ESTIMATION OF DIRECT RECHARGE ON NATURAL VEGETATIONS OF THE LAKE AQUIFER

(A case study of Lake Naivasha Basin, Kenya)

Elizabeth Nalugya
March 2003

ESTIMATION OF DIRECT RECHARGE ON NATURAL VEGETATIONS OF THE LAKE AQUIFER

(A case study of Lake Naivasha Basin, Kenya)

By

Elizabeth Nalugya

Thesis submitted to the International Institute for Geo-information Science and Earth Observations in partial fulfilment of the requirements for the degree of Master of Science in Water Resources and Environmental Management specializing in Groundwater Resource Evaluation and Management

Degree Assessment Board

Chairperson:	Prof. Dr. A.M.J. Meijerink, Head WREM Division, ITC
External Examiner:	Drs. J.W.A. Foppen, IHE
Supervisor:	Drs. Robert Becht, WREM Division, ITC
Member:	Dr. M. W. Lubczynski, WREM Division, ITC

INTERNATIONAL INSTITUTE FOR GEO-INFORMATION SCIENCE AND EARTH OBSERVATION
ENSCHEDE, THE NETHERLANDS

Disclaimer

This document describes work undertaken as part of a programme of study at the International Institute for Geo-information Science and Earth Observation. All views and opinions expressed therein remain the sole responsibility of the author, and do not necessarily represent those of the institute.

Abstract

Groundwater use in Naivasha basin is a fundamental importance to meet the rapidly expanding agricultural water requirements, around the area. Due to the (semi-) arid climatic conditions of the area, this resource is almost the only key to economic development; hence the quantification of its current rate is a necessity for the efficient and sustainable groundwater resource management.

The availability of recharge estimate techniques differs climatically. Sources and processes of recharge in humid areas are different compared with (semi-) arid areas; hence the need to proceed from a well-defined conceptualisation of different recharge processes is essential, as is the need to use more than one technique for verification of results.

Generally the most factors contributing to recharge in the area are rainfall, evapotranspiration rates and soil types. The area experiences an annual rainfall of 640mm, which is characteristic of a semi arid climate. Since the potential evapotranspiration of the area was estimated to be higher than rainfall, direct recharge is not a permanent process in the area, but a process which occurs during rain seasons and, only when there is high intensity. The process of evapotranspiration occurs through the year for those areas that are covered with both grassland and thick natural vegetation.

High recharge values are estimated in areas that are mainly dominated by grassland type of vegetation and low values in areas covered by shrubs and thick vegetation. Due to structural uniqueness of the rooting system of Acacia trees, it is proved that these trees have a big influence on the recharge and groundwater system in the study area.

Field measurements are the basis of recharge investigations since they give a realistic idea on recharge processes. They should work hand in hand with models for better estimations of groundwater recharge.

Acknowledgements

Glory and honour to the almighty God for his provision towards my life, most especially his guidance and care during this period of stay in Netherlands. "He who begun a good work in me is ready to accomplish it….."(Philippians 1:6).
First and foremost, I wish to express my gratitude to the Government of Netherlands for the fellowship offered to pursue my studies at ITC. My sincere thanks go to Eastern Centers, Water and Sanitation Project for granting me this opportunity for further studies. Special thanks to Engineer D. Kavutse, the project coordinator for his advice and immediate response towards all the paper work involved in acquiring the scholarship. I cannot forget my immediate boss Mr. Kagaba who helped in processing all the necessary documents for my study extension.

I am greatly indebted to my supervisor, Drs. Robert Becht, for his dedication and supervision of this project, right from fieldwork to the final writing of this report, more especially, his professional approach during the modelling part. I acknowledge the support and guidance received from the entire staff of WREM towards my studies. I express my gratitude to Dr. M. Lubczynski and Dr. A. Geiske for their advice and critical comments towards this project. I thank Mr. Boudewijn de Smeth and Ms Barbara Casentini, for the support during the long and crucial laboratory analysis of the field data.

I would like to express my appreciation for the support I received from the following individuals and organisations during my field work in Kenya; Ministry of Natural resources and Environment, Shell limited, LNRA, the managers of the local farms in particular the Manager of Three Point farm, field assistants, Mr.Tanui, Mr.Joseph and Mr. Kimiri.

I would like to acknowledge my fellow MSc colleagues for their support in one way or another during our study and stay in ITC. Special thanks go to the following; Uan (Thailand), Arlan (Indonesia), Tefo Boyboy (Botswana), Dorji (Bhutan), Stephan (Bolivia), Liu (China) while not forgetting Cate (Uganda), for her moral support and encouragement, during tough times throughout the study period.
Thanks to my fellow believers, the ITC Christian fellowship and members of Pniel church. Many thank go to Pastor Henk, Adrie and Ginny for their prayers and spiritual encouragement.

I express my sincere gratitude to the Ugandan and East Africa community. Special thanks go to Mike, Charles and Alex for their friendship and also their contribution in one way or another towards this research. To my sister Anita, thank you for being a good ambassador back home during my absence.

Last but not the least, I would like to express my heartfelt appreciation to my Parents, uncle Kiyingi, and aunt Martha for their invaluable moral support and sacrifices to help me achieve my educational goal.

Dedication

To my beloved Brother, John

TABLE OF CONTENTS

LIST OF FIGURES

LIST OF TABLES

LIST OF APPENDICES

LIST OF PLATES

1. INTRODUCTION

1.1. GENERAL INTRODUCTION

Groundwater plays a vital role in the rapidly expanding Urban, industrial, and agricultural water requirements, in the study area. Therefore the quantification of the current rate of groundwater recharge is a necessity for the efficient and sustainable groundwater resource management.

Groundwater recharge is generally considered as that amount of water, which contributes to the temporary or permanent increase of groundwater resources. From the mechanism of groundwater recharge it is quite obvious that the highest percentage of water is of meteoric origin. Other sources such as juvenile water of volcanic, magmatic and cosmic origins contribute little to the ground water recharge (Simmers, 1987). The actual recharge reaching the water table may be considerably less than the potential recharge due to the influence of the unsaturated zone. Water-resource evaluation requires information on recharge over large spatial scales and decadal time scale, which requires detailed information on spatial variability and preferential flow (Scanlon et al., 2002). Therefore, the complexity of water movement has to be followed critically from the very time it enters the soil profile, until it reaches the water table.

1.2. RESEARCH PROBLEM

The status of water recharge on lake Naivasha basin is not fully known, as previous studies did not have sufficient data for its estimation. Due to this fact, it is difficult to plan how the resource can be sustainably exploited. In most of the researches water recharge has been estimated and modelled from other parameters like transmissivity, but the direct research on recharge estimate has not been carried out.

In this research the study will be on estimation of recharge, focusing more on direct recharge from rain, in unconfined aquifer surrounding Lake Naivasha, since this is the most available and affordable water and mostly liable to depletion in the study area.

As in many (semi-) arid areas, it is of great importance to recognize the role of water cycle elements, such as evapo (transpi) ration and rainfall, how they are linked to groundwater, rivers and lakes, still the need to understand the role of vegetation in the hydrological cycle, particularly the interactions between vegetation and groundwater is important.

1.3. RESEARCH OBJECTIVES

1.3.1. Overall Objective

The main aim of the research is to estimate groundwater recharge around the lake aquifer. Direct recharge from unsaturated zone will be estimated using Soil- Water Atmosphere-Plant (SWAP) numerical model together with field measurements. By the use of stable isotopes, more highlights on how much recharge is contributed by both the lake (lateral inflow) and rain toward the southern parts of Lake Naivasha.

1.3.2. Specific Objectives

- To estimate physical properties and hydraulic properties of different soil layers in unsaturated zone. This will mainly include soil particle size and organic matter determination, soil moisture and saturated hydraulic conductivities estimates.
- To carry out infiltration tests on the unsaturated zone
- To analyse $\delta^{18}O$ and δD isotopic composition in unsaturated zone,
- To estimates spatial variability of recharge in different soils types
- To understand the impact of vegetation on groundwater recharge
- To improve on spatial variations in the groundwater flow patterns around the lake aquifer

1.4. RESEARCH QUESTIONS

- Where are the recharge potentials of the lake aquifer and how much do recharge contribute to groundwater flow of the lake aquifer.
- How much water does Acacia tree extract from groundwater.

1.5. OUTLINE OF THESIS

Chapter 1: This is the introduction of the research. It includes the importance of the research, the problem and the objective of the research followed by research questions to be answered at the end of the research.

Chapter 2: It comprises of the literature of the study area, mainly about the research topic.

Chapter 3: This description of the study area in terms of location, topography, climate, soil and vegetation, geological and hydrological settings and finally groundwater recharge and groundwater flow of the entire basin.

Chapter 4: It outlines the processes involved, right from the preparations before fieldwork until the completion of the project.

Chapter 5: This focuses on recharge estimates from applied techniques. It also discusses the influence of vegetation on recharge, emphasis being directed to the Acacia trees located in the study area.

Chapter 6: This broadly discusses the results from the analysis, including their successes and limitations.

Chapter 7: It incorporates the conclusions and recommendations for further studies based on the output of all the analysis carried out.

2. LITERATURE REVIEW

2.1. THEORY OF UNSATURATED FLOW

Movement of precipitation into the ground consists of a series of hydrological processes; the entry of water across the soil-atmosphere interfaces, filing of storage, transmission of water through the soil profile, deep drainage and recharge of the underlying groundwater system. All these five processes are related to the potentials energy of water in the soil, which in turn comprises of other several components:

The matric potential ψ is caused by both the attraction of water molecules to each other and to the solid surface. Water in the unsaturated zone possesses a negative potential, and the negativity of soil matric potential increases as films of the water around the soil pore walls becomes thinner as a soil dries and at this moment, the remaining soil water is held under a greater tension and the zero matric potential occurs when the all the soil pores are filled with water, which is the case below the water table.

Other forms of potentials include; the gravity potential ***z***, due to the elevation difference between soil water and the reference pool for example the water table; the pressure potential ***p,*** due to the weight of water or gas pressure, it is equal to an opposite sign of gravity potential. In this case ***p*** is zero in saturated soils; the osmotic pressure ***o,*** caused by salts dissolution in the soil water. Water will always moves from a weaker to stronger solution in order to balance the solutions concentrations (Buttle, 1998). The total potential (Φ) can be defines as:

$$\Phi = \psi + z + p + o \qquad \textbf{(2.0)}$$

2.1.1. Factors affecting the water movement to the water table

Soil factors, include, the soil water properties such as particle sizes, determined from the size distribution of individual particles in a soil sample, bulky density, which the ratio of weight of dry solids to the bulk volume of the soil, the soil porosity which is the total volume occupied by pores per unit volume of soil, the water retention characteristics described in equation, (2.0) above, and the hysteresis, which is illustrated in the matric potential water content $h(\theta)$ and $K(\theta)$ relationships as the soil is de-

sorbing or absorbing. For practical applications, hysteresis has been avoided. Hydraulic conductivity is another soil physical property that affects infiltration. It is a measure of the ability of soil to transmit water. It is affected by the soil properties like, total porosity, pore-size distribution and pore continuity, and the fluid properties like viscosity and density. The hydraulic conductivity for water content at or above the saturation point ($h \geq 0$) is referred to as saturated hydraulic conductivity and that for water content below the saturation point ($h<0$) is called unsaturated hydraulic conductivity.

The surface factors, also do affect the movement of water through the air-soil, interface. Areas with cover materials like grass and trees protect the soil surface, whereas areas with bare soil form crush during raindrops, which inhibit infiltration. Agriculture management systems affect the soil properties like soil porosity, bulky density that can also affect infiltration rates. Increase in organic matter of soil lowers the bulky density, increases porosity and this leads to increase in infiltration. Natural factors, such as precipitation, temperature, and moisture, vary with space and time, and interact with other factors in their effect on infiltration (Rawls et al., 1993).

The time of movement of infiltration water is a function of the thickness of the unsaturated zone and the vertical unsaturated hydraulic conductivity. In (semi-) arid environments, with very occasional recharge and great depths to the water table, water may take years to pass through the unsaturated zone. When the unsaturated zone is thinner recharge can reach the water table first resulting in localised groundwater piles. This normally occurs in areas, which are topographically low, like lakeshores. Soil moisture percolating through the unsaturated zone beneath the upland areas, takes a longer time, and if there exist a temporary water table which is initially levelled, localized high spots can develop on it and immediately, localised flow system develops that transfers water laterally from this temporary groundwater piles towards the water table beneath the uplands. Immediately the water table beneath the uplands will rise owing to both vertical percolation of infiltration water and the lateral movement from temporal groundwater piles (Fetter, 1994). Localised flow reversals can also take place with the groundwater first flowing from beneath the lowland towards the upland in response to the formation of localised recharge piles and then moving in the positive direction as the water table beneath the upland is finally recharged, by the percolating soil moisture. It would be expected that the flow reversals would affect only the water moving in the very top of an unsaturated flow system.

Furthermore, the interaction of climate, soils, vegetation and geology (figure 2.0) also determines the groundwater recharge processes. Thick vegetations extract soil water in dry season. The poor vegetation cover, on permeable soils or fractured porous bedrocks near the surface, together with high rainfall intensity creates a favourable condition for recharge. The presence of low-permeability material, like silt and clays can retard the rate of recharge, even when the layers are thin. Recharge is normally delayed by thick alluvial soils, which have high retention storage during wet seasons.

Normally, in (semi-) arid climatic zones, the potential evapotranspiration exceeds rainfall, so groundwater recharge in these areas depends on rainfall intensity, accumulation of rainwater in depressions and streams, and the ability of rainwater to escape evapotranspiration by rapid percolation through cracks, fissures, or solution channels. Thick vegetations do extract soil water, mostly in dry seasons and poor vegetation cover, on permeable soils or fractured porous bedrocks near the surface, together with high rainfall intensity creates a favourable condition for recharge. Recharge can also be delayed by thick alluvial soils, which have high retention storage during wet seasons

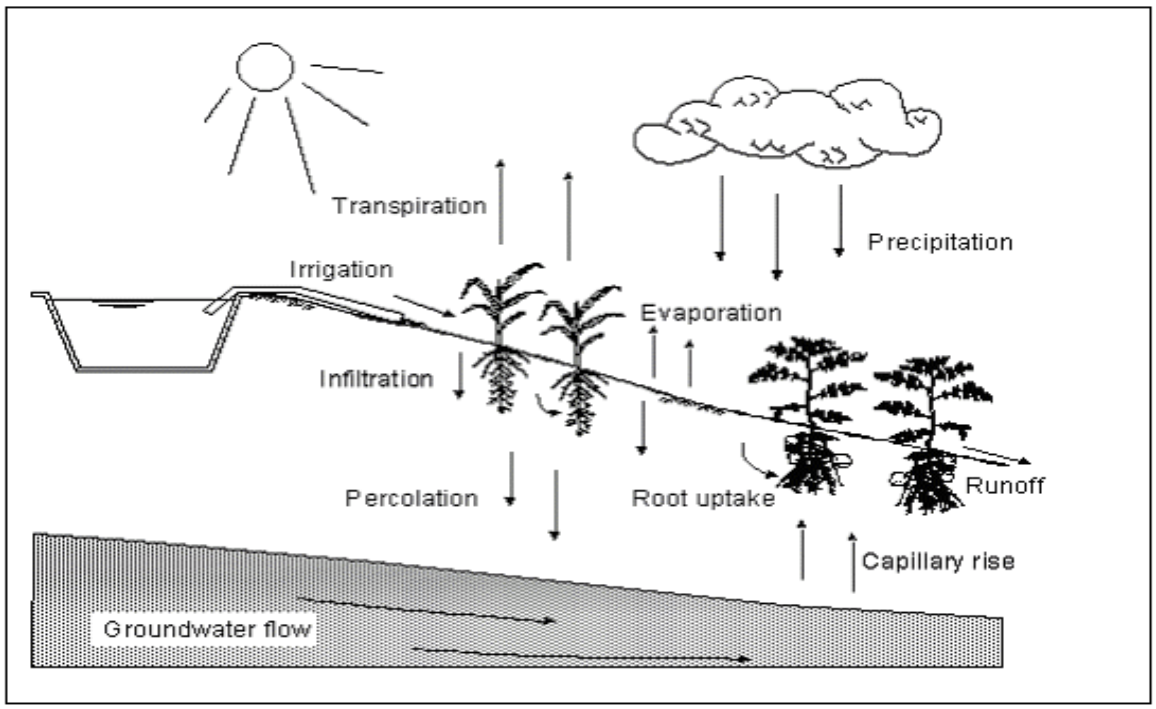

Figure 2.1: Hydrological processes at field scale

2.1.2. Governing Equations for Water Movement in unsaturated zone

Usually water flows in the soil under unsaturated conditions, where the soil pore space is always occupied by air and water. Flow conditions within the unsaturated zone are far more complex than the flow mechanisms in a saturated aquifer. The main difficulty is that the three parameters, that is the moisture content, the matrix potential or fluid pressure, and the hydraulic conductivity, which are inter-related. The relationship among these parameters is very sensitive; a slight change in the volumetric water content can correspond to a big change in the hydraulic conductivity and fluid pressure. The soil hydraulic conductivity $\boldsymbol{K}$ is a function of the volumetric soil water content, θ, that is $K=K(\theta)$, sometime referred to as capillary conductivity. Soil water potential in an unsaturated soil can be nega-

tive due to the capillary suction forces since it is a function of θ, $h = h(\theta)$. The $h(\theta)$ is referred to as the Soil water matrix potential head and its absolute value is called the matric suction head $\tau(\theta)$.

For one-dimensional unsteady vertical flow:

$$q = -K(\theta)\left[\frac{\partial h(\theta)}{\partial z} - 1\right] \qquad \textbf{(2.1)}$$

where q is the specific discharge or flow rate per unit cross sectional area of soil (ms^{-1}), often called Darcy's velocity or flux, z is the soil depth, taken positive downwards.

The term $K(\theta)$ can also be written as $K(h)$, when θ is assumed to be a unique function of h, the matric potential head.

Combining Darcy's law (equation 2.1) with the law of conservation of mass results into a one dimension vertical flow in an unsaturated soil:

$$\frac{\partial \theta(z,t)}{\partial t} = \frac{\partial}{\partial z}\left[K(\theta,z)\frac{\partial h(\theta,z)}{\partial z} - 1\right] \qquad \textbf{(2.2)}$$

The above equation has two dependent variables h and θ. With an assumption that θ is a unique function of h, the function $\partial\theta/\partial t$ can written as:

$$\left(\frac{\partial \theta}{\partial h}\right)\frac{\partial h}{\partial t} = C(h)\frac{\partial h}{\partial t} \qquad \textbf{(2.3)}$$

from the above equation Richard's equation is obtained:

$$C(h,z)\frac{\partial h(z,t)}{\partial t} = \frac{\partial}{\partial z}\left[K(h,z)\frac{\partial h(z,t)}{\partial z} - 1\right] \qquad \textbf{(2.4)}$$

where $C(h)$ is the Specific moisture capacity, (cm^{-1}) and **t** is the time.

Some portions in soil horizons become saturated in the course water flow, then the term $C(h)$ becomes zero and $K(h,z)$ becomes a constant saturated value $Ks(z)$.

Richards's equation has a clear physical basis at a scale where the soil can be considered as a continuum of soil, air and water.

2.1.3. Mechanism of Water Movement in Unsaturated soil

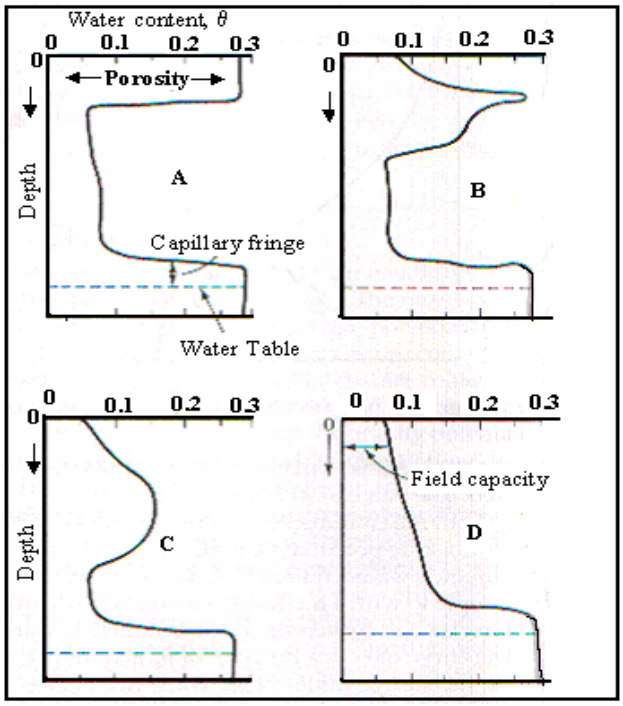

Figure 2.2: Moisture profiles of the downward passage of a slug of infiltrated water, (Fetter, 1994).

During infiltration (part A), the topmost soil layer is brought to saturation. When the rainfall rate exceeds the infiltration capacity so the vertical hydraulic conductivity of the soil starts controlling the rate of downward movement. When infiltration ceases, (part B), the slug of infiltrated water begins to move downward, although only a small layer remains at the saturated moisture content. Eventually all of the downward-moving slug at an unsaturated state, and K (θ_v) control the downward movement (part C). Lastly the slug reaches the water table and raises it (part D). At this moment gravity drainage has reduced the upper soil layer to field capacity (Fetter, 1994). The water table separates the unsaturated zone and the underlying saturated zone of groundwater when all the pores are filled with water.

2.2. THE ORIGIN OF GROUNDWATER RECHARGE

Recharge is that amount of water that reaches the water table by percolation of precipitation in excess of evaporation, through the unsaturated zone. During this process as described above, there is a downward movement of water through the saturated zone under the influence of gravitation force whose direction is determined by hydraulic conditions.

Most of groundwater recharge is of meteoric origin. Other sources such as juvenile water of volcanic, magmatic and cosmic origins contribute little to the ground water recharge (Simmers, 1987). As groundwater recharge is generally considered as that amount of water, which contributes to the temporary or permanent increase of groundwater resources, the complexity of the process has to be considered from the very time water, which is transformed by interception, enters the soil profile.
The actual recharge reaching the water table may be considerably less than the potential recharge due to the influence of the unsaturated zone.

2.3. TYPES OF RECHARGE MECHANISMS

(Lerner et al., 1990)classified recharge in three types; direct recharge, which is that added to the groundwater reservoir, in excess of both soil-moisture deficits and evaporation by direct percolation through the vadose zone; indirect recharge is that type where water percolates to the water table through the beds of surface watercourses; localised recharge, is an intermediate form of groundwater recharge resulting from horizontal (near-) surface concentration of water in the absence of well-defined channels.

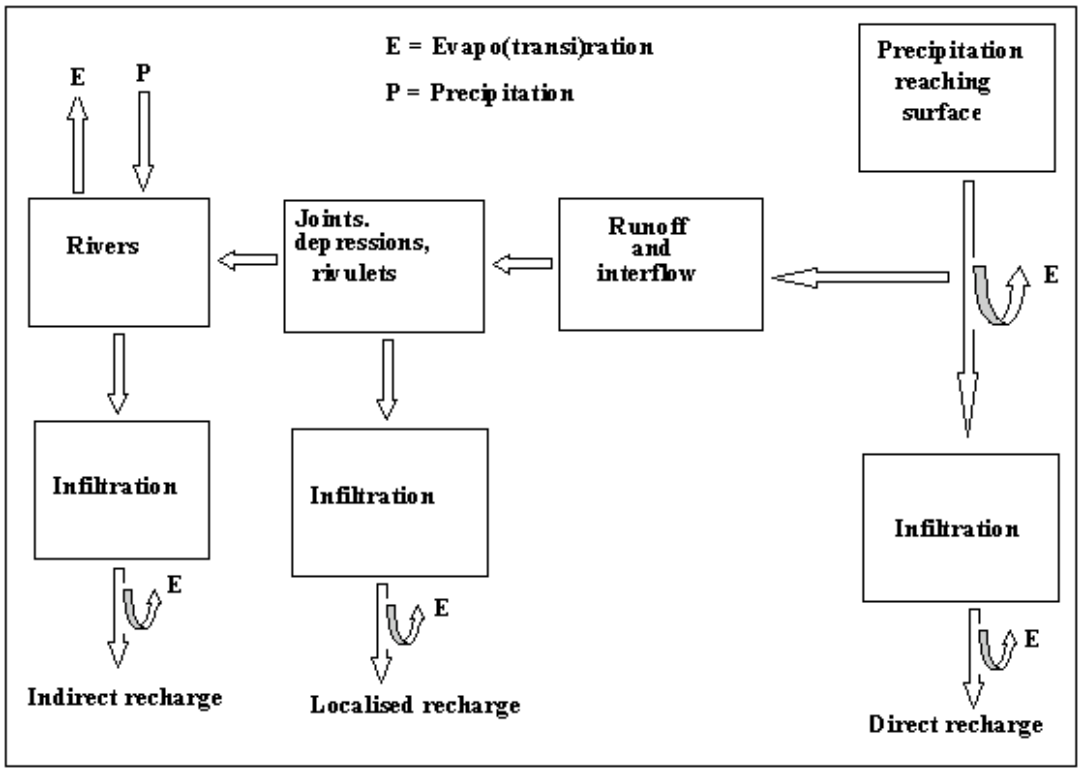

Figure 2.3: Various mechanisms of recharge in (semi-) arid areas (Simmers et al., 2002)

2.4. INFLUENCE OF VEGETATION ON RECHARGE IN SEMI-ARID AREAS

Vegetation on a big scale determines the amount of net rainfall, infiltration rate, deep drainage and the available storage capacity of groundwater system. When all the above factors are combined, the potential recharge is determined. The effect of vegetation can either be positive or negative. A slight change in vegetation, say from forest to grassland can have a large effect on recharge. The nature of land cover has a big influence on recharge, hence groundwater recharge modelling should not assume that vegetation is a constant factor (Scott and Le Maitre, 1998).

(Allison et al., 1994; Leduc et al., 1997) illustrated the crucial influence of vegetation on recharge in (semi-) arid areas through the historical evapotranspiration changes. The removal of the indigenous vegetation in large parts of southeastern Australia more than 100 years ago caused a significant increase in ground water recharge. The landuse in Niger resulted in an increase in recharge from a previous 5mm/year to the present 20mm/year, which has induced a longer water table rise. By clearing the vegetation, the hydraulic properties of topsoil changed, an increase in runoff occurred, which lead to concentrated water in depression and resulted in an improved recharge.

Previous studies in Kalahari Desert have detected acacia species from depths exceeding 50 meters (De Vries et al., 2000).

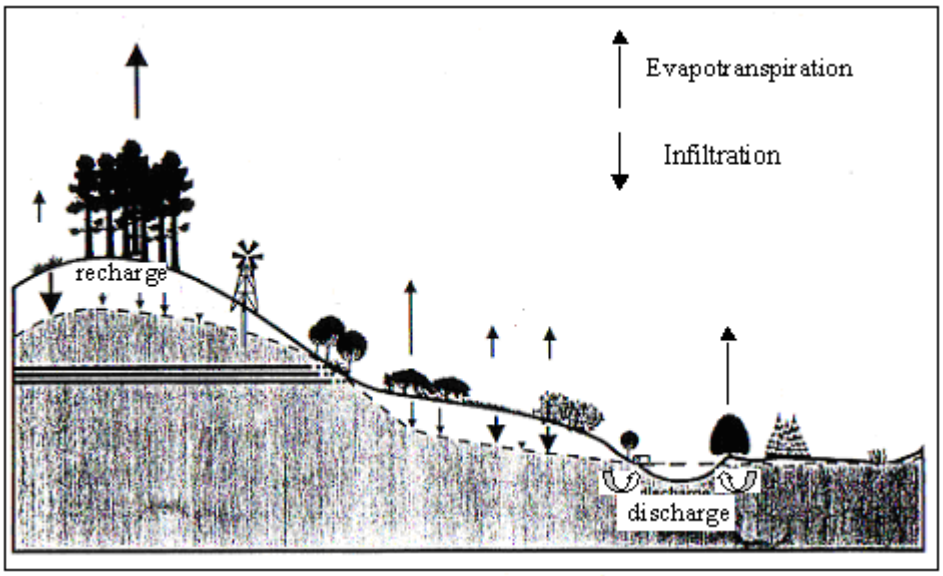

Figure 2.4: Illustrates typical interactions between vegetation and groundwater (Scott and Le Maitre, 1998)

In (semi-) arid areas where the annual precipitation is always less than 700 mm, recharge fluxes always turn out to be very small in quantity. The natural vegetation in these areas has often developed root systems such that almost all the precipitation that is received is consumed by evapotranspiration (Simmers et al., 2002).

2.5. SOIL-WATER-ATMOSPHERE-PLANT (SWAP)NUMERICAL MODEL

The Soil-Water-Atmosphere-Plant (SWAP) is a computer model developed by Wageningen Agricultural University and DLO Winand Staring Centre. SWAP simulates vertical transport of water, solutes and heat transport in unsaturated- saturated zones in relation to vegetation growth. In this research only the water transport module will be used to simulate bottom fluxes, which will be referred to estimation of groundwater recharge.

The system boundaries at the top are defined by the soil surface with or without crops or vegetation and atmospheric conditions. The lateral boundary simulates the interaction with surface water systems. The bottom boundary is located in the unsaturated zone or in the upper part of the groundwater and describes the interaction with regional groundwater.

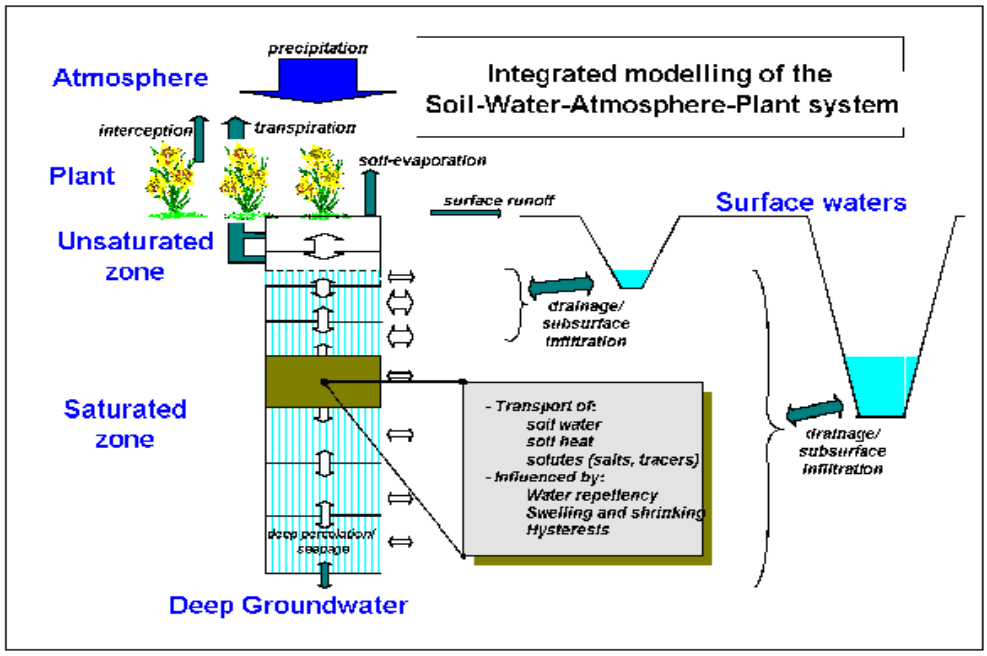

Figure 2.5: A schematised overview of the modelled system; adapted from the user's guide of Swap model version 2.0, (Kroes et al., 1998).

2.5.1. Soil water flow

As described in Darcy's equation (2.1), the flow of soil water is caused by spatial differences of the soil water potential. SWAP solves the Richards' equation (2.4) numerically when it is subjected to specific initial and boundary conditions, with a known relation between the soil hydraulic functions that is, θ, h, and K. these soil hydraulic functions area either measured directly in soil or obtained from basic soil data. During the process of water movement in unsaturated zone, the effect of roots on this

process is so crucial. This factor is added to the equation as a sink term S_w, expressing the rate of water uptake by roots per unit volume of soil.

$$\frac{\partial \theta(z,t)}{\partial t} + Sw(z,t) = \frac{\partial}{\partial z}\left[K(\theta,z)\frac{\partial h(\theta,z)}{\partial z} - 1 \right] \qquad \textbf{(2.5)}$$

The model solves equation (2.4) numerically, if subjected to specific initial and boundary conditions and with known relations between θ, *h*, and *K*. These relations are called soil hydraulic functions and can be measured directly in the soil or obtained from the basic soil data. The soil hydraulic functions are described by analytical expressions of Van Genuchten (1980) and Mualem (1976) or by tabular values.

By applying the different scaling factors, SWAP generated for each scaling factor the soil hydraulic functions and the corresponding water balance. The actual mobile volume at a certain depth depends on the soil water pressure head. In this case the Richards' equation applies.

2.6. ISOTOPE HYDROLOGY

Isotopes are elements with the same atomic number but different atomic weights due to varying numbers of neutrons in the nucleus. 18-Oxygen and Deuterium are some of the stable isotopes used for identifying processes and origin of the water though have some difficulties in quantification of recharge estimates since they are not conservative and are subjected to fractionation by evaporation (Simmers et al., 2002).

According to Barnes and (Allison, 1987), as cited by (Buttle, 1998), stable isotopes such as $\delta^{18}O$ and $\delta^{2}H$ have been used to estimate groundwater recharge in (semi-) arid regions where recharge is thought to occur only during heavier rainfall events. He noted that sites with high recharge rates should have soil water that is more similar to isotopic signature of incoming water than sites with lower recharge where greater evaporation continuously enhances the isotopic enrichment of soil water.

2.6.1. Global Meteoric Water Line (GMWL)

According to (Craig, 1961), as cited by (Kendall and Caldwell, 1998), when the isotopic composition of precipitation samples from all over the world are plotted relative to each other on δ18 O versus δD plots, the data form a linear band of data can be described by the equation:

$$^{2}\delta = 8^{18}\delta + 10 \qquad \textbf{(2.6)}$$

This is a linear relationship between δ2 and δ8 values representing worldwide fresh water sources their isotopic composition in precipitation and it can be used to unravel the processes, like evaporation and mixing trends, which affect the rainwater or soil moisture. Regionally and for certain period, Local

Meteoric Water Lines (LMWL) may be found, depending on the conditions for forming the local water source of each region.

In region with arid type of climate the $^{2}\delta$-$^{18}\delta$ slope is less than 8, it ranges between 4 and 6 due to evaporative process in the atmosphere. With different sources of vapour having differing isotope contents, and varying evaporation and exchange processes below the cloud base, result in a complex relation between the two deltas values which leads to a large scatter of data points in a $^{2}\delta$-$^{18}\delta$ diagrams (Rozanski et al., 1993).

Stable isotopes investigations in unsaturated zone are aimed at examining the isotopic modification of soil moisture as it infiltrates through the unsaturated zone to the aquifer. In such a case, the stable isotopes are used to determine the distributed groundwater recharge rates, groundwater mechanisms and its evaporation rates from groundwater discharge zones (Selaolo, 1998). In most cases, unsaturated and dry soils show $^{2}\delta$-$^{18}\delta$ slopes of between 2 to 5, depending on the moisture content of the soil. The lower slope observed for dry soils results from laminar flow, which dominates over turbulent flow during diffusion of the isotopes to the atmosphere (Allison, 1987).

2.7. PREVIOUS STUDIES ON NAIVASHA BASIN

Quite a number of ITC students and other researchers have done a fundamental work on Lake Naivasha basin. Previous groundwater modelling clarify that the major factors controlling the groundwater flow near lakes include; geometry and heterogeneity of the geological framework, hydraulic conductivity of geologic units, lake depth and distribution of recharge as reflected by the configuration of the water table.

2.7.1. Groundwater recharge and flow

(Farah, 2001) determined the evapotranspiration using satellite data of different soil and vegetation units covering the Naivasha basin. The rate of potential evapotranspiration in the study area is higher than precipitation. Groundwater recharge from precipitation occurs only during heavier rainfall events. Researches on groundwater flow in the study have proved that Lake Naivasha has a big contribution towards the groundwater recharge in the area.

(Owor, 2000) researched on long-term interaction of groundwater with lake Naivasha. The regional groundwater flow patterns indicate major outflow areas to the south and southeastern part and lesser to the north and northeastern part of the basin. Transmissivity and groundwater recharge in the area has been modelled using available data from individual wells. His model calibrated for low recharge values ($<5 mmyear^{-1}$) in the lake sediments in the vicinity of the Lake. The volcanic tuffs intercalated with ash that are bounded by south Kinangop fault to the east receives recharge of ($75\text{-}80 mmyear^{-1}$), most

likely derived through intensive fractures systems in the area. A recharge of (20-25mmyear^{-1}) was estimated for the rest low gradient area, which is underlay, by the mixture of sediments and reworkable volcanic materials. He recommended that in order to have a clear description of the groundwater flow patterns, estimation of spatial variation of recharge is required.

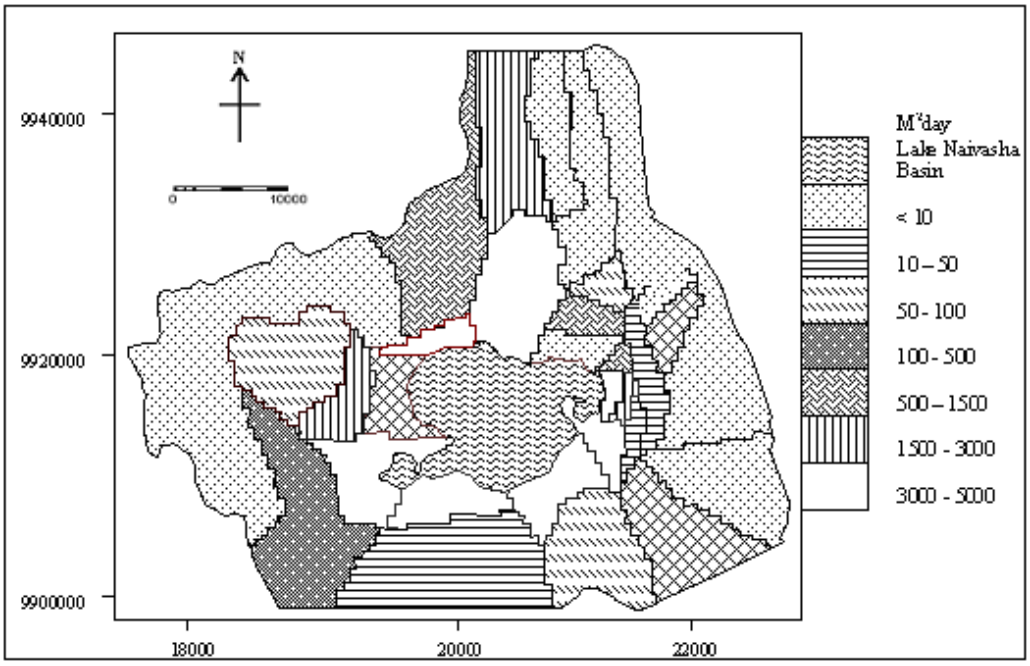

Figure 2.6: The distribution of Transmissivity in the study area, modelled by (Owor, 2000).

2.7.2. Effect of faults on groundwater flow systems

The structure of the rift valley, especially the major rift faults have a substantial effect on the groundwater flow systems of the area. Generally Faults have two effects on the fluid flow, they can provide channels of high permeability or barriers to the flow by offsetting zones of relatively high permeability. With little evidence it is thought that in areas where horizontal flow predominates, faults are thought of as hydraulic boundaries in groundwater flow systems whereas in areas predominated by vertical flows, they are considered to provide conduit for flow (Clarke et al., 1990).

The effect of Rift faulting appears to be less in the Kinangop Plateau areas where the piezometric contours are more widely spread and the little evidence from boreholes located in Mau Escarpment to the west of the Naivasha basin, suggests that the flow towards the lake are not greatly affected. Dry boreholes to the west of Suswa indicate that the rift faulting may inhibit lateral ground flows in this area.

The geology of the area has a major control over the fluid movements in the study area. Recent studies (Ogoso Odongo, 1986) state that the faults in Olkaria region act as barrier, redirecting the southerly flow from Eburru to the south-west, towards Suswa, though the evidence for such behaviour is rather

small. So in general faulting has an effect on groundwater flow. It causes it to flow from the sides of the Rift towards the centre where it follows longer flow paths reaching greater depths, and it aligns the flows within the Rift along its axis.
(Nabide, 2002) developed a 3-D geological model which will be used as an input to modflow in a later study

2.7.3. Isotopic composition of Groundwater

Stable isotopes results confirm that many Naivasha wells contain lake water. It is understood that the lake is recharged by a combination of river and groundwater from the northwest, which then undergoes evaporative concentration before eventually discharging underground to the south and north of the lake, which lies at the termination of the Rift floor. Thus mixing between a lake water and shallow groundwater would occur along flow paths away from the lake, giving rise to isotopic properties of Naivasha group of well waters (Clarke et al., 1990).
(Oppong-Boateng, 2001) carried out isotopic analysis on saturated zones in the southern part of the lake and came up with groundwater flow directions induced from isotopic data. From his studies, he observed that that the Deuterium, Oxgen-18, tritium and carbon-14 isotopic signatures of both the surface and groundwater provide evidence for the sources of recharge into the groundwater flow system in the lake aquifer. There is a gradual variation in the isotopic composition due to physical factors during different storms at sampling sites, which these waters encounter in the process of recharging, before reaching the groundwater flow system. Isotopic signatures of groundwater have confirmed that the southern aquifers are recharged by Lake Naivasha and direct recharge, whereas the north aquifers are recharge by rain and river Malewa. There is a distinct inflow from the west from Mau escarpment and Ndabibi plains towards the lake. The main groundwater out flow zone is located in the southern part of the Lake. The wells from the northern part of the lake have relatively a different isotopic composition from that of the lake. Their isotopic signature is a mixture of direct recharge and Malewa River. From Isotopic Mass Balance Method, based on 18-Oxygen isotopic composition of the lake and specified wells, estimated isolines of lake water contribution, as a percentage of the total contribution towards the study area was obtained (Oppong-Boateng, 2001).

3. DESCRIPTION OF THE STUDY AREA

3.1. LOCATION

The Naivasha basin is situated in Nakuru District, about 100 km northwest of Nairobi (figure 3.1). It is located in the central rift valley of Kenya with Universal Time Meridian zone 37, south and covers an area of about 3500km^2, with the following coordinates:

X_{min} 190000 X_{max} 221000

Y_{min} 9934000 Y_{max} 9907000

The lake basin has become a major fruit and vegetable producer as well as a commercial producer of fresh flowers for export. Agricultural farms, flower plantations and fishing provide huge employment opportunities for residents of Naivasha. These employment opportunities have led to an invasion of people into Naivasha town and to large flower farms around the lake. The population of 20,000 about 20 years ago, now stands at about 250,000.

The Naivasha basin incorporates lake Naivasha, the Ndabibi plains which lie to the west of the lake and the llkek plains which lie immediately to the north. On the floor of the eastern Rift valley lies Lake Naivasha. Lake Naivasha dominates the Naivasha basin, with an elevation of 1885 m.a.s.l and covers an area of 150km^2 and a mean depth of 4.7m. This is the largest freshwater lake along the Kenyan section of the Rift valley. Lake Naivasha is a relict lake that once belonged to a large freshwater body that comprised Lakes Naivasha, Elmenteita and Nakuru. The large freshwater body is believed to have dried up due to changes in climatic conditions and increase in water obstruction since 1996. Lakes Nakuru and Elmenteita became saline but Lake Naivasha remained a freshwater lake, a characteristic that makes it unique among the rift valley lakes. This makes it valuable to people as a source and store of water. There are no known outlets, yet the water remains fresh, thus leading to suggestions of possible unique and hydro-geological mechanisms involving underground seepage in this part of the Rift Valley. Its freshness is attributed to incoming water from dilute rivers and precipitation, loss of solutes via seepage out and due to geochemical and biochemical sedimentation. The lake and its environment are important because of their biological diversity, and the lake function as a freshwater resource.

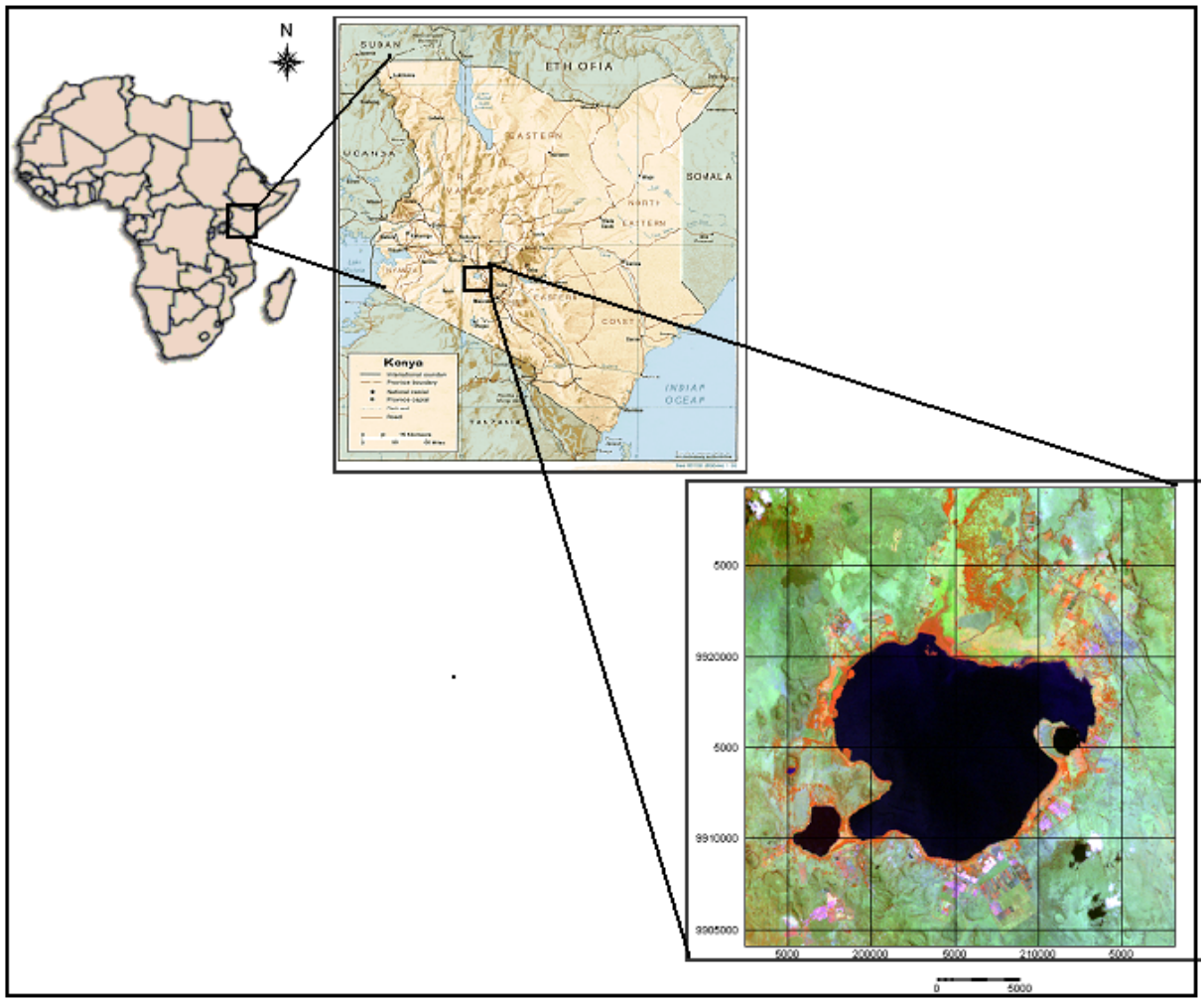

Figure 3.1: The Location of the study area

3.2. PHYSIOGRAPHY

The study area has three types of landscape, Kinangop plateau to the east, Mau escarpment to the west, the Mt Longonot with its lava flow fields to the south and IIkek plains to the north (figure 3.2).

The Mau escarpment on the western fringe rises up to a maximum of 3080 m.a.s.l. The escarpment is deeply incised with numerous faults and scarps. There is also a rise of topography to the south towards the Olkaria volcanic cones of up to 2430 m.a.s.l at Olkaria Hill. The Ndabibi plains extend up to 9km west of the Lake and it separates the Olkaria and Eburru volcanic complexes. The Kinangop plateau to the east rises to a maximum altitude of 2740 m.a.s.l. Its plains are about 1980masl along their western margin and slope gently eastward to the Lake (Clarke et al., 1990). To the north, we find the llkek plains, which are 23 km north of the Lake. They slope gently southward with a maximum elevation of 2000 m. Its width is about 13km near the Lake, and 4 km near Gilgil town.

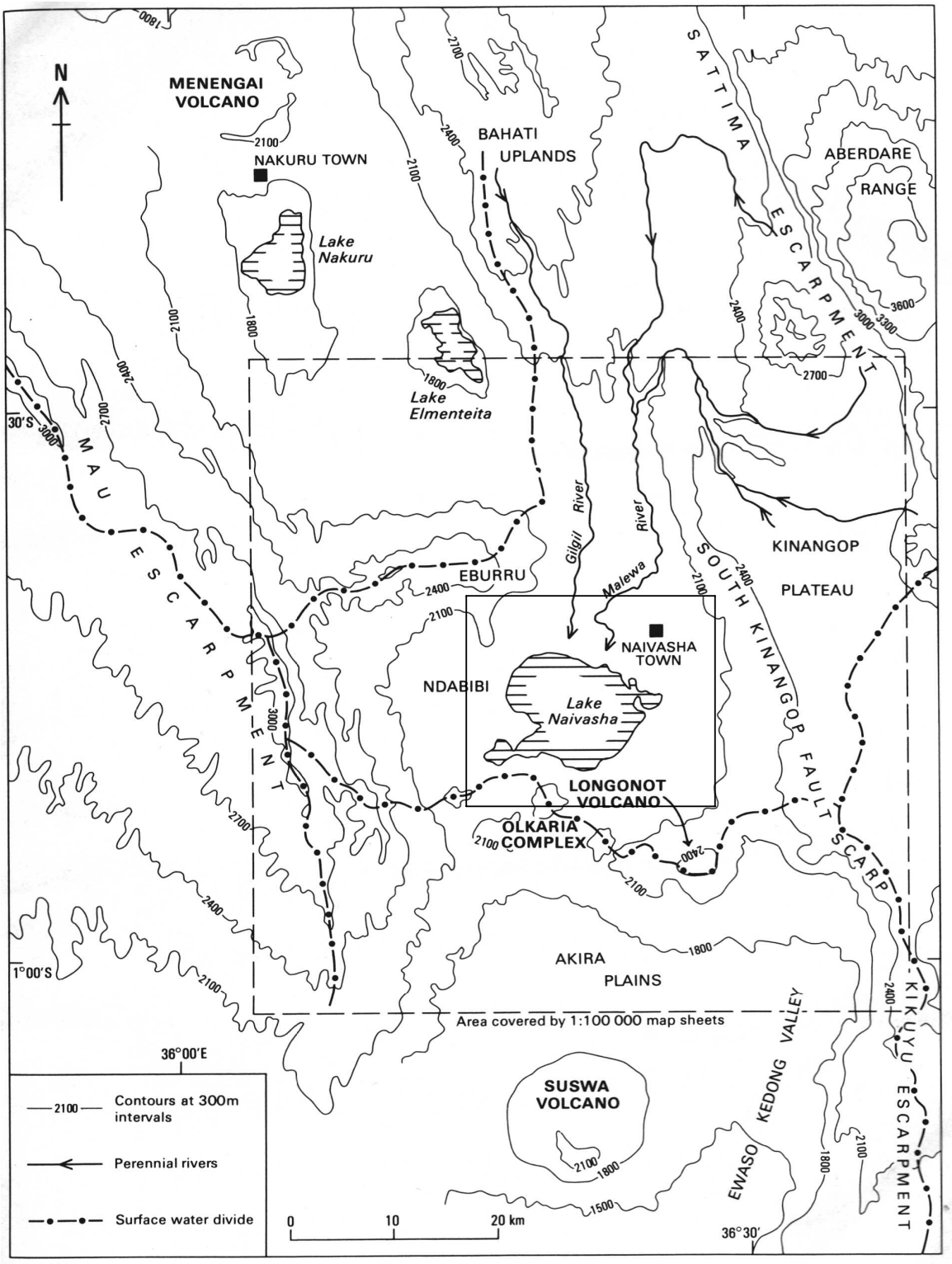

Figure 3.2: The Study area and Physiography of the central Rift Valley (Clarke et al., 1990)

3.3. GEOLOGICAL SETTINGS

The basin is characterised by prominent morphological and structural features due to numerous tectonic episodes that produced volcanic rocks and Quaternary lacustrine deposits that dominate the area. The oldest rocks found *in situ* in the area are Tertiary.

On the basis of surface outcrops, the main products of volcanism within the Olkaria Volcanic Complex (termed the Olkaria Volcanic Group) are alkali rhyolite (comendite) lava and pyroclastic rocks. Trachyte and basalt-hawaiite lava have been minor products, but widespread trachytic pyroclastics to the north-west, west and south-west of the complex are believed to have been erupted from vents. The Longonot volcano constitute the Longonot Volcanic Group which incorporates seven formations, the major ones are; the building of an early shield which is Represented by the Longonot Volcanic Formation-poorly exposed pyroclastics and lavas in boreholes; the Caldera formation, represented by the Kedong Valley Tuff Formation; the building of a pyroclastic and lava cone, represented by the Akira pumice. Other formations include the summit crate, accompanied by the Longonot Ash formation, the flank and crater floor lave eruption, represented by the Upper Trachyte Member (flanks) and the Upper Mixed Lava Member (crater), in which the Pyroclastics-ashes, agglomerates and tuffs make up a considerable proportion in the area, and it covers the whole volcanic plain (Clarke et al., 1990).

3.4. HYDROGEOLOGICAL SETTINGS

Flows toward lake Naivasha from the Mau escarpment and the Kinangop plateau are definite and some of the water from the western side of the rift eventually forms part of the discharges at Olkaria and Eburru.

Around the lake Naivasha, the groundwater level is between approximately 1880m and 1890m. The rise in groundwater contours, in the east and north parts indicate flow towards the lake, while the fall in contours to the south part, indicate groundwater flow away from the lake. This also explains why the lake is fresh despite the fact that it has no outlet and it lies in an area of high evaporation. The position of the lake at a culmination of the Rift floor, suggests flow both to the north and to the south. The southern flow from the Lake Naivasha is estimated to be between 27 $mcmyear^{-1}$ and 270 $mcmyear^{-1}$, and the shallow northerly flow from the lake is estimates to be 11 $mcmyear^{-1}$ and the deep flow to be 0.3 $mcmyear^{-1}$ (Clarke et al., 1990). (Ojiambo, 1996) indicated that lake Naivasha has a subsurface outflow of about 40 $mcmyear^{-1}$ from its eastern and south-western shores. The flow to the south was estimated to be between 50-90% of the total flow. The conclusion from the above analysis indicated that much of the subsurface outflow from the Lake catchment is towards the south.

There is a considerable local variation in permeability of rocks in the rift valley though this variability is less noticed. In most cases aquifers are found in fractured volcanics or along weathered contacts

between different lithological units. These aquifers are either normally confined to semi-confined associated with low storage coefficients. Areas where sediments are covering parts of the rift floor, mainly around Lake Naivasha, have aquifers with moderately high permeabilities. Such aquifers in most cases are unconfined and will always have high specific yields. Tectonic movements of the Rift valley have important effects on aquifer properties, both on a small scale by creating the local fracture systems, which comprise many aquifers, and on the large scale by forming regional hydraulic barriers or shatter zones of improved permeability.

The basin is drained by three rivers: Malewa, Gilgil and Karati Rivers. The floodplains of the two largest rivers, the Malewa and Gilgil, have a delta, which enters the lake from the north. Malewa, with an area of 1600 km^2, contributes about 80% of the discharge into lake Naivasha, Gigil, and Karati contribute the remaining percentage, with catchment areas of 527 km^2 and 149 km^2 respectively.

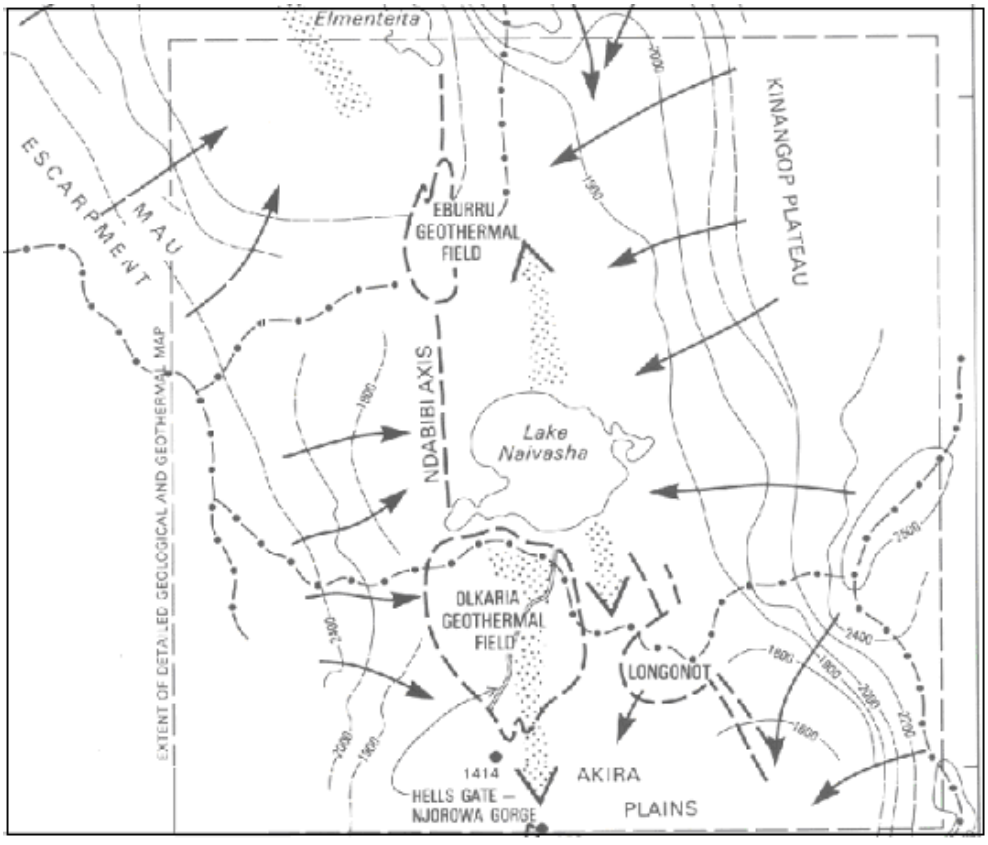

Figure 3.3: Structure and general groundwater flow direction in the study area (Clarke et al., 1990)

3.5. SOILS

Due to the prominent morphological and structural features developed from numerical episode, the area is characterised by volcanic rocks and Quaternary lacustrine deposits, which have contributed much on the distribution and properties of the soils around. Recent soil studies have been mainly car-

ried out in the southern part of the lake, which concentrated on mapping soil properties relevant for the proper management of the irrigated areas (figure 3.4)

The soils are mainly sediments of the former large lake, the origins of the basin deposits. The Lacustrine plain, have their soils developed on sediments mainly from volcanic ashes. They are divided into two sub-types, the first consists of well drained soils, with moderately deep to deep dark brown, friable and slightly smeary, fine gravely, sandy clay loam to sandy clay, with humic topsoil. The second sub- type consists of imperfectly drained soils, with moderately deep to deep, strong brown, mottled, firm and brittle, sandy clay to clay (Atkilt et al., 2001).

The soils of volcanic plain are developed on ashes and other pyroclastic rocks of recent volcanoes, they are also divided into two sub-types, the first one consists of excessive to well drained soils, with very deep to deep dark greyish brown to olive grey, stratified, calcareous loose fine sand to very friable sandy clay loam. The second consists of deep to very deep dark brown, friable, slightly gravelled, loam to clay, loam, with humic topsoil (Atkilt et al., 2001).

The content of the volcanic glasses, which are mainly obsidian, and ashes decrease as one goes from the high volcanic plain to the low Lacustrine plain.

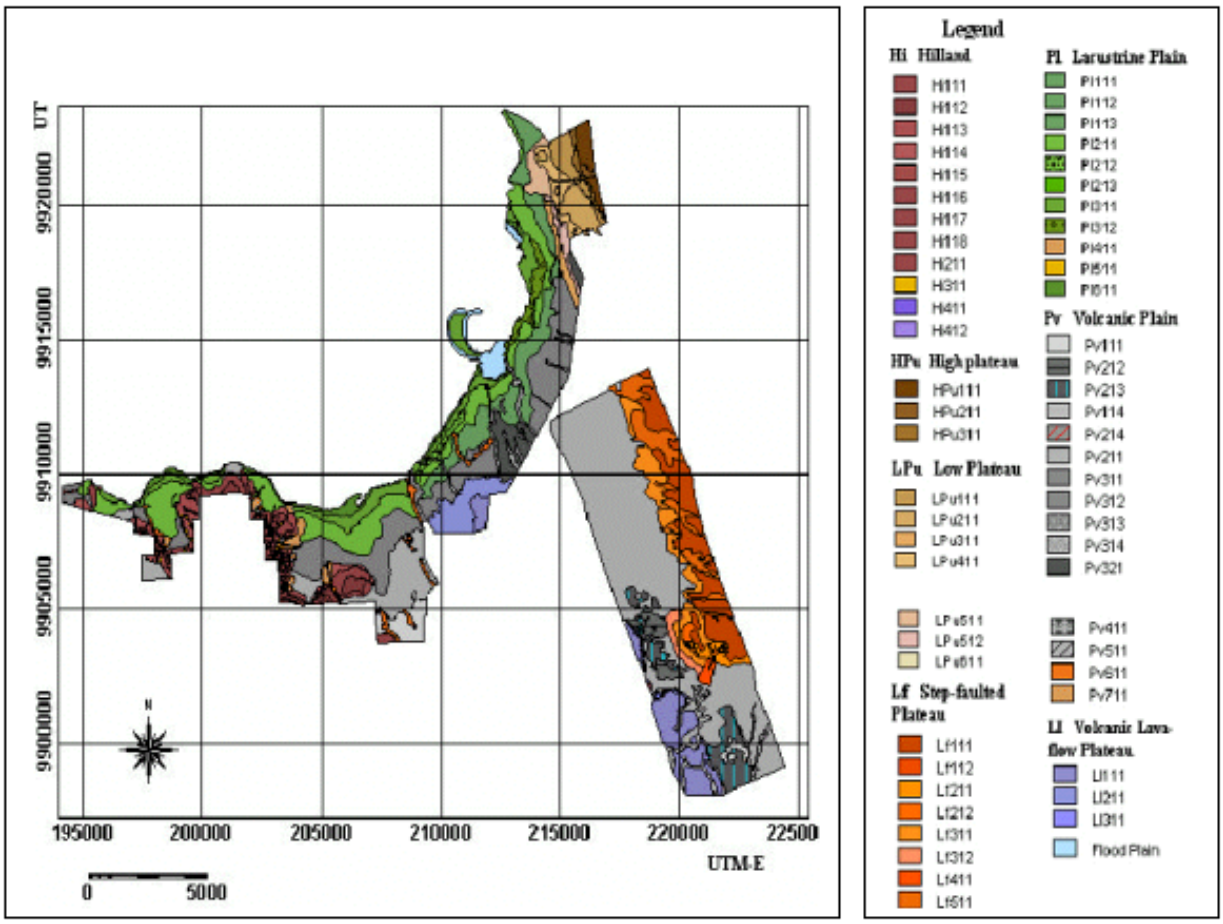

Figure 3.4: The Geopedological soil map-southern part of Lake Naivasha,(Atkilt et al., 2001). The full legend description, in Table 3.1

Table 3.1: Legend description of soil map- southern part of Lake Naivasha

LANDSCAPE	RELIEF	PARENT MATERIAL	LANDFORM	SOILS
VOLCANIC PLAIN (PV)	Slightly undulating lava flow Pv 1	Akira Pumice and Alluvial deposits Pv 11	Tread Pv 111	Andic Xerochrepts
	Long Ridges Pv 2	Akira Pumice and Alluvial deposits Pv 21	Raised ridge Pv 211	Lithic Xerorthents
	Excessive slightly dissected plain Pv 3	Lower Longonot mixed Basalt/Trachyte lava flows and Pyroclastic cones Pv 31	Tread Pv 311	Andic Xerorthents
LACUSTRINE PLAIN (PL)	High Terrace PL 1	Lacustrine Sediments PL 11	Tread PL 111	Typic Haploxeralfs
			Riser PL 112	Typic Haploxeralfs
	Middle Terrace PL 2	Lacustrine Sediments PL 22	Tread PL 222	Typic Eutrochrepts
			Riser PL 223	Typic Xerochrepts; Loamy over clay
	Low Terrace PL 3	Lacustrine Sediments PL 33	Undulating Tread PL 331	Typic Xerochrepts; Clayey over sandy
			Almost level Tread	Typic Xerorthents

3.6. LANDUSE AND LANDCOVER

Agriculture is the main activity carried out in areas around the Lake. This includes irrigated crop farming. Flower farming, is the major one, its products are exported to both European and American countries. Other crops such as vegetables, cabbages and fruits, are grown mainly for local consumption. Dairy farming is also practised mainly on large estates on the shores of the lake.

The wetland around the shores of the lake is dominated by papyrus swamps and other parts which are a bit far from the lake are occupied by natural vegetations, mainly grassland, acacia, and shrub.

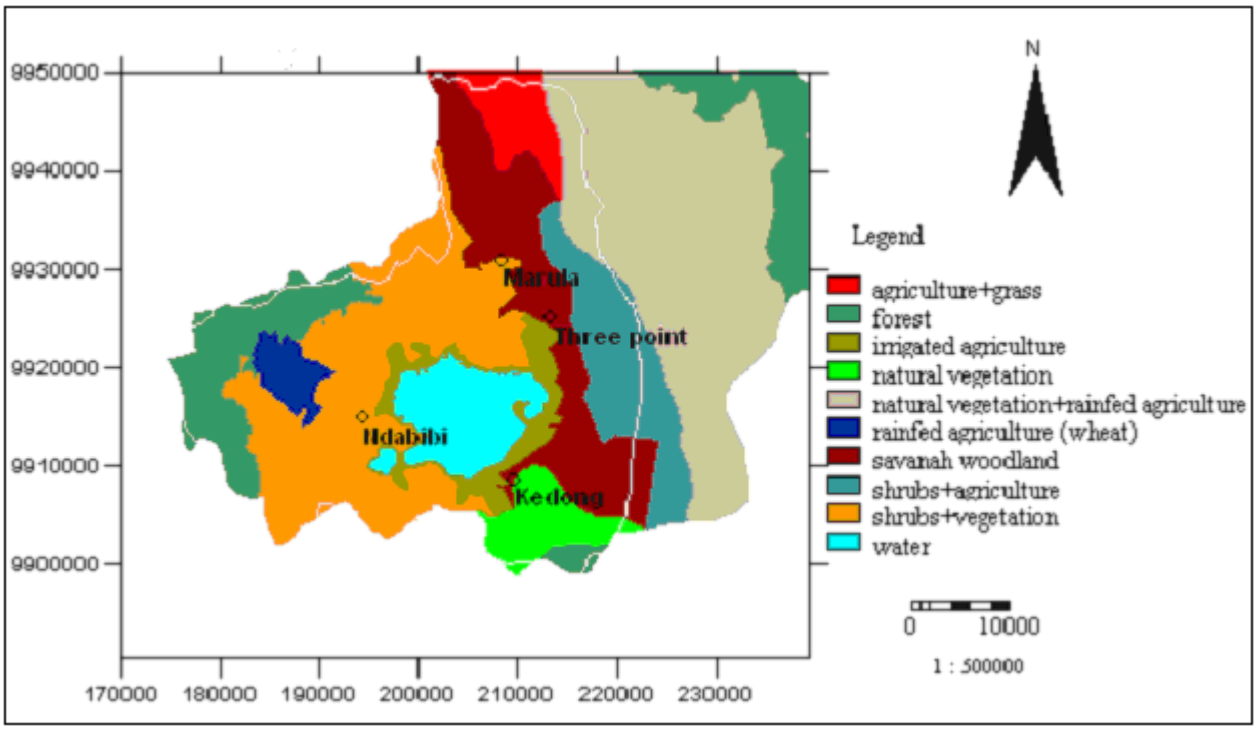

Figure 3.5: Landuse map with site areas

3.7. CLIMATE

The basin experiences a semi-arid climate. Rainfall is the most important climatic element in this area. Rainfall is concentrated into two main seasons; the main rain season is between March and May and the short rain season is between October and November. Rainfall is a function of topography; high rain is received along the Mau and Aberdare escarpments, with an average ranging from 1250-1500 mm annually. In the valley areas, including Lake Naivasha area, an average of 650 mm, is received. The monthly potential evapotranspiration on the floor of the basin exceeds the rainfall by a factor of 2 to 8 for every month except April when the potential evaporation still exceeds rainfall. The average maximum daily temperature in the Rift valley varies between 9^{o}C at night to 25 ^{0}C during the day. The winds are general calm in the morning while in the afternoons they can attain a speed of 11-15 kmhr^{-1}. They are strongest in the months of August to October, with a speed of 21 kmhr^{-1}. Their direction is from the southeast and northwest depending on the season. Extremely strong winds have been reported to occur through the window between the Longonot and Kijabe Hill (Ataya, 2000). The area experiences a relative humidity of less than 75%.

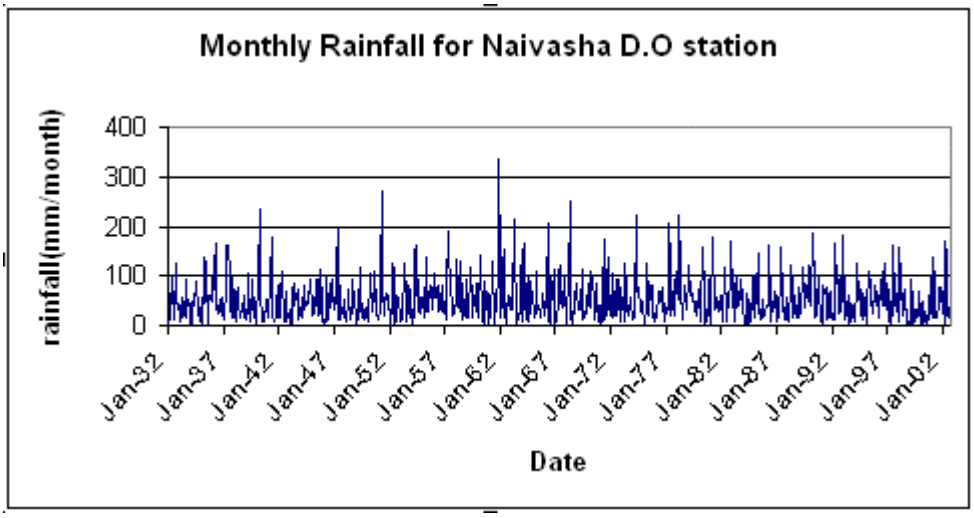

Figure 3.6: Monthly Rainfall for Naivasha between year 1932 and 2002

3.8. GROUNDWATER FLOW

Lake Naivasha is unique among the East Africa Rift Valley lakes in that it is fresh. It has no outlet and yet the water budget of the lake to a large extent depends on groundwater flow to and from the lake. This suggests that there exist an underground outlet, which caters for the groundwater flow. This is also evidenced from previous studies of chemistry of the lake. High conductivity zones are predicted by very high yielding wells in close areas of very low yielding wells or totally dry wells (Nabide, 2002).

The piezometric contour map shows a depression on the north-eastern side of the study area. This is due to constant abstraction of water from that part. Further abstraction from the well fields will result to increased hydraulic gradient in the direction from the lake to the field well. The lack of isotopic signature in the well field is due to the fact that the depression in the well field is a recent event; time is not enough for water to emigrate from the Lake to the well field.

Further more, on the north side of Lake Naivasha, deep wells (91 m) have water which is equal or less than 20 years old. Water from these wells has stable isotopic values resembling those of nearby rivers, and high-elevation eastern Rift water. This indicates that this water recharges from rains from high eastern Rift Valley escarpments. Many of the shallow wells on the south side of the lake have ages between four and 17 years. The young ages and the Oxygen-enriched signature of the water from these wells indicate that they are recharged by a mixture of water from the lake, Rift flanks, and water from deep pumping wells that is recharged during irrigation. Water mixing ratio calculations using isotopes show that about 50% to 70% of the southern ground water system is derived from the lake, while the

Olkaria geothermal reservoir water shows that 40% to 50% of this water is originally lake water. Estimated horizontal velocity from age dating between Lake Naivasha and a well about 3 km to the south is 75 myr^{-1}, giving average horizontal hydraulic conductivity of 6 $mday^{-1}$ (Ojiambo et al., 2001).

3.9. DESCRIPTION OF THE FIELD WORK AREA

The study area was based on four locations; the natural areas around Kedong Ranch, Ndabibi, Three Point, and Marula Farms, all constrained around the lake aquifer (figure 3.5)

Table 3.2: Location sites for the study area

Location of natural area	UTM-X	UTM-Y
Kedong	209691	9908544
Ndabibi	194490	9914863
Three Point	213403	9924948
Marula	208444	9930840

4. METHODOLOGY

4.1. PRE-FIELD WORK

Pre-field mainly involved review of the existing literature of the study area based on ITC database and Internet. The following information on Naivasha basin was compiled: Meteorological data, Topographical data, Data on irrigated areas (Dung, 2001, Chisakuta, 2002), Land cover information, Soil data (Siderius, 1980, Kwacha, 1998, Ataya, 2000, Tilaye, 2001) and Isotopic data, from 1996 to 2001.

4.2. FIELDWORK

4.2.1. Field measurements and Experimental techniques

After literature review of the study area, fieldwork was conducted for three weeks, that is, between 9th September and 3rd October on four study areas (figure 3.5).

Table 4.1: Parameters determined for recharge estimates and the technique applied.

Parameters	Technique
Soil moisture content (cm3/cm3)	Hand-auger and Theta Probe
Saturated hydraulic conductivity (cm/day)	Inverse augering
Soil texture	Hand feel
Vegetation rooting depth	Hole-digging around acacia tree track using Spades and Shovel
Layer thickness	Hand augering from field
Sample collection for Particle size, organic per-centages and stable isotopic analysis	Hand-auger

Hand augering was conducted up to depths below the rooting zones of grass. Samples for each layer were collected, sealed and transported to ITC laboratory for analysis.

Unsaturated soil samples for isotopic analysis were collected at depths of 2m, 4m, and below the rooting zone for each of the four the study locations. Two groundwater samples from Kihoto boreholes in Naivasha town were also collected for the same analysis. Tightly sealed in polythene bags, for the case of soil samples and water bottles for the groundwater samples, were transported to Austria, at ARC Seibersdorf Research, from where the analysis was conducted.

4.3. POST FIELDWORK

This phase involves processing of the data, both from literature and field. On addition to the Laboratory analysis, other analyses were carried out using ILWIS, a geo-information system software; Excel spread sheet and SWAP (Soil-Water-Atmosphere-Plant) modelling.

Particle Size And Organic Matter Analysis

Particle size analysis is the separation of soil into various size fractions and determination of the proportional of these fractions. Four main types of soils were analysed, sand, silt and clay. Fine earth material was obtained with a 2mm sieve. To each 20grams portion a solution of Hydrogen peroxide was added continuously to remove organic substances. After overnight shaking the suspension with a dispersing agent on an end-over-end shaker of about 30 prm, sand was separated from clay and silt with a 50μm sieve. The clay and silt fractions were determined by pipette method. Then the aliquot for the three samples, sand, silt and clay were fractionated by overnight oven drying under temperature of 105^0C. Sand (50-2000μm), silt (2-50μm) and clay (<2μm) fractions were determined.

Organic Matter analysis was carried out following the Walkley-Black procedure. This involves a wet combustion of the organic matter with a mixture of potassium dichromate and sulphuric acid at about 125^0C. The residual is then titrated against ferrous sulphate. The empirical correction factor *1.3* is applied in the calculation of the result.

The carbon content of the soil was obtained by the equation:

$$\%C = Mx\frac{V1 - V2}{s}x0.39xmcf \qquad \textbf{(4.1)}$$

Where;

M= molarity of ferrous sulphate solution (from blank titration)

V1= millilitre ferrous sulphate solution required blank

V2 = millilitre ferrous sulphate solution required for the sample

s = weight of air-dry sample in grams

0.39 = $3x10^{-3}$x100% x1.3, where 3 is the equivalent weight of carbon

mcf = moisture correction factor

1.3= is the compensation factor for the incomplete combustion of the organic matter in this procedure.

And multiplying the above results with empirical factor 2 does the conversion of % carbon to % organic matter:

$$\% \text{ Organic matter} = 2 \text{ X } \% \text{ carbon} \quad \textbf{(4.2)}$$

4.4. FRAMEWORK FOR ENTIRE RESEARCH

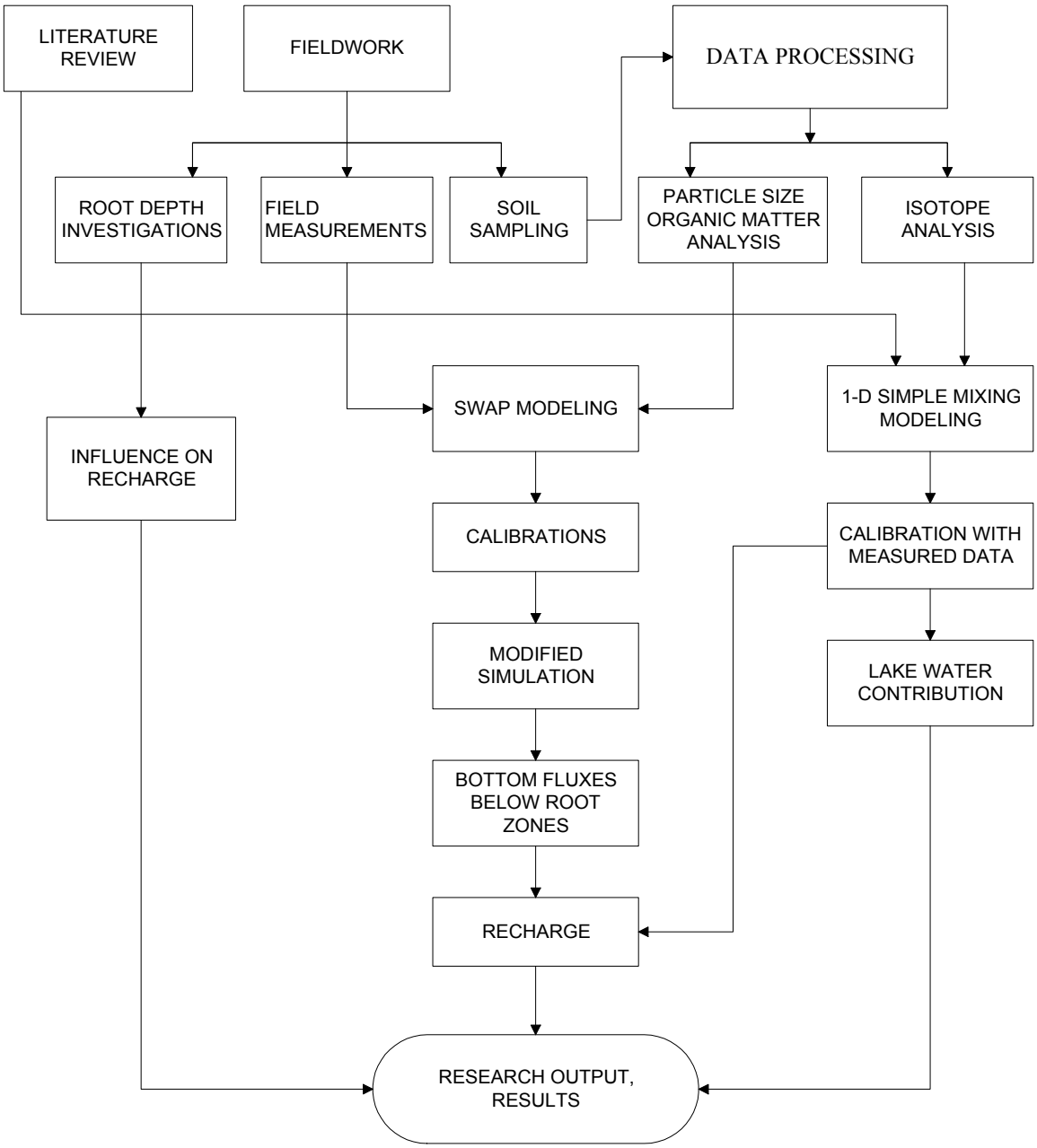

5. ANALYSIS

5.1. INITIAL FIELD CONDITIONS AND INFILTRATION TESTS ANALYSIS

5.1.1. The Initial soil moisture conditions for the study area

In figure 5.1 illustrate initial soil moisture content of the four locations, as a function of depth.

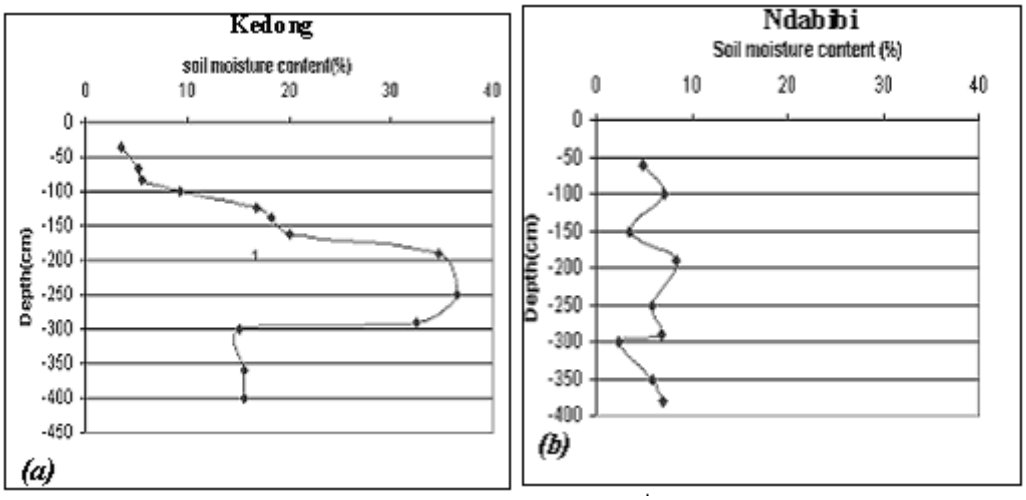

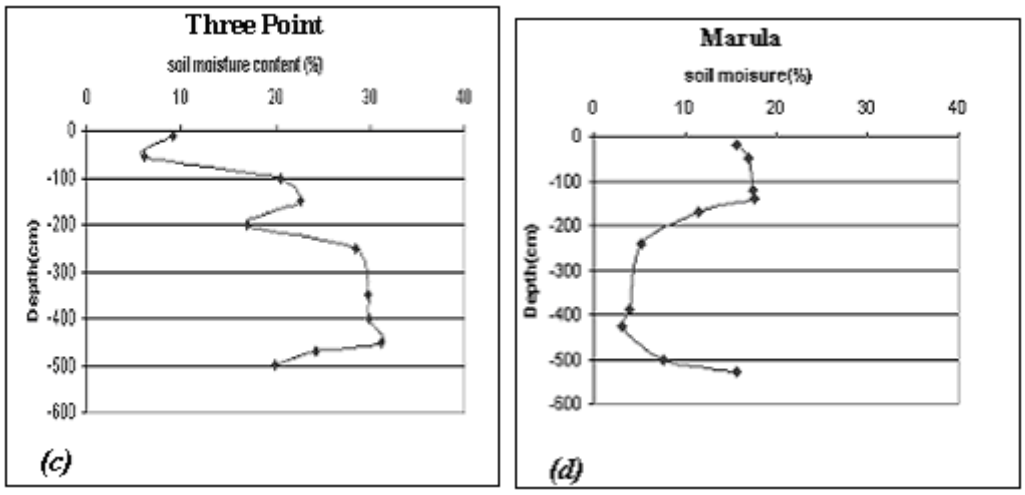

Figure 5.1: The initial soil moisture graphs (a-d) for the four field locations

5.1.2. Saturated hydraulic conductivity, K (sat)

These were conducted in situ using Inverse auger-hole method. Auger holes were made to a given depth in soils above the water table. The $K_{(sat)}$ was determined for each separate layer. At each location, a hole with a known diameter was dug and filled with water, up to a required depth. The draw down ***h'(ti)*** of the water level at each time step, were measured with the help of a stopwatch and measuring tape and recorded consecutively. The water level, ***h(ti)*** was obtained by subtracting ***h'(ti)*** from the total depth (Landon, 1984).

From the data obtained from inverse auger-hole method, ***Log (h(ti)+d/2)*** was plotted against the time. In the beginning the line curves, which later becomes a straight line, when the soil gets saturated. From the slope **ε** of this straight part, saturated conductivity (K_{hsat}) was calculated using the equation:

$$K_{(sat)} = 1.15 * r * \log \varepsilon \qquad \textbf{(4.0)}$$

Where ***r*** is the radius of the augered hole.

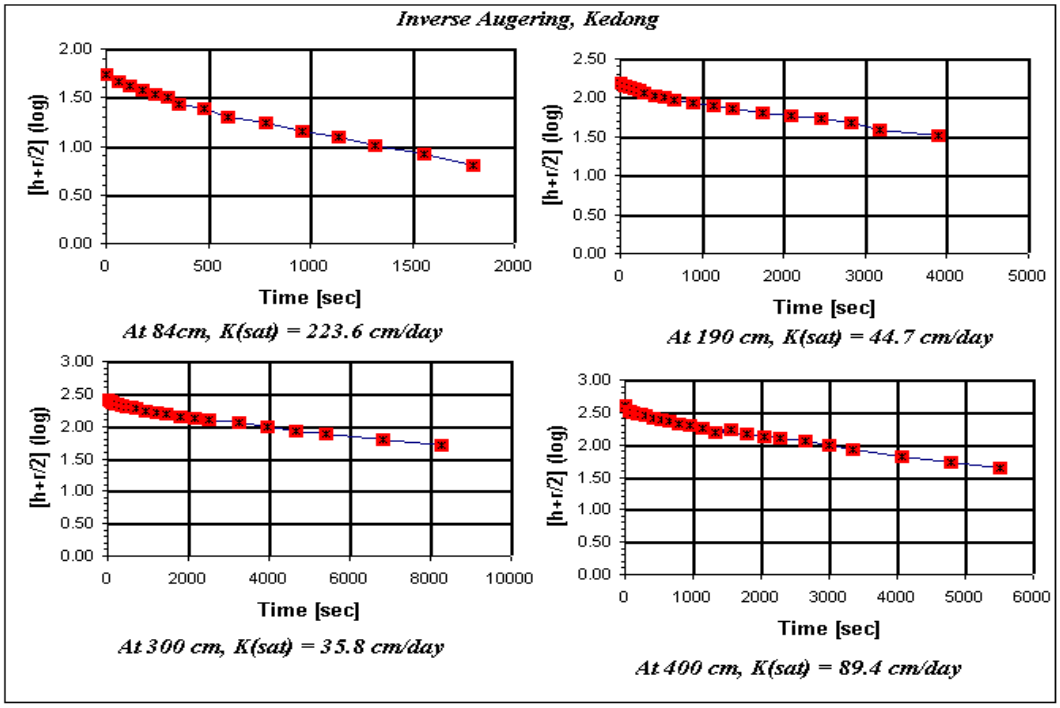

Figure 5.2: Saturated hydraulic conductivities, Kedong area.

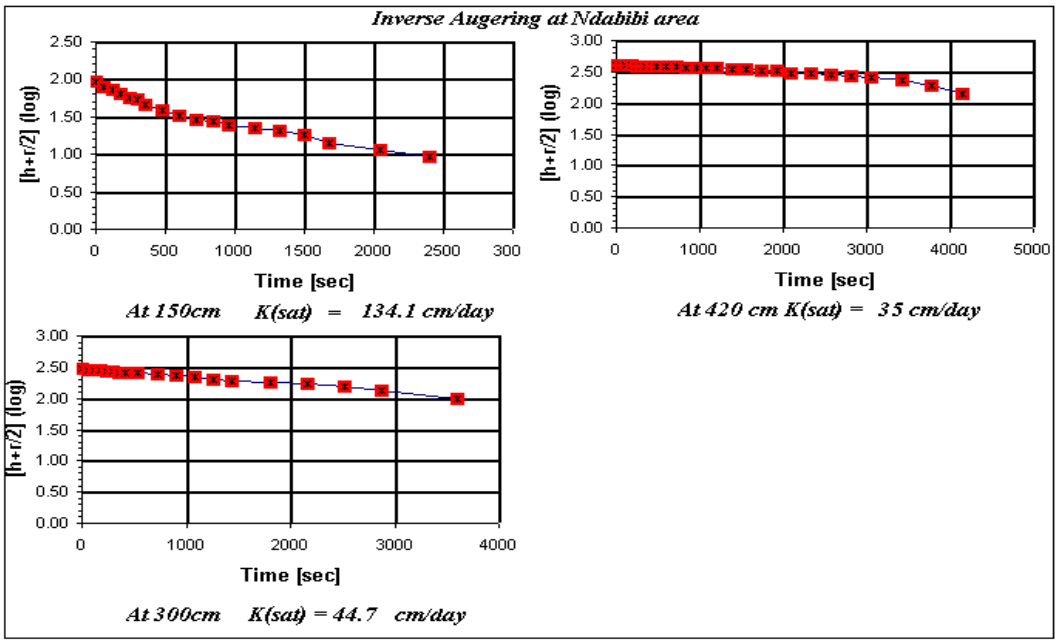

Figure 5.3: Saturated hydraulic conductivities, Ndabibi area.

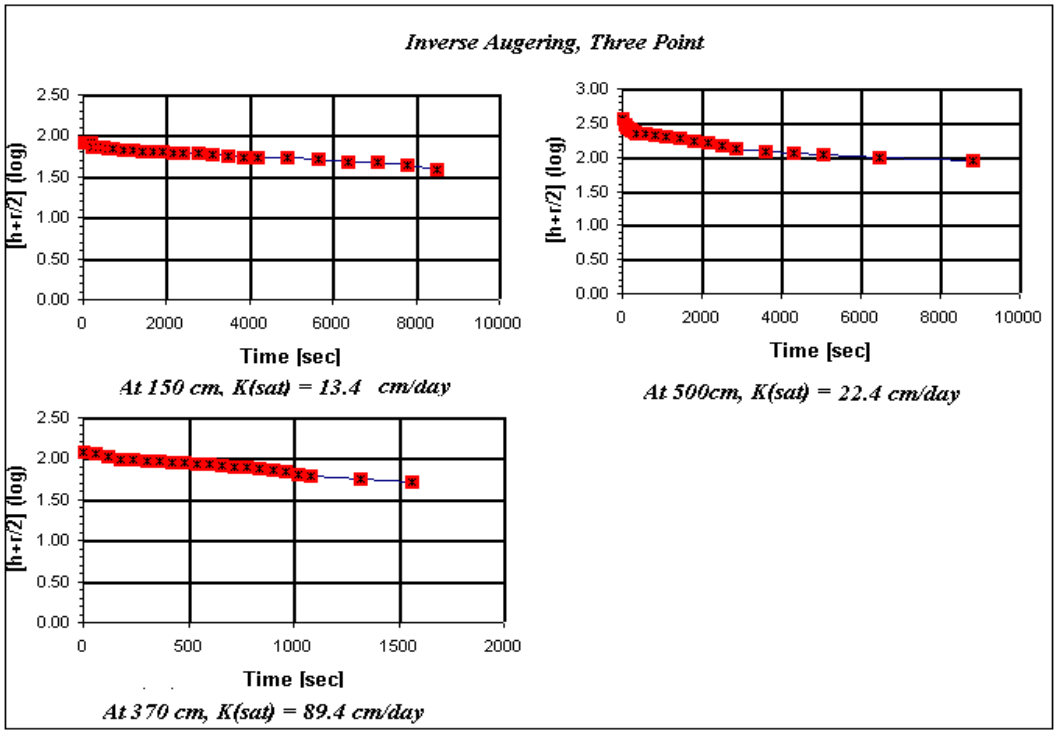

Figure 5.4: Saturated hydraulic conductivities, Three Point area

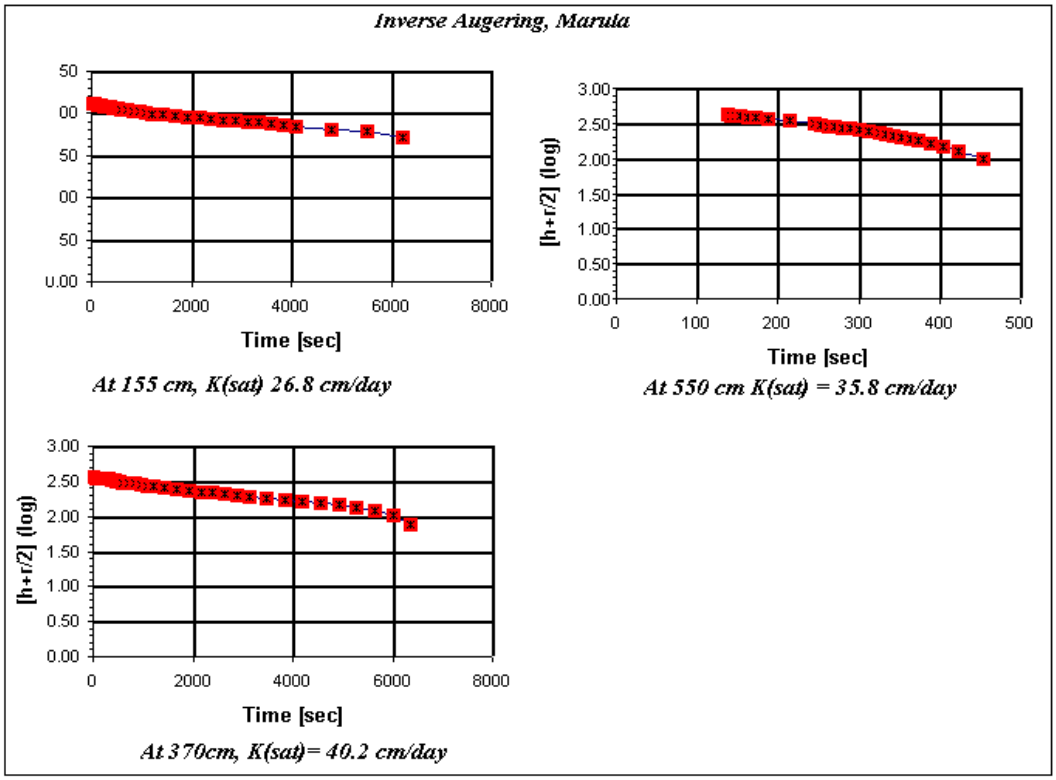

Figure 5.5: Saturated hydraulic conductivities, Marula area.

Table 5.1: Summary of Saturated hydraulic conductivities for the four locations at various depths

Location	Depth (cm)	$K_{(sat)}$ ($cmday^{-1}$)
Kedong	84	223.6
	190	44.7
	300	35.8
	400	89.4
Ndabibi	150	134.1
	300	35.0
	420	44.7
Three Point	150	13.4
	370	22.4
	500	89.4
Marula	155	26.8
	370	35.8
	550	40.2

5.1.3. Infiltration Tests results

In figures 5.6-5.9, illustrate soil moisture content as a function of depth from the four infiltration tests, including the initial conditions, prior to the test.

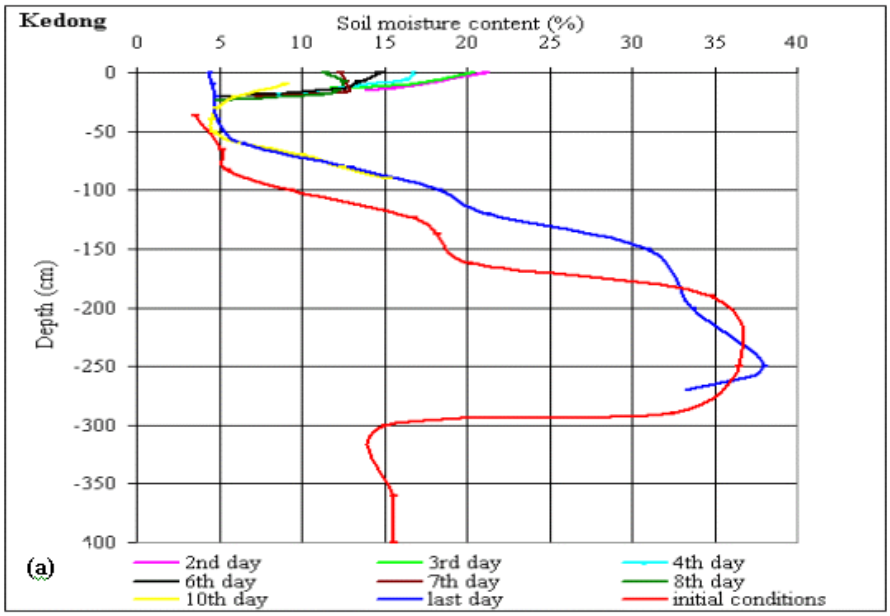

Figure 5.6: Infiltration tests with initial conditions, Kedong area.

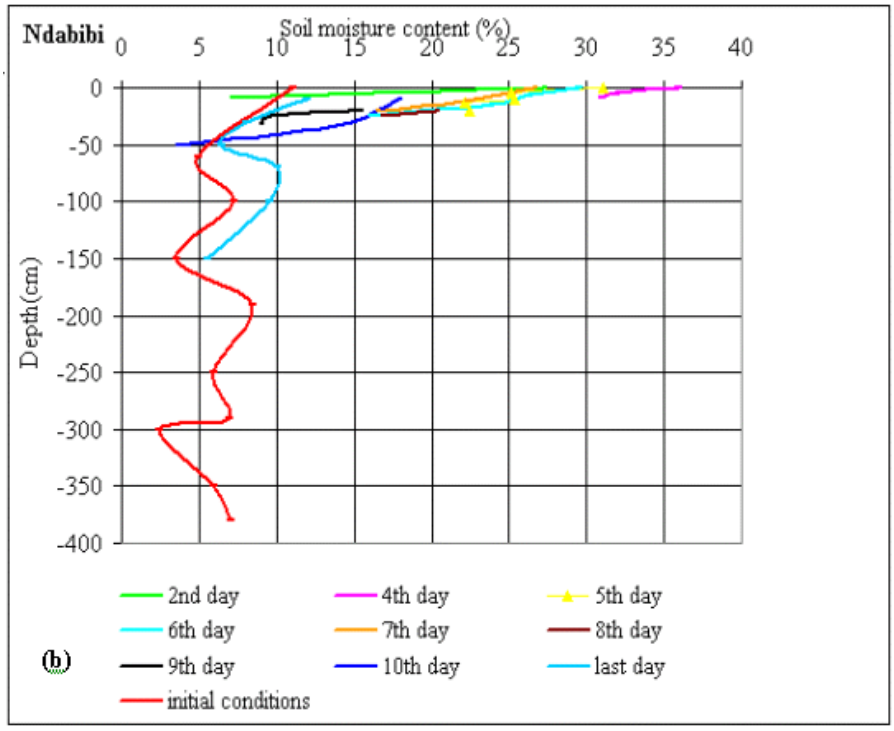

Figure 5.7: Infiltration tests with initial conditions, Ndabibi area.

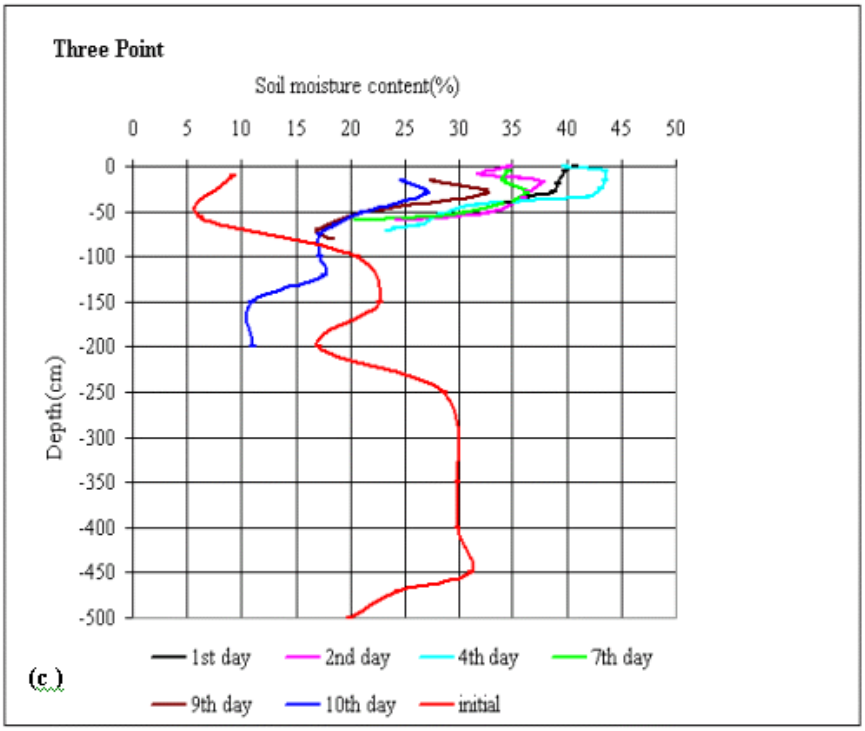

Figure 5.8: Infiltration tests with initial conditions, Three Point area.

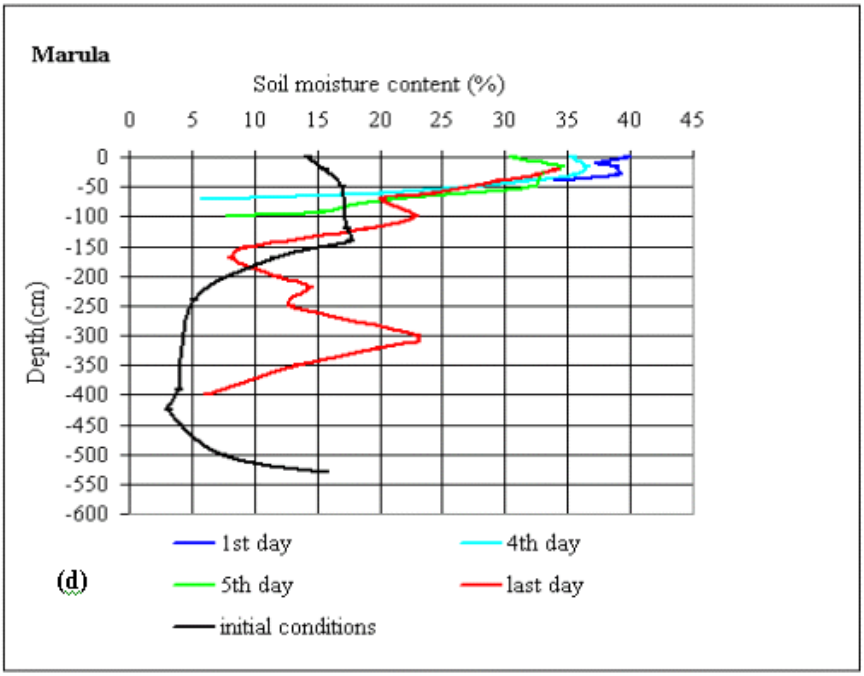

Figure 5.9: Infiltration tests with initial conditions, Marula area.

5.2. SWAP MODELLING IN ESTIMATION OF DIRECT RECHARGE

SWAP model caters for both surface and soil factors, influencing the soil movement in unsaturated zones. It simulates vertical transport of water, and subtracts what goes out in form of interception evaporation, transpiration, from what goes in form of rainfall, and comes up with change in storage and extra water. This is assumed to be the potential recharge if the simulation is below the rooting depth.

5.2.1. Model Set Up

The daily rainfall data for the eight years, was obtained from the regression analysis was carried out on six meteorological stations located in the vicinities of the four study areas. Table 5.2 and figure 5.10 display the locations of stations.

Table 5.2: Rainfall stations, used in recharge estimates

Station	Name	ID	UTM-X	UTM-Y
Kedong	Naivasha D.O	9036002	214315	9920714
	Naivasha W.D.D	9036281	216173	9918872
Three point and Marula	Naivasha Marula	9036109	208742	9928088
	Naivasha K.C.C	9036073	208743	9926243
Ndabibi	Naivasha Kongoni Farm	9036062	195758	9909639

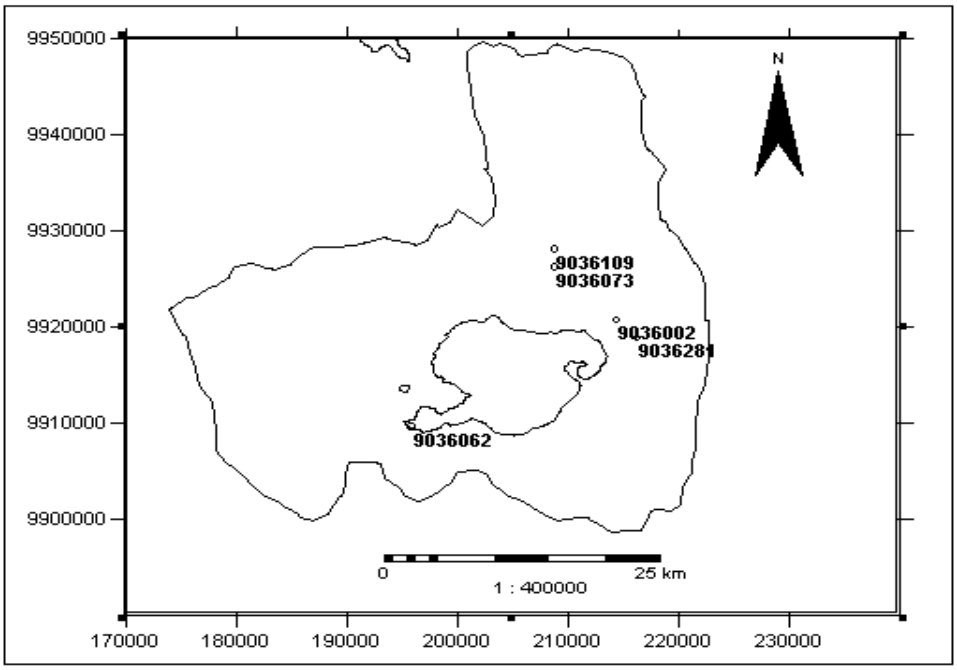

Figure 5.10: Rainfall stations

Each profile was divided into layers according to the soil types and bottom compartments were assigned to each. The first compartments, near the surface, were set to a thickness of one centimetre, for easy calculation of top boundary fluxes. A maximum of 40 compartments was allowed for each soil profile. Table 5.3, displays the total length and number of layers for each location, with maximum rooting depth set at 1000 cm. A simple crop model was used, where the potential evapotranspiration (ET_o) is calculated using actual evapotranspiration (ET_{ref}) and the crop factor is as per FAO manual 56, (Allen et al., 1998).

Table 5.3: The geometry of soil profiles used in the model

Location	Total length (cm)	Number of layers
Kedong	560	5
Ndabibi	402	4
Three Point	500	4
Marula	555	5

The bottom boundary, located in the unsaturated zone, is set to free drainage. The drainage can only occur if the pressure heads in the last bottom compartments increases above zero. The soil hydraulic properties were obtained from the soil particle and organic matter properties analysed from the Laboratory (appendix 5), together with the analytical expressions of Van Genuchten (1980) and Mualem (1976) using Pedotransfer function. The initial pressure heads were estimated from the initial soil moisture curves (figure 5.1).

The model was run for eight years. During the first periods, the conditions were too wet, and it took sometime, approximately three years for the simulation to stabilise. So the final pressure heads were used as initial pressure heads and the simulation was repeated. Figures 5.11 and 5.12 below illustrate the results.

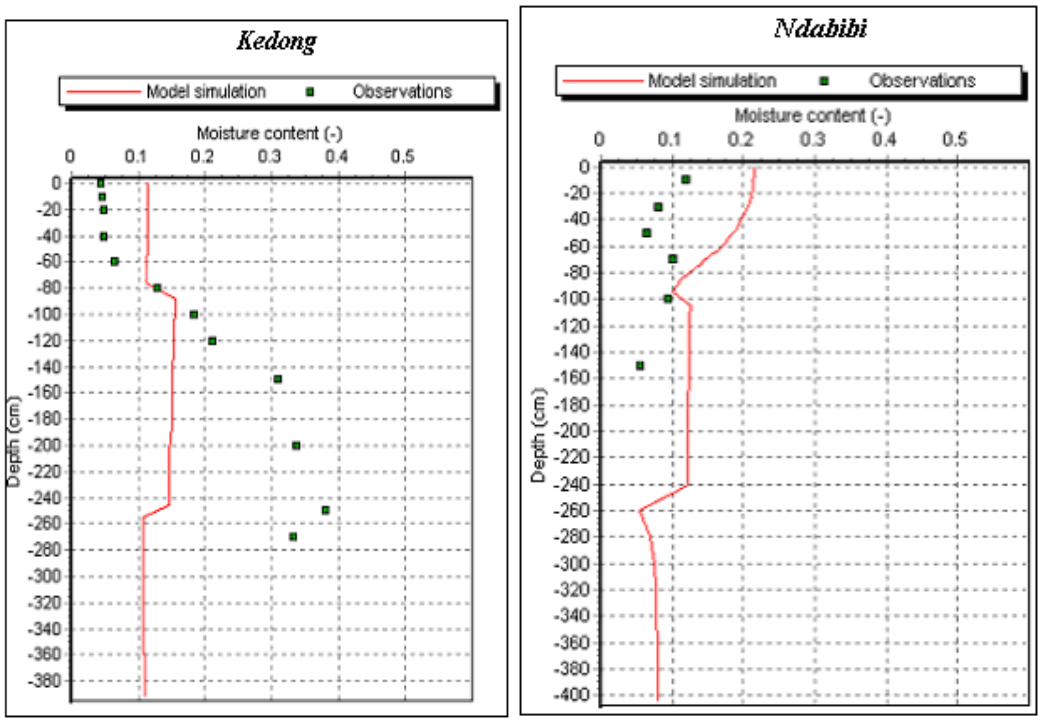

Figure 5.11: Field measurements and model simulation, Kedong and Ndabibi areas

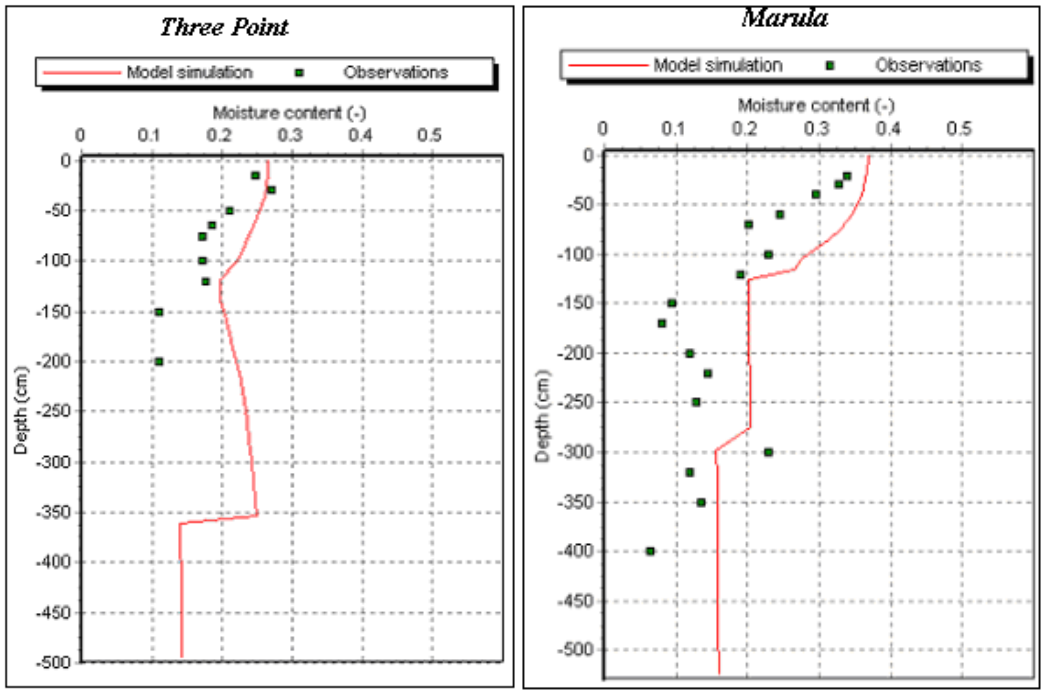

Figure 5.12: Field measurements and model simulation, Three Point and Marula areas

The soil moisture curves of the simulated model were not in match with initial soil moisture obtained from field measurements (figure5.1).

5.2.2. Infiltration Tests

These tests were carried out from 15th September to 30th September 2002. The last rain received during this period was on 29th of August, before the beginning of fieldwork. For the entire fieldwork, no rain-fall occurred. This time is generally dry, with little rainfall.

Using a locally made filtering can, the soil was fully wetted to some centimetres below, and covered with a sheet of polythene to reduce the evaporative losses to a minimum. Soil moisture contents were taken at successive depths, every 24 hours, for a number of days until the soil moisture profiles stabi-lised. Table 5.4 shows the amount of application together with the length for each test.

Figure 5.13: The infiltration tests procedures during fieldwork, Kedong area.

Table 5.4: Artificial rain in form of infiltration tests to the four location studies

Location	Amount of water applied	Date of application	Last day of measurements
Kedong	30 mm	15/09/02	26/09/02
Ndabibi	1st application, 30mm	16/09/02	
	2nd application, 50mm	19/09/02	30/09/02
Three Point	100 mm	18/09/02	30/09/02
Marula	100 mm	21/09/02	30/09/02

Another simulation was conducted basing on both soil moisture curves before and after the infiltration tests. The tests were conducted towards the end of each simulation in the month September. All the

rain days between the day of 29th August and 30th September 1998, were excluded from the simulation and applied the amount of water used during infiltration for each location. The actual reference evaporation is set to zero since there is no evapotranspiration-taking place. At the end of the run, the soil moisture curves, before and after the tests were not in match with those simulated from the model, (figures 5.14 - 5.16) display the results.

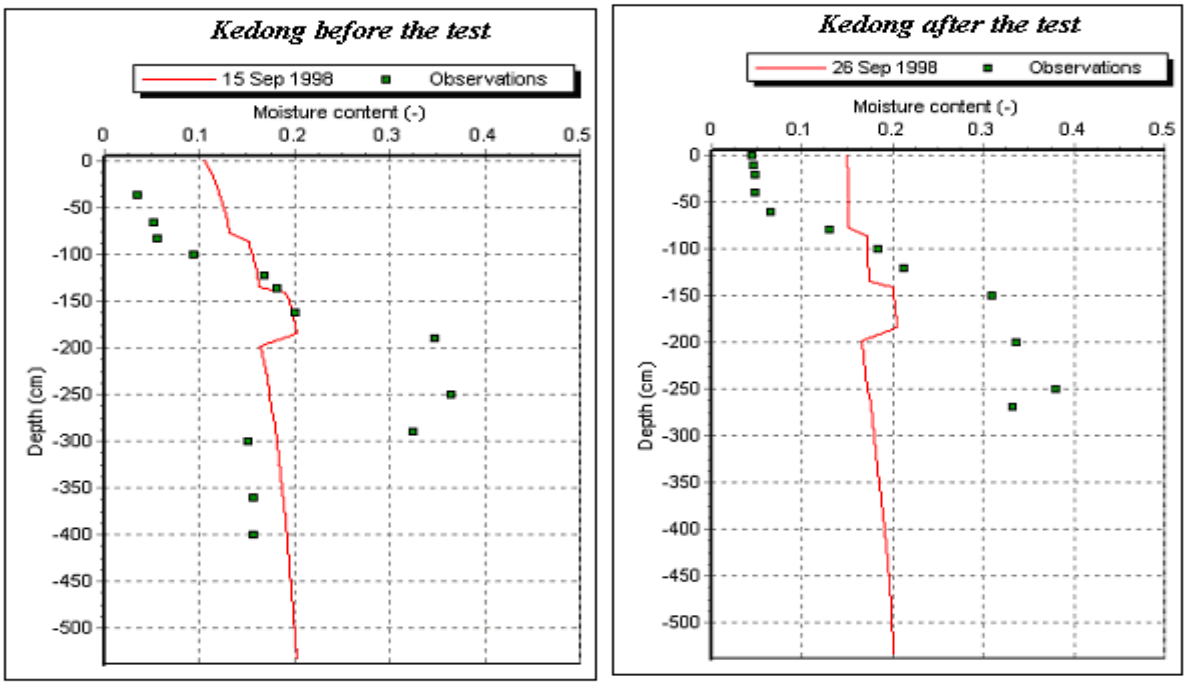

Figure 5.14: Field measurements and model simulation before and after infiltration, Kedong area.

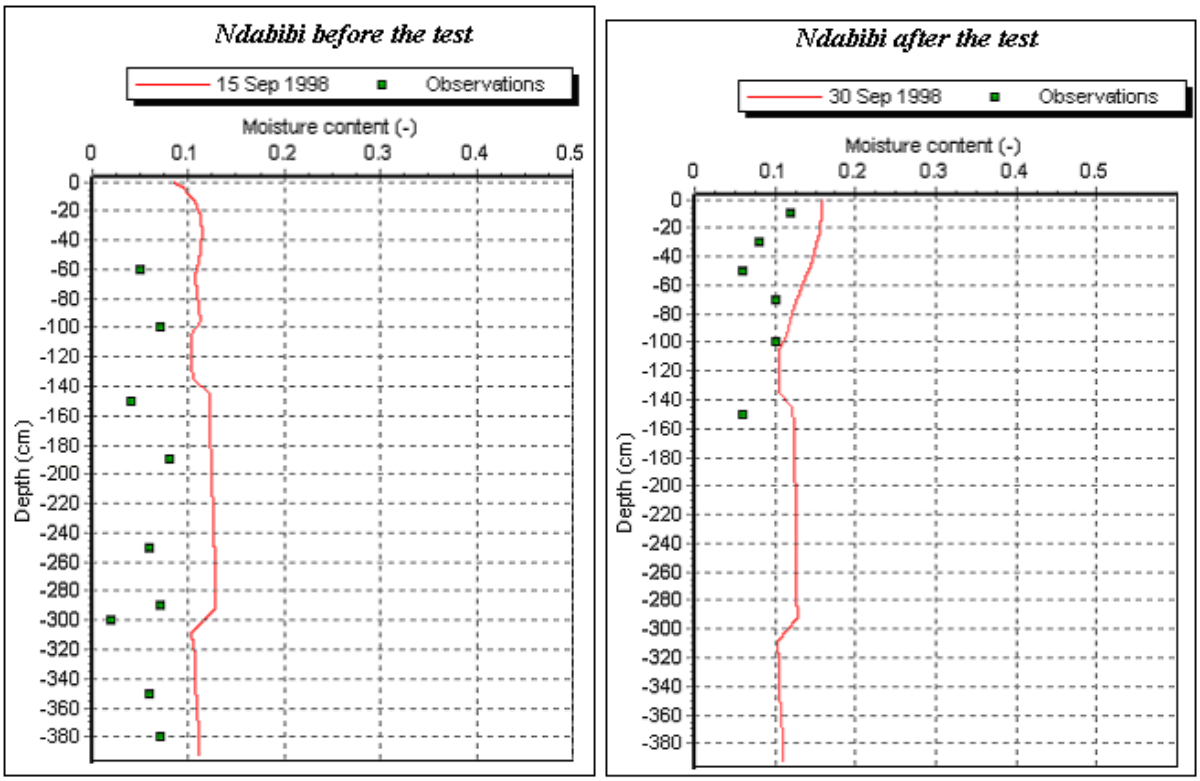

Figure 5.15: Field measurements and model simulation before and after infiltration, Ndabibi area.

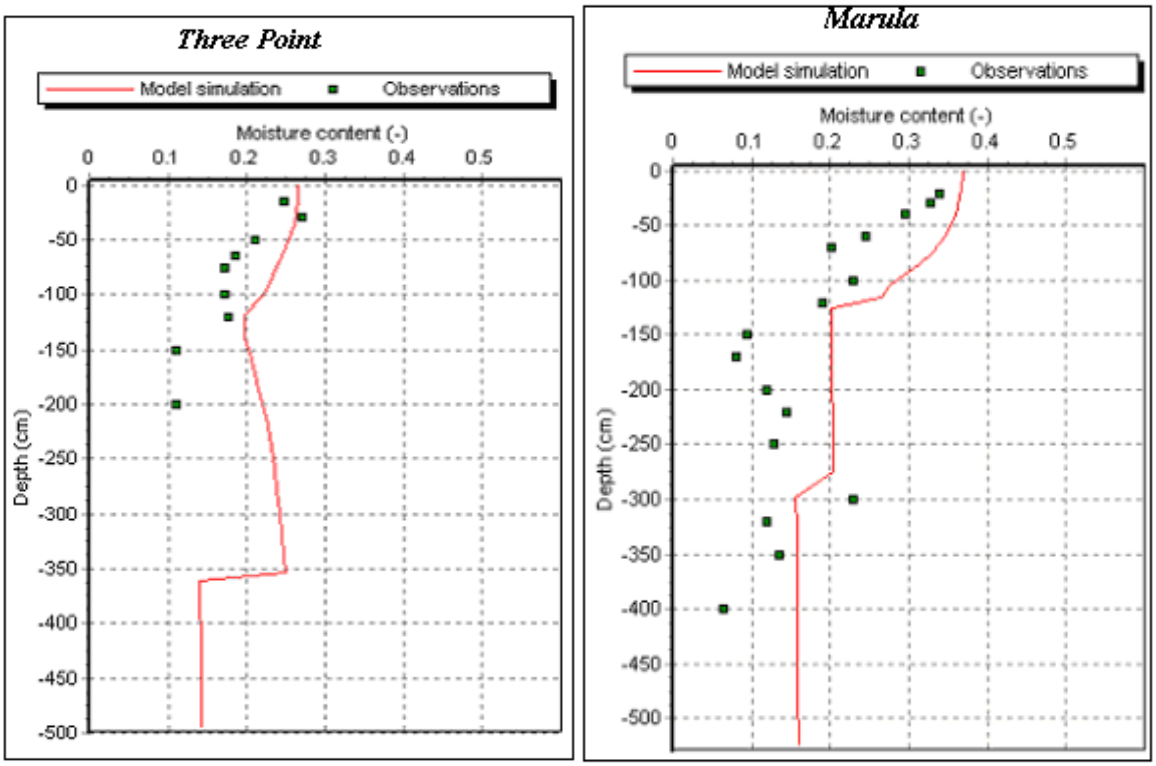

Figure 5.16: Field measurements and model simulation after infiltration, Three Point and Marula areas.

Application of soil particle size and organic matter properties analysed from the laboratory do not simulate the actual conditions in field. The model either exaggerates or limits the hydraulic properties of the soil.

5.2.3. Calibration of infiltration measurements

Calibration of infiltration measurements in the above model was conducted by applying some modification on the soil hydraulic properties. Alteration of soil hydraulic properties was performed basing on the initial soil moisture and saturated hydraulic conductivity measurements conducted from field along with the soil hydraulic properties given by Carsel and Parish, (1988) given in SWAP manual Figure 5.17 and 5.19, display the calibrated soil moisture profiles before and after infiltration tests.

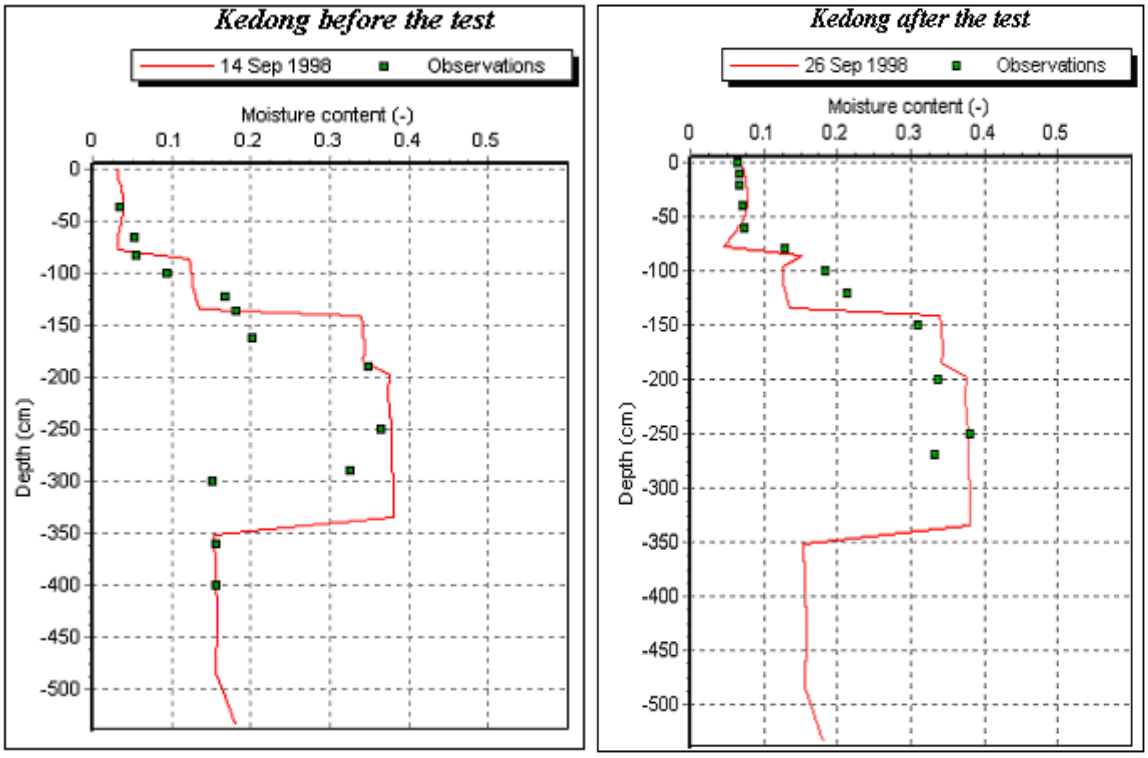

Figure 5.17: Field measurements and model simulation before and after infiltration test, Kedong area.

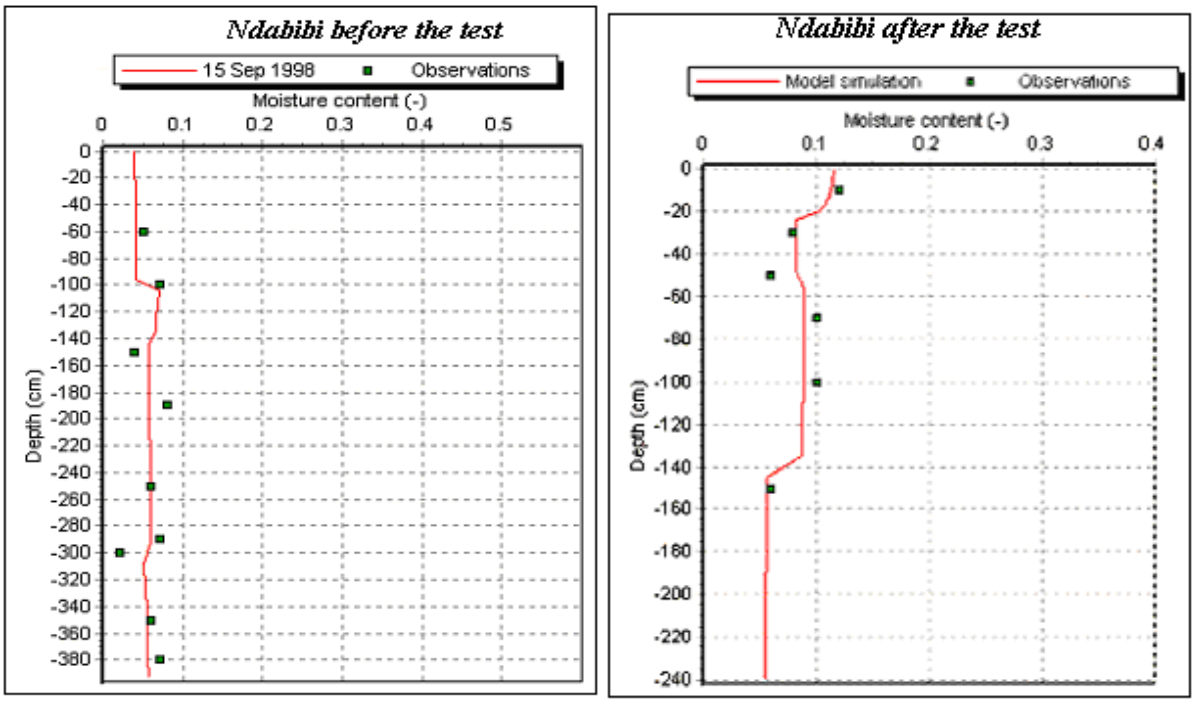

Figure 5.18: Field measurements and model simulation before and after infiltration test, Ndabibi area.

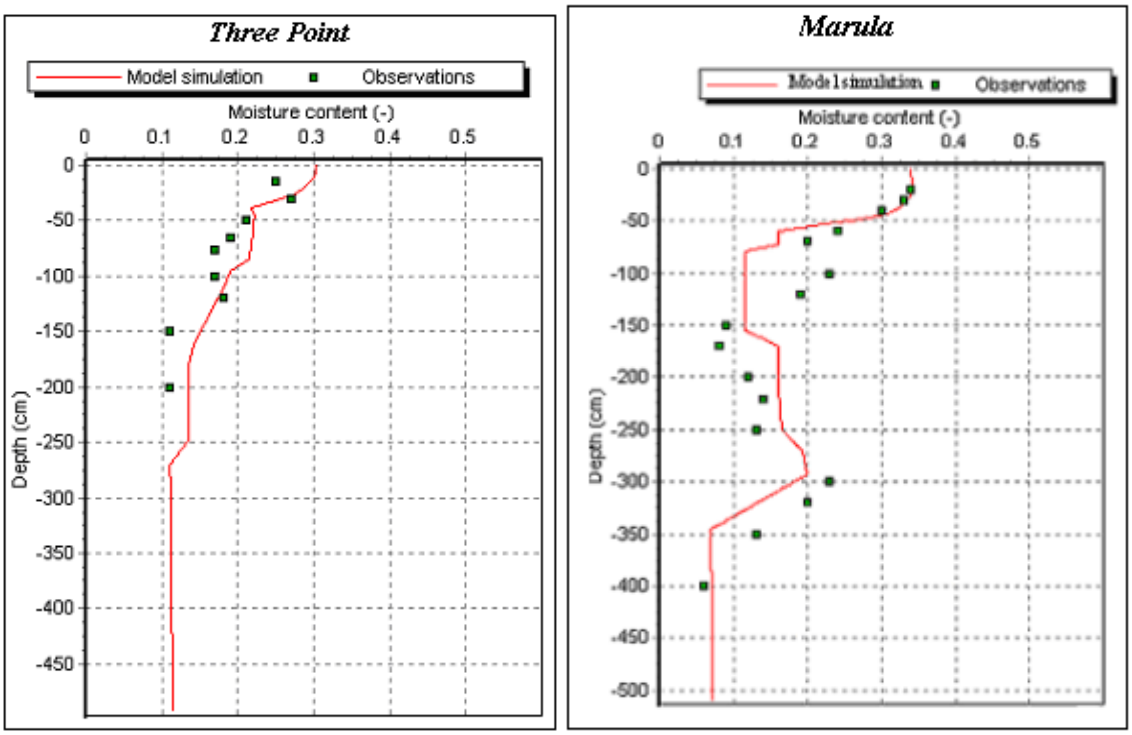

Figure 5.19: Field measurements and model simulation after infiltration test, Three Point and Marula

5.2.4. Bottom flux calculations from the modified Model

Assuming that the model has calibrated the actual conditions of the study area, the above modification was maintained. Excluding the infiltration tests, the bottom fluxes were simulated for eight years. Since the boundary conditions were set to lysimeter with free outflow, the drainage will only occur if the pressure head in the bottom compartment increase above zero. It is observed that the soil layers take sometime to reach field capacity, which limits the bottom flux movement at the boundary. Due to this limitation, the bottom fluxes are estimated from a level, one meter above the bottom boundary. Figures 5.20 to 5.23 illustrate the distribution of bottom fluxes before and after El Nino period, and tables 5.5and 5.6 display the results for each location.

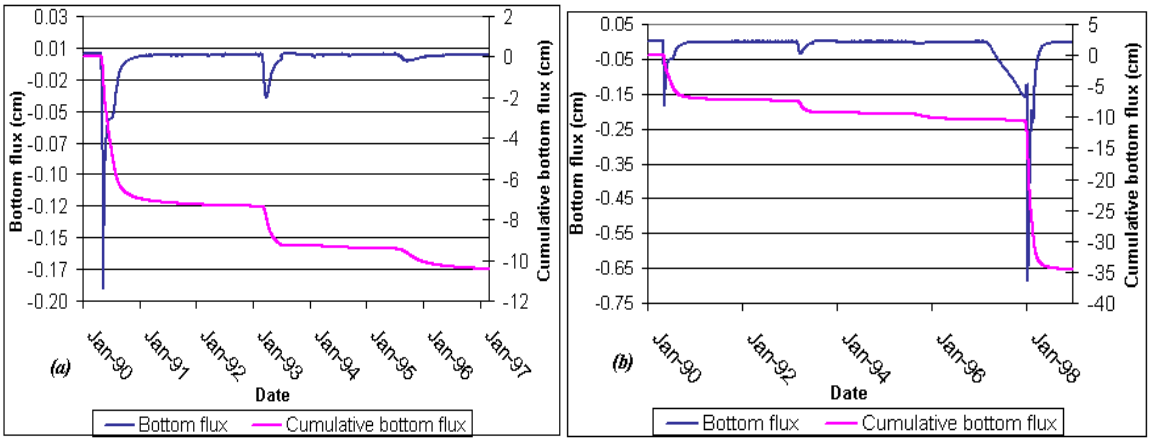

Figure 5.20: Bottom fluxes at depth of 500 cm before (a) and after (b) El Nino Kedong area.

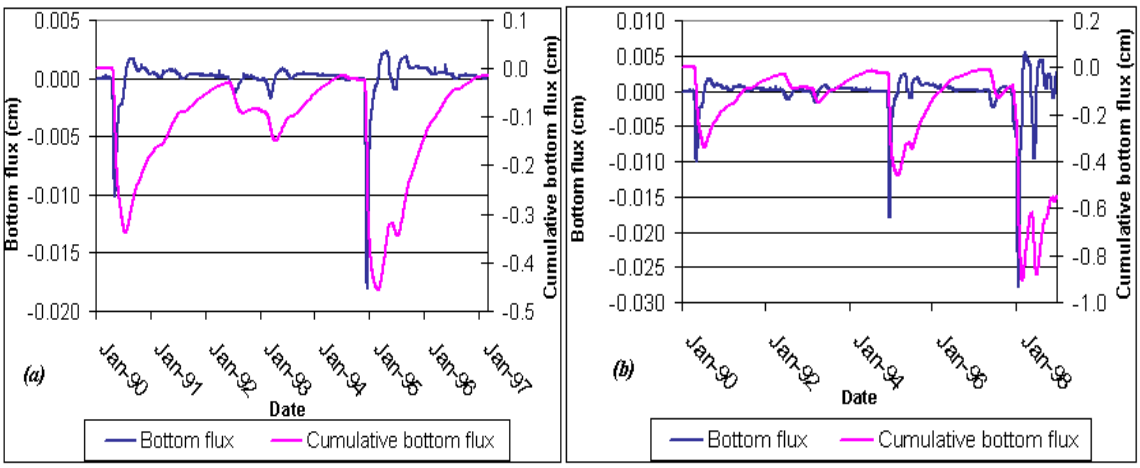

Figure 5.21: Bottom fluxes at depth of 400cm before (a) and after (b) El Nino Ndabibi area.

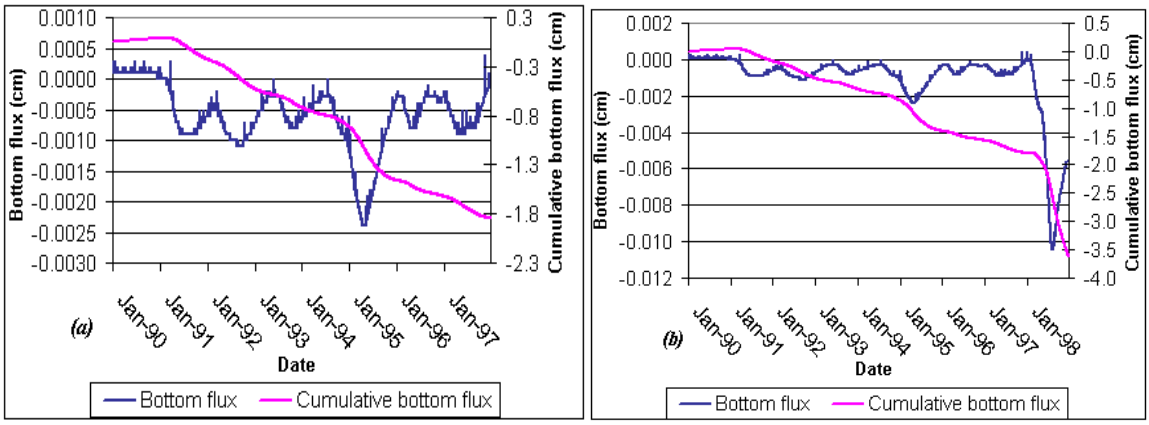

Figure 5.22: Bottom fluxes at depth of 400cm before (a) and after (b) El Nino, Three Point area.

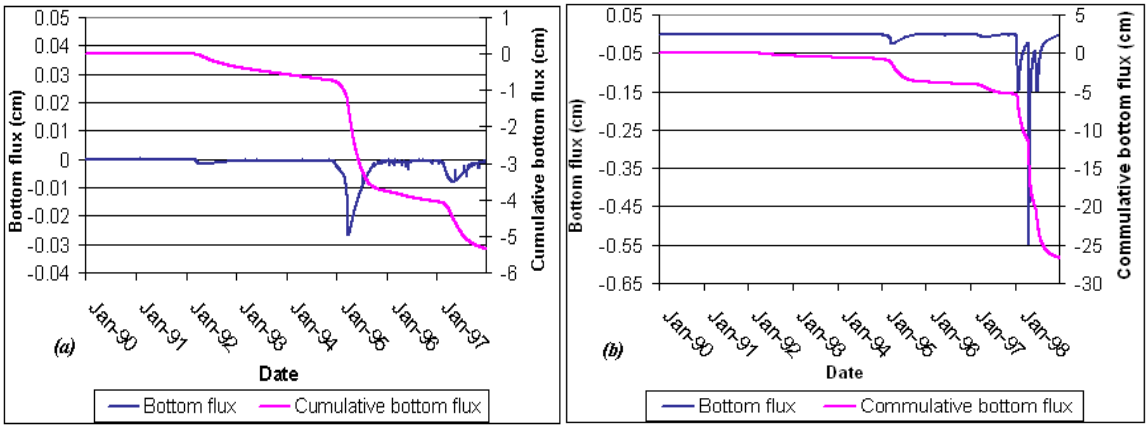

Figure 5.23: Bottom fluxes at depth of 450cm before (a) and after (b) El Nino, Marula area.

5.2.5. Interpretation of results

Since the bottom fluxes are simulated from depths below the rooting zones, it is assumed that these fluxes reach the water table. The average water table in the study area is between 20 and 30 meters deep. For the bottom fluxes to reach this level will depend on the recession period.

Table 5.5: The recharge received before the El Nino (1990-1997).

Location	Recharge ($mmday^{-1}$)	Total recharge (1990-1997) (mm)	Average re-charge ($mmyear^{-1}$)
Kedong	0 – 1.90	100	14.29
Ndabibi	0 – 0.18	0.2	0.03
Three Point	0 – 0.024	18	2.57
Marula	0 – 0.28	52	7.43

Table 5.6: The recharge received after the El Nino (1990-1998).

Location	Recharge ($mmday^{-1}$)	Total recharge (1990-1998) (mm)	Average recharge ($mmyear^{-1}$)
Kedong	0 – 7.00	350	43.75
Ndabibi	0 – 0.27	5.5	0.69
Three Point	0 – 0.10	35	4.38
Marula	0 – 5.50	270	33.75

There was an occurrence of El Nino in the year 1998. During this period the areas received an extraordinary amount of rainfall, which resulted into an increase in downward movement of bottom fluxes.
From the graphs it is clearly indicated that Kedong and Marula received the highest recharge, during the seven years. This is probably due to pumice formation in these two areas, which allows easy infiltration of water during rainy seasons. Additionally, Kedong area gets the highest recharge compared with the other due to the type of vegetation around. The widest part of the area is covered with savannah type of grassland with shrubs and scattered trees. High evapotranspiration do occur only during rain seasons when the grass is green, and this is catered for by rainfall. During dry seasons, low evapotranspiration takes place since the grass at this time is dry, and unable to transpire. Little evapotranspiration can only occur from some scattered trees like acacia, which are always green even during dry periods.
On daily basis, the natural area of Ndabibi receives more than Three-Point. This is probably due high intensity of rainfall received in the area, which leads to high rate of downward movement of water flux during rainy season. The pumice type of soil formation in the upper layer of the area also contributes to the easy infiltration. Ndabibi ends up receiving the lowest recharge per year due to evapotranspiration from trees during dry seasons. This is indicated by the intensive upward movement of water fluxes (figure 5.21). This is caused by evapotranspiration from the dense vegetation around, especially from acacia trees, which dominate the area. Since water takes some time to reach the water table, depending on the recession period, trees trap these water fluxes on its way down, towards the water table.

The natural area around Three-Point farm, on the other hand, receives low recharge on the daily basis, but due to lack of thick vegetation, a high percentage of the water fluxes infiltrate in the deeper parts, and it is assumed to reach the water table.
The year 1998 was quite different from the rest of seven years. It was year of floods caused by an extraordinary amount of rainfall. The area received a big rise in bottom fluxes, which resulted in a big increase in recharge, mostly in areas with no limitations of water movement towards the water table.

5.2.6. Limitations of the model

SWAP model allows for three options of input files from crop calendar, that is; the simple crop, detailed crop and detailed grass model. Due to lack of parameters for the detailed grass crop model, a simple crop model was used. The natural grass of the study area is permanent through the year, with a cycle of 366 days. Three different types of grass in terms of crops had to be created in the simple crop model to represent the grass cycles. These cycles were marked by the beginning and end of rainy seasons. During dry seasons, the grass dries up, but it remains covering the soil surface. In this condition it cannot expire since the leaves are completely dry. Simple crop model does not account for this. It assumes that during dry seasons, when crops are being harvested, the soils are bare, and evaporation do occur due to lack of soil cover. It simulates the actual soil evaporation rates in terms of soil water flux, the maximum soil water flux occurring when there is maximum dryness of the soil.

Further The study area consists of different land cover types, but the modelling was restricted to only grass, introduction of trees causes confusion since both grassland and trees behave differently during rain and dry seasons.

The model works by Darcy, law equation (2.1) as the change in soil moisture content ($\partial\theta$) becomes smaller, numerical problems develop in the software. The soil moisture becomes constant in all the compartments. And this affects the water movements and hence the bottom fluxes.

5.3. ISOTOPIC ANALYSIS OF DEUTERIUM AND OXYGEN-18 ISOTOPES

Data processing for isotopic analysis

Each sample was extracted in a vacuum under at temperature of 180^0C for a period of five hours. Results illustrated in table 5.7 below.

Table 5.7: Isotopic analysis for δ18O and δ2H from both unsaturated and saturated zones.

Location	Sample number	Depth (cm)	$\delta^{18}O$ of sample (‰)	$\delta^{2}O$ of sample (‰)
Unsaturated zone				
Kedong: Utm-X: 211875 Utm-Y: 99044706 Altitude: 2009 masl	ST1 KD1	50	-1.02	-27.9
	ST1 KD2	150	-2.18	-23.1
	ST1 KD3	450	-3.03	-17.7
Ndabibi: Utm-X: 194432 Utm-Y: 9914858 Altitude: 1958 masl	ST3 NDA1	78	-1.10	-24.1
	ST3 NDA2	172	-2.44	-27.7
	ST3 NDA3	350	-1.42	-21.1
Three Point: Utm-X: 213398 Utm-Y: 9924946 Altitude: 1940 masl	ST4 3PT1	80	-2.76	-23.0
	ST4 3PT2	210	-3.20	-14.1
	ST4 3PT3	460	-3.78	-26.7
Marula: Utm-X: 208448 Utm-Y: 9930834 Altitude: 1928masl	ST5 MRu 1	72	-2.97	-29.1
	ST5 MRu 2	180	-2.88	-27.0
	ST5 MRu 3	440	-2.80	-23.6
Saturated zone				
Kihoto BH1: Utm-X: 214125 Utm-Y: 9919894 Altitude: 1865masl	K1	Groundwater level	3.21	23
Kihoto BH1: Utm-X: 214125 Utm-Y: 9919894 Altitude: 1865masl	K2	Groundwater level	3.78	25.5

The isotopic composition for unsaturated zone in Kedong, Ndabibi and Three point areas decrease with increase in depth. There is generally a high isotopic enrichment of soil moisture at the top layers of the profiles, which is attributed to direct atmospheric Evaporation. Water uptake by roots is not selective on the isotopic compositions; hence has no effect on their variation with depth.

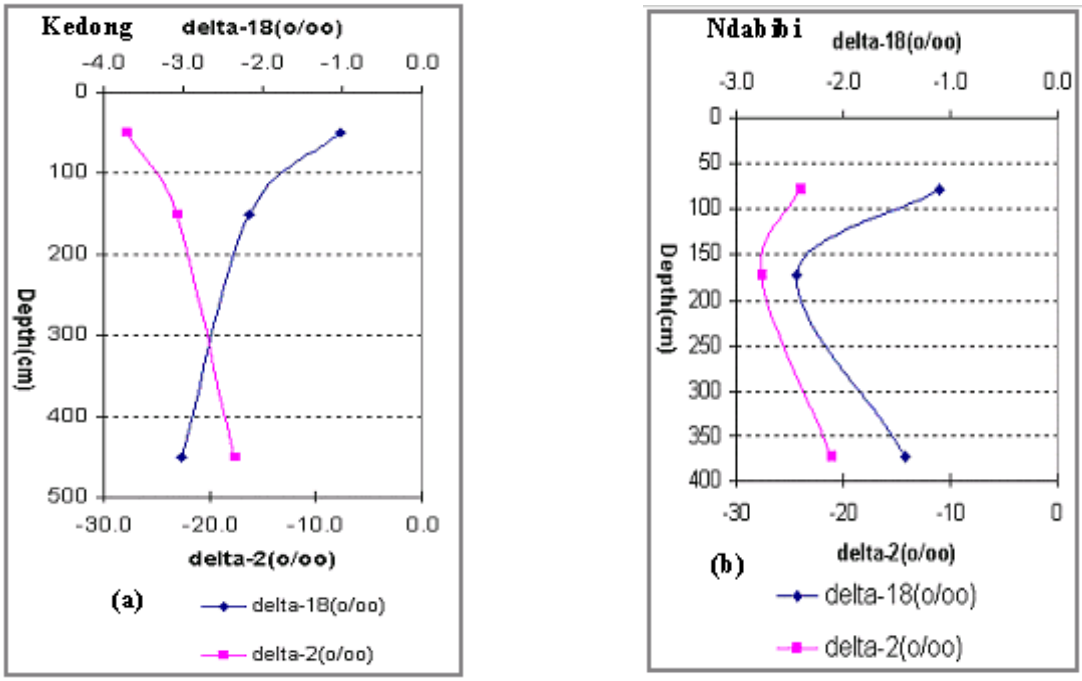

Figure 5.24: Variation in isotopic composition with depth, Kedong and Ndabibi

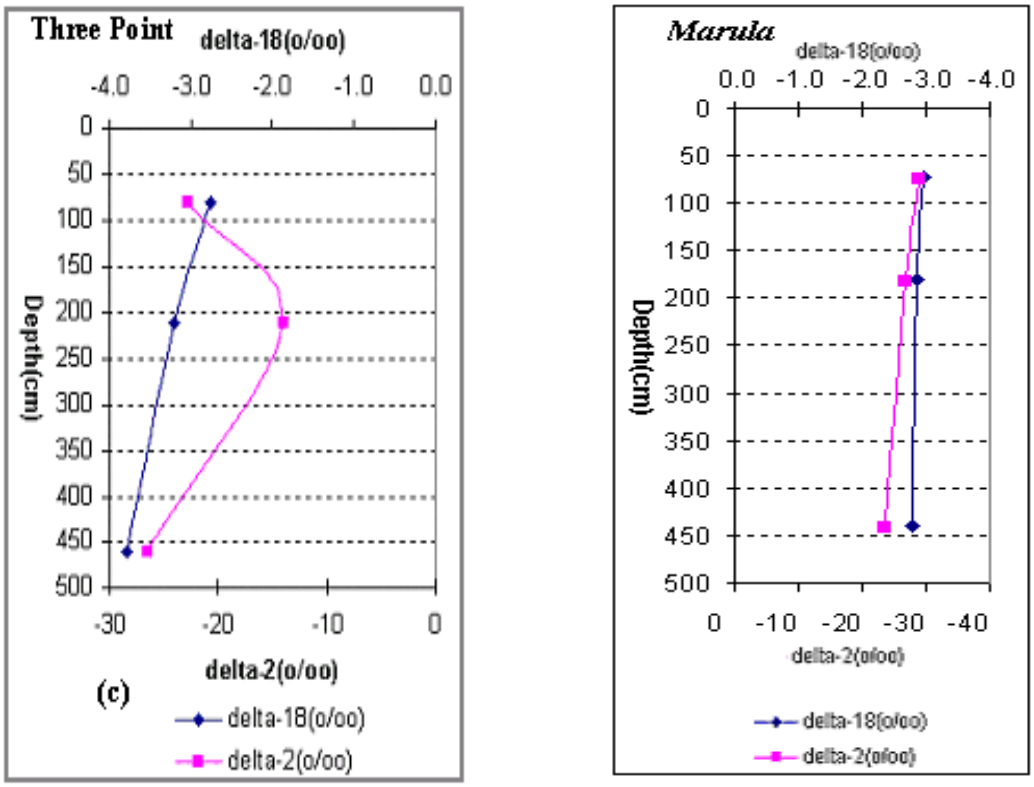

Figure 5.25: Variation in isotopic composition with depth, Three Point and Marula

According to previous studies the isotopic composition of Marula and 3 Point Farm BHM (appendix 10) signifies that these boreholes have their source of recharge from precipitation and river Malewa (Oppong-Boateng, 2001). This is also confirmed from the isotopic composition of unsaturated zone of Marula ($\delta^{18}O$ = -2.80 $^{o}/_{oo}$, $\delta 2H$ = -23.6 $^{o}/_{oo}$) and Three Point ($\delta^{18}O$ = -3.78 $^{o}/_{oo}$, $\delta^{2}H$ = -26.7 $^{o}/_{oo}$) which are a mixed of river Malewa and rain.

The constant profile in the isotopic composition of Marula area (figure 5.25d), according to (Selaolo, 1998) implies that almost no evaporation occurred during infiltration period. This is a typical situation for areas with high rates of infiltration and recharge (Buttle, 1998). In case of Marula, it is probably due to pumice type of formation in the area that has a good hydraulic conductivity, allowing little time for evaporation to occur.

The isotopic composition of the unsaturated zone for Ndabibi is similar to that of rain. It shows some depletion with increase in depth up to 1.8 meters, and then it starts getting enriched probably due to interflows in form of infiltrations from precipitation.

The isotopic composition of the unsaturated zone for Kedong has no significant similarity with that from boreholes located in this area. This confirms the previous research that the groundwater in the southern part of the lake has mixed waters from Lake Naivasha and direct-localised recharge.

The isotopic signatures from the unsaturated zones, below the rooting system for grass, and those from the two the boreholes (table 5.7), were plotted together with the compiled isotopic data sets for the study area since 1992 (appendices, 10-14).

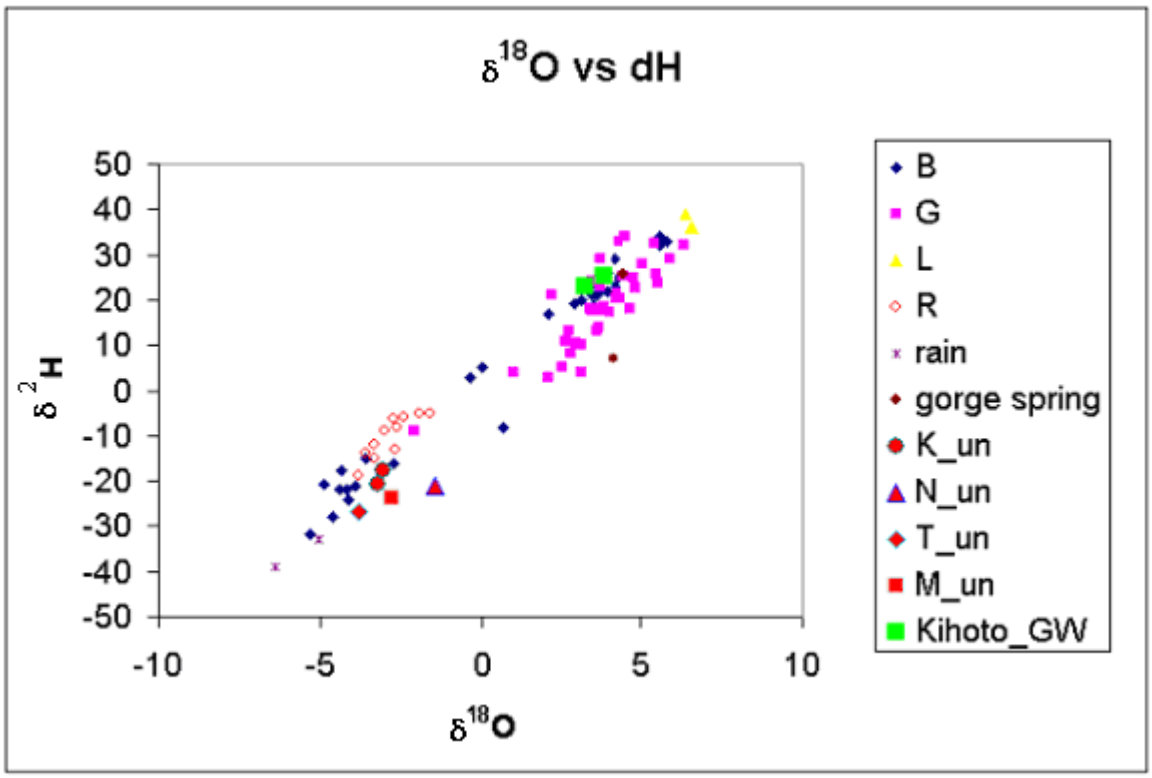

Figure 5.26: Local meteoric water line for Naivasha basin; Isotopic evaporation line for water from rain-fall, Lake Naivasha, river, boreholes and unsaturated zone.

Explanation:

B: Borehole

G: Geothermal well

L: Lake

R: River

K_un: isotopic value for unsaturated zone around Kedong area

N_un: isotopic value for unsaturated zone around Ndabibi area

T_un: isotopic value for unsaturated zone around Three-point farm

M_un: isotopic value for unsaturated zone around Marula Farm

Kihoto_GW : Isotopic composition for Kihoto boreholes, K1 and K2 (Naivasha town)

The isotopic signatures obtained from the unsaturated zone are relatively similar to those from rainfall and rivers. Marula and Three Point areas are being recharged from direct rain, River Malewa and Gilgil. Ndabibi area is recharged by direct rain and ephemeral streams, whereby the highest percentage comes from rain. Kedong area receives its recharge from rain and Lake Naivasha, and according to previous studies, the highest percentage recharge comes from Lake Naivasha. The boreholes K1 and

K2 located in Naivasha town (Kihoto area) have similar isotopic composition with those from the geo-thermal wells.

5.4. RECHARGE ESTIMATES USING A SIMPLE 1-D MIXING MODEL

A simple model (Appendices 8 and9) using Excel spread sheet was applied to the area in the southern part of the lake lying between the piezometric levels of 1888m, near lake Naivasha, and 1884m, 10km away from the lake. The isotopic signatures of boreholes (Table 5.8) were taken as measured and reference values. From the transmissivity distribution modelled by (Owor, 2000), figure 2.6, the aquifers lying between the above mentioned piezometric levels has the transmissivity values ranging between 3000 and 5000 m^2day^{-1}.

During each simulation, the following parameters were always kept constant; the transmissivity, concentration of lake and unsaturated zone (in terms of isotopic values), direct recharge. The piezometric heads at the ends were kept constant throughout the calibration. By applying changes in both the transmissivity and recharges every after each simulation, different isotopic signatures falling between the specified piezometric heads were calibrated.

Table 5.8: Boreholes from the southern part of the lake with mixed water.

SITE	$\delta^{18}O$	$\delta^{2}H$	X-UTM	Y-UTM
C562	4.30	25.0	210900	9911000
C7829	3.90	26.0	206610	9908050
C2071	3.40	18.0	202800	9909500
OLSULWA	3.53	23.0	204888	9908150
C210	3.10	20.1	208867	9909074
HEATHER	4.19	29.2	214281	9909564
C4366	3.40	21.0	198050	9909400
KONGONI	3.25	23.0	194823	9909906
C562	4.30	25.0	210900	9911000

The validity of the model is tested by the plots of both the simulated and the measured isotopic signatures values from existing wells, figures 5.27 and 5.28 display the results.

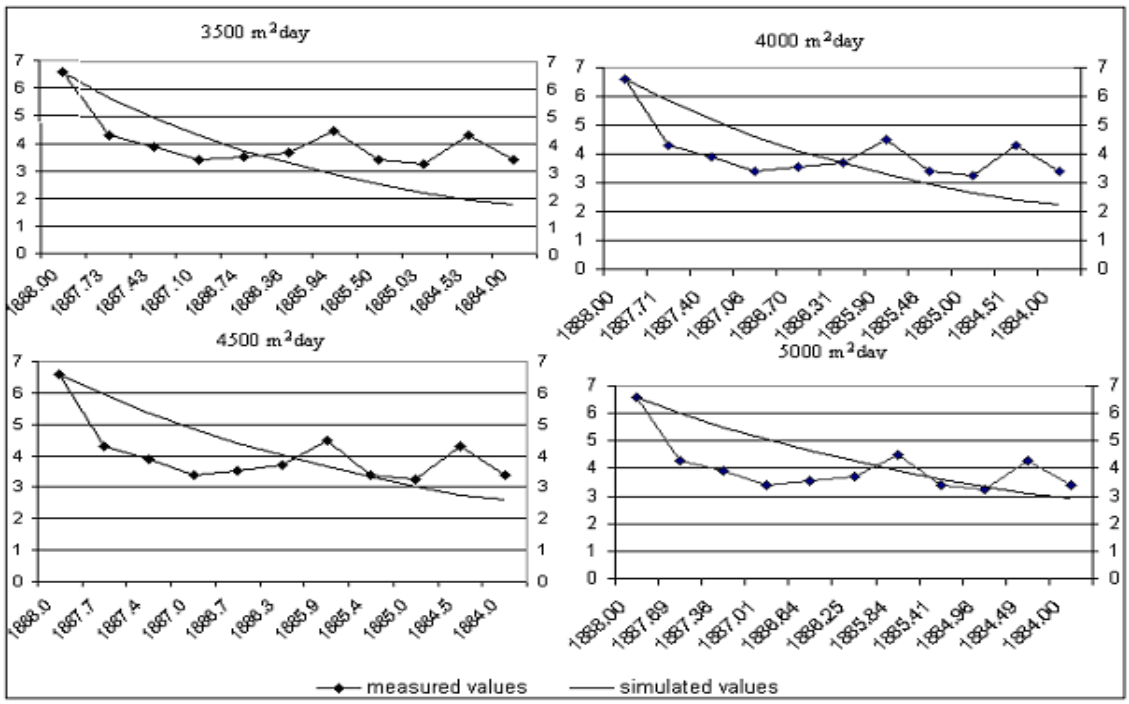

Figure 5.27: Validity of model simulations with measured values for δ18O composition.

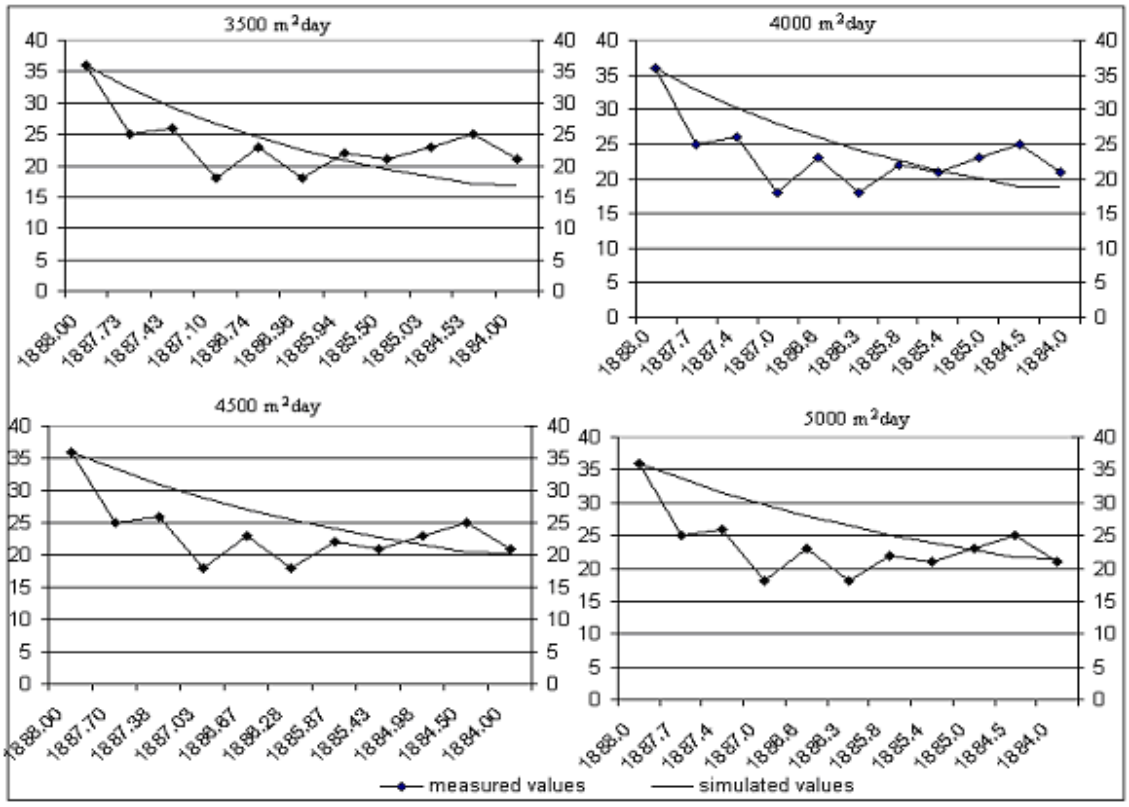

Figure 5.28: Validation of model simulations with measured values for δ^2H composition.

A high correlation between the measured and simulated isotopic values, confirms strength of the model. Some variations do occur probably due to incorrect piezometric heads imposed on the wells used. Table 5.9, below displays the results.

Table 5.9: Direct recharge estimates in southern part of the lake aquifer, *simulated by a simple 1-D Mixing Model.*

Stable isotope	Range	mmday^{-1}	mmyear^{-1}
18-Oxygen	3 – 6 $^{o}/_{oo}$	1x10^{-5} – 7x10^{-5}	3.65 – 25.55
Deuterium	18 – 36 $^{o}/_{oo}$	3x10-5 – 7x10-5	10.95 – 32.85

5.5. INFLUENCE OF VEGEATATION ON RECHARGE IN THE STUDY AREA

5.5.1. Grassland

This extraction of water by roots is not only constrained by atmospheric demand but rather by the nature of plant, physical obstructions in the soils for example impermeable layer and the effect on the rooting depth. Detailed analysis of soil pits and auger holes show that the roots of grassland in the study area go up to 2.5 meters.

In such areas water uptake by roots only occur within the depth and only takes place during the rain season. No evapotranspiration from grass takes during dry seasons, since by this time the grass is completely dry and cannot transpire.

Figure 5.29: The behaviour of different types of vegetation during dry seasons, Kedong area.

5.5.2. Acacia trees

There are two common types of species in Naivasha area, the Acacia Xanthophloea (yellow fever) and Acacia Drepanolobium (Whistling Thorn) species. The Yellow fever species are found in areas with abundant supply of water and fertile soils, normally the vicinities of Lake Naivasha and grow up to twenty meters in height. The Yellow fever species can survive drought conditions because of their tap-roots, which can reach deeper profile layers.

Whistling Thorn can survive in drier climates more than the Yellow Fever Acacia. Vast fields of this species are dominant in areas towards Masai Mara. They look more like bushes than trees, because they do not grow very tall. Unlike the Yellow Fever species, which can grow twenty meters in height, this species can only reach a height of 18 feet (Benders, 2000).

Acacia trees in the study area have been termed as shallow rooted trees. This has been disproved, basing on the research carried in the study area, together with other researches by other authors.

The field research was conducted on two acacia trees, of the same species, located at Three Point farm. The first one was already exposed in a dry trench of river Karati and another one, its root system was exposed by digging a hole of 8 meters with a diameter of 1.80 meters and trenches following the lateral roots.

These acacia trees have lateral roots, with diameter range of 5-9cm. The highest rooting density is consigned within a depth of 65cm. They extend horizontally to a depth of 9 meters, and beyond this, they grow vertically and branches into small other lateral roots, which later develop intensive hair roots. The taproot of this acacia tree was estimated to go beyond 8 meters. It starts with one big trunk, with diameter of 60cm up to a depth of about 70 cm. From then onwards, it starts dividing into other branches.

Figure 5.30: The lateral roots of acacia in the upper zone, Three Point Farm.

Figure 5.31: The Main taproot of acacia in the upper zone, exposed with its lateral roots, Three Point Farm.

The young acacia tree (yellow fever) that was exposed in the dry trench of Karati River, with a diameter of 40cm and its taproot was extending beyond eight metres. The lateral roots extend horizontally beyond 15 m, and small other lateral roots branch off, in the process, which later develop intensive hair roots. These hair roots extend vertically to a depth of 6m

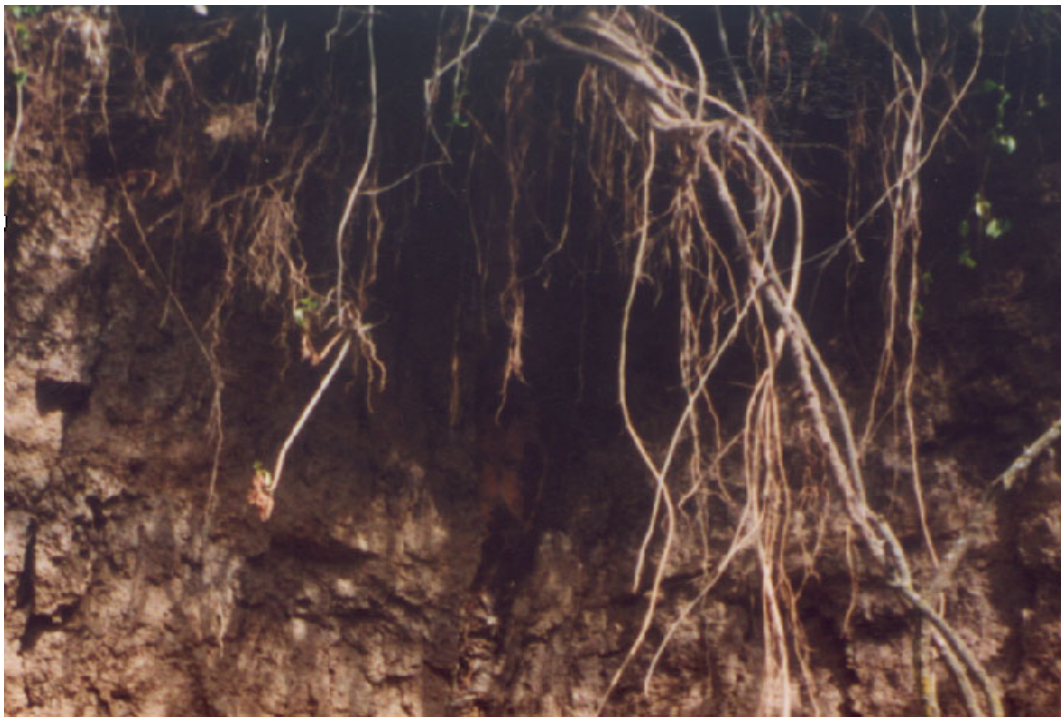

Figure 5.32: Exposure of the intensive small lateral roots of Acacia, branched off the main lateral roots, (from a dry trench of Karati river), Three point Farm

Figure 5.33: Taproot of Acacia at 7 meter depth (from a dry trench of river Karati), at Three Point Far- The acacia Xanthophloea that are located in the study area not shallow rooted, as it has been thought but rather deep rooted and have the potential to extract water from the water table.

Their lateral roots grow horizontally but when they encounter a soft or hard fractured formation, they divert to vertical growth and branches into small other laterals, which also divides into small intensive hair roots. The system continuously extracts water from wider parts of the unsaturated zone.

Their taproot start as a single trunk, beyond 70cm, it starts branching into other taproots, with hair roots. These trap water from deeper parts of the soil profile. From the diameter of the taproot at the bottom of the hole, it is assumed that this taproot has the ability to extent beyond 20m and could be extraction water from the water table.

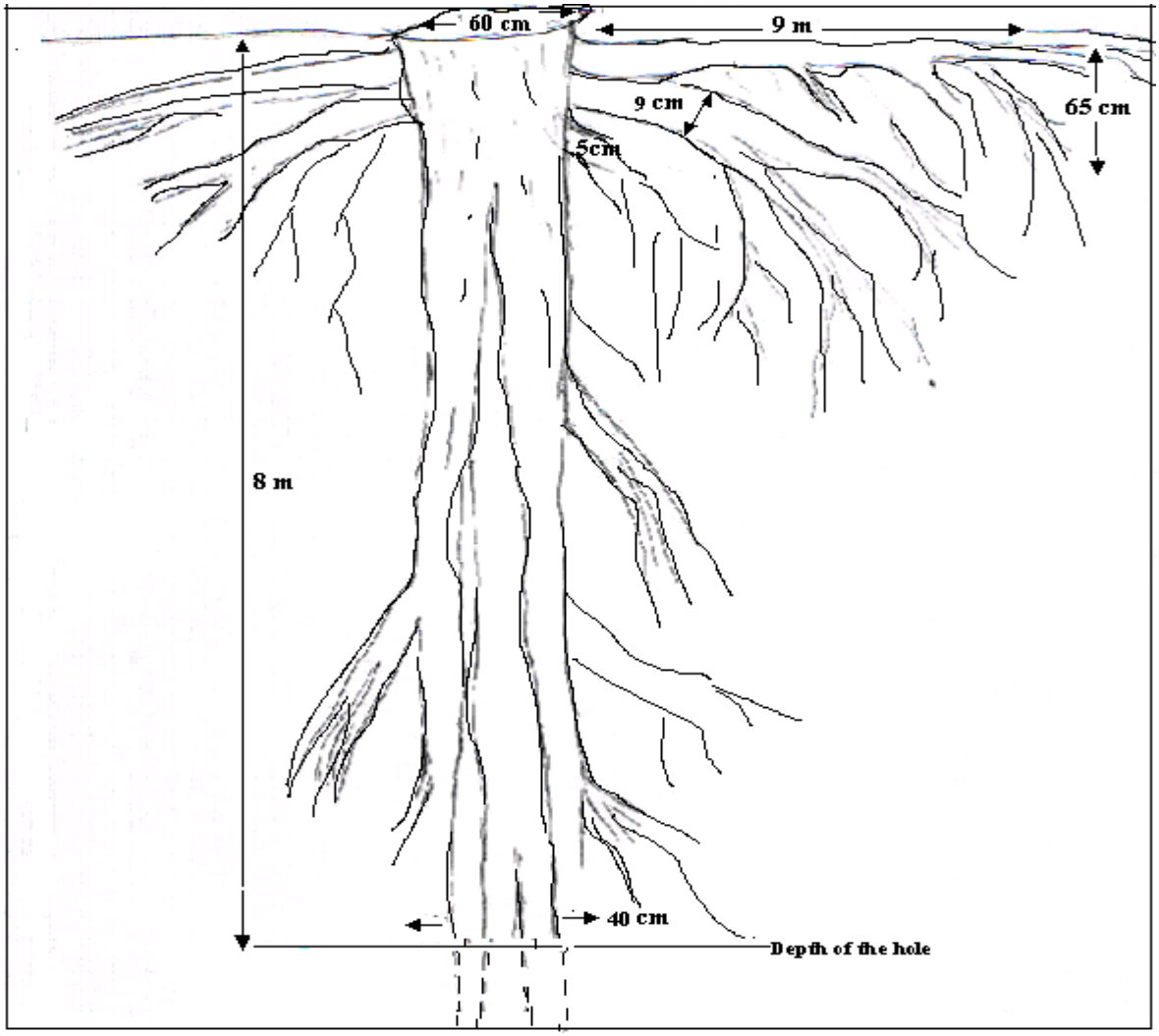

Figure 5.34: Sketch of Acacia Xanthophloea , dug out from a hole, exposing its root system

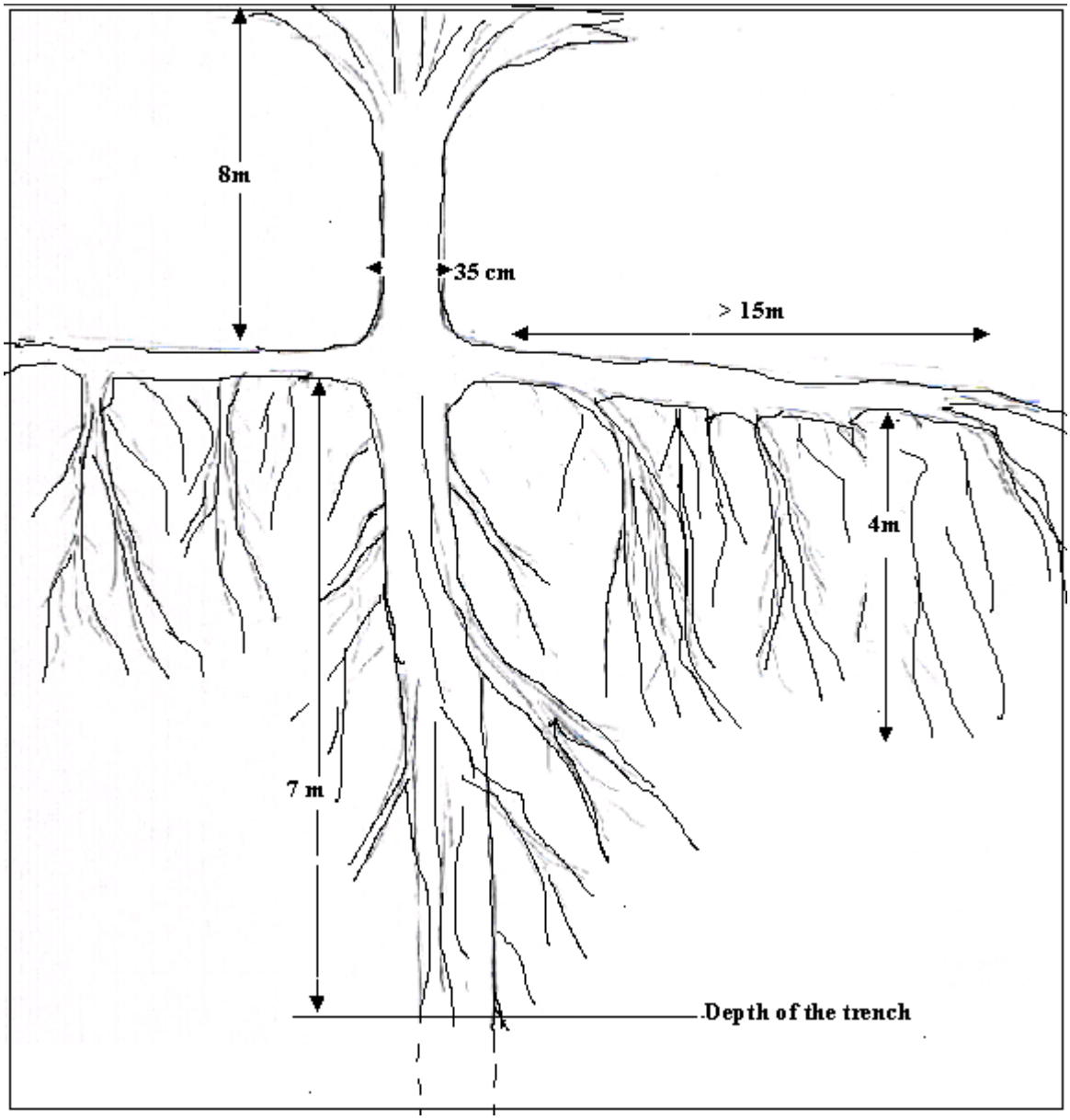

Figure 5.35: A Sketch of young Acacia Xanthophloea , exposed in a dry river trench, exposing its root system

6. DISCUSSIONS AND LIMITATIONS

6.1. DISCUSSIONS

In (Semi-) arid environments like the study area much of the precipitation evaporates or is transpired by plants back into the atmosphere, thus evapo(transpi)ration is a very important factor for determination of recharge and available groundwater in these areas.

Unsaturated zone techniques for estimating recharge are mostly applied in semiarid and arid regions, where the unsaturated zone is thick. They generally provide estimates at points or small scales, however these estimates may represent many large areas. These techniques provide estimates of potential recharge based on drainage rates below the root zones, however in some cases, drainage is diverted laterally and does not reach the water table(Scanlon et al., 2002). In the study area it is assumed that all the diverted drainages, in one way or another reach the water table, depending on the residence period, though the drainage rates in thick unsaturated zones do not always reflect the current recharge rates at the water table.

There are three main sources that contribute to recharge in the study area; the direct recharge from rain, and localised recharge from depressions, like lake Naivasha, indirect recharge from rivers and lakes like lake Naivasha, river Malewa, Gilgil and ephemeral streams. Tables 6.1 and 6.3 summarise the results from the two models.

Table 6.1: Direct recharge estimates from SWAP model (1990-1997), before El Nino.

Location	Recharge ($mmday^{-1}$)	Total recharge (1990-1997) (mm)	Average recharge ($mmyear^{-1}$)
Kedong	0 – 0.19	100	14.29
Ndabibi	0 – 0.18	0.2	0.03
Three Point	0 – 0.024	18	2.57
Marula	0 – 0.28	52	7.43

Table 6.2: The recharge received (1990-1998), after the El Nino

Location	Recharge ($mmday^{-1}$)	Total recharge (1990-1998) (mm)	Average recharge ($mmyear^{-1}$)
Kedong	0 – 7.00	350	43.75
Ndabibi	0 – 0.27	5.5	0.69
Three Point	0 – 0.10	35	4.38
Marula	0 – 5.50	270	33.75

Table 6.3: Direct recharge estimates from a 1-D mixing model.

Type of recharge	Stable isotope	$mmday^{-1}$	$mmyear^{-1}$	Average recharge ($mmyear^{-1}$)
Mixed recharge; Lake, rain,	18-Oxygen	$1x10^{-5} – 7x10^{-5}$	3.65 – 25.55	14.6
	Deuterium	3x10-5 – 7x10-5	10.95 – 32.85	21.9

The groundwater recharge in the study is influenced by climate, soils, vegetation, lithology and geomorphology of the area. The area experiences an annual rainfall of 640mm. Since the potential evapotranspiration (1700mm) of the area is much higher than rainfall, direct recharge is not a permanent process in the area, but a process which occurs during rain seasons and, only when there are high intensities, this explains those periods during model simulations which show zero bottom flux.

From the previous studies, the aquifers of Marula and Three Point, in the northern part of the study area obtain their recharge from Precipitation and river Malewa; the largest percentage comes from the river. Ndabibi plains, is recharged by precipitation and Kedong area, by Lake Naivasha and precipitation, the highest percentage being contributed by the Lake.

The main factors influencing the water movement in the unsaturated zone are the rooting density and depth of vegetation, and the types of soil layers in the profiles. Most part of the study area is flat, with no indication of valleys, hence no runoff. So when it rains, due to high rate of evaporation, much of it evaporates and that which remains infiltrates, through the pumice sand to the deeper parts of unsaturated zone. If a water flux is obtained at a depth in a profile where no further abstraction by roots occur, it is estimated to be equal to groundwater recharge (Allison, 1987). The rooting depth of grass in the study area is about 2.50 meters, beyond which no evapotranspiration from grassland is assumed

occurs. The water movement at this stage is still influenced by other factors in the unsaturated zone, before it reaches the water table.

The studies carried out in Kalahari semi- arid environment (De Vries et al., 2000) detected the extraction of water by acacia species from a depth exceeding 50 metres. The research on acacia trees in the study area, together with the other studies carried out in other semi arid environments clearly proves that Acacia species extracts water from deeper depths. Clearing of native vegetation and establishment of shallow-rooted pasture and crops, increase the local recharge, which will still be variable in time due to variability of rainfall (Balek, 1987).

The native vegetation, particularly acacia trees, have developed root system (Figure 5.32 and 5.33) that extracts a big percentage of water during it movement towards the water table. Since the water table is deep, water movement continues even during dry seasons, hence the process of evapotranspiration occurs throughout the year for those areas that are covered with both grassland and acacia trees.
The roots of acacia trees have a constant affect on groundwater recharge, since they continue to transpire even during dry seasons (Plate 1). During this period, water movement from the last rainfall events could still be taking place, probably due to the long residence period and the deep water table.

Kedong is a flat area widely dominated by grassland type of vegetation. Evaporation mostly occurs during rainy seasons, when the leaves are green and have the potential to transpire.
In other areas, Ndabibi, Marula and three point, the water flux below the rooting depth of grass is still affected by the presence of acacia trees, whose roots continue extracting water from deeper parts of the unsaturated zone and could even go up to the water table. The total amount consumed by these trees depends on their percentage coverage in the respective areas.

A simple 1-D mixing model simulated direct recharge in the southern part of the lake Naivasha aquifer, 10 km away from the lake. From the piezometric map, the isotopic signatures of boreholes (Table 5.8) located within this area; with heads between 1888-1884 metres were used in model calibration. These were taken as measured values during the simulation. Their signatures range between 6 - 3 $^{o}/_{oo}$ for 18-Oxygen and 36 – 18 $^{o}/_{oo}$ for Deuterium. From the simple 1-D mixed model, the simulated recharge between these limits was of the range (3.65 – 25.55) mmyear^{-1}, giving an average recharge of 14.60 mmyear^{1}, which figure correlates well with the direct recharge simulated from SWAP model before El Nino (Table 6.1), in Kedong area. This is assumed to be the average contribution of direct recharge towards southern part of the lake aquifer, in a radius of 10km. The lake water percentages

(appendices 8 and 9) agree with the previous estimates on lake water contribution (Oppong-Boateng, 2001) towards the aquifer.

The evaluation of validity of the simple model with measured isotopic values was based on a general piezometric range (1888-1884), due to lack of independent piezometric heads for each borehole.

6.2. LIMITATIONS

Recharge in (semi-) areas can be determined through the vadose zone from direct calculation of water fluxes, either by applying or establishing a vadose-zone water balance on the basis of soil, climate, and vegetation data. However this is not a straightforward process, since the small recharge calculated from the difference between rainfall and actual evapotranspiration is still less than the accuracy range of recharge (Simmers et al., 2002).

Since all the Darcy's law solution for water movements in the unsaturated zone require knowledge of the soil-water retention curves, and since their determination is difficult, indirect methods for estimating soil hydraulic properties has been developed from many practical applications (Van Genuchter et al). The simulation obtained was not matching with infiltration curves obtained from fieldwork. The soil moisture content of simulated curves is exaggerated. SWAP modelling does not simulate exactly was in field. The soil basics found in SWAP model were generated basing on both surface and soil properties from temperate type of climate, which is mainly influenced by summer and winter seasons. These properties somehow differ from those for (semi-) arid type of climate. These humid environments are characterised by high rainfall intensities, little evapotranspiration, shallow groundwater levels, thin unsaturated zone, and hence high rates of groundwater recharge.

Generally the Naivasha basin has a homogenous type of soil, the pumice sand, with bulk density, which is less than that for water ($<1 gcm^{-3}$). Its rate of sacking up water and releasing it is very high. These soils cannot hold water for a long time. So when it rains, all the water infiltrates to the deeper soil layers. SWAP generally bases on three soil types; sand, clay, and silt to classify their hydraulic properties. Sand is taken as a quartz material with bulky density ranging between 1.20 gcm^{-3} and 1.80 gcm^{-3} (Landon, 1991). Due to its big bulky density and porosity, it can hold water for sometime before releasing it, which is quite different from pumice type of sand found in the study area. To obtain better results, modification of soil properties with the use of field measurements was necessary.
The initial pressure heads were estimated from the initial conditions of soils, basing on soil moisture measurements. Due these rough estimates, the water fluxes in the first periods were exaggerated. The conditions were too wet, and it took sometime, approximately three years to attain its equilibrium. The

final pressure heads for the last year were used as initial pressure heads and the simulation was re-peated.

7. CONCLUSIONS AND RECOMMENDATIONS

7.1. CONCLUSIONS

The ephemeral streams in the study areas can also be source of recharge especially during dry seasons when ephemeral rivers terminate in depressions groundwater recharge can also occur. In this case topography of the region plays a dominant role.

The low values of direct recharge are caused by mainly two factors, the little and irregular distribution of rain and, high rates of evapotranspiration in the study area. And not every rainfall event causes recharge, direct recharge only occurs during wet seasons and only when there is a heavy storm.

The natural areas around Kedong received the highest recharge (43.75mmyr^{-}1), followed by Marula (33.75 mmyr^{-}1). Ndabibi and Three Point receives the lowest, 0.69mmyr^{-1} and 4.38mmyr^{-1} respectively. The highest recharge was received in the year 1998, during El Nino period. The big variation in recharge is associated with the different types of vegetations and soils in the study area.
The mechanisms of Groundwater recharge dominating the study area are; direct recharge from rain, indirect recharge from river Malewa and Gilgil in the northern part, localised recharge from the Lake Naivasha.
Model simulation has to be appropriate to the actual conditions in the field. Applying of hydraulic properties on soils using the inbuilt datasets from SWAP model resulted in simulations that did not match with field measurements. Matching curves were obtained after the modification of the soil hydraulic properties by referring to both the datasets and field measurements. Field measurements are the basis of recharge investigations since they give a realistic idea on recharge processes. So models must work hand in hand with them for better estimations of groundwater recharge.

7.2. RECOMMENDATIONS

Recharge in (semi) arid areas is intermittent and concentrates in small areas; such conditions influence the choice of its estimation. It is therefore recommended to have a well-defined theory of different recharge processes as well as using more than one technique for result verification.

There are normally very low water fluxes in semi-arid environment and are highly variable in time, therefore, the application of physical methods, which rely on direct measurements of hydrological parameters is a problem. Because of the low water fluxes, changes in these parameters are very small and difficult to detect, and due to their variability in time, these measurements must be made over several years to come up with an estimated mean value. This can be avoided, for the case of the study area, by massive application of chemical and isotopic techniques on unsaturated zone. The diffusivity of trace elements is much less variable with change in water content or soil type than the diffusivity of soil water, so the former gives a better indicator of water movement in the porous medium (Allison, 1987). The physical methods are more advantageous in wetter environment where the fluxes are higher and constant in time.

Since in developing countries like the study area, it is difficult to obtain adequate data to result into a reasonable recharge estimates, a flexible approach to recharge determination is needed. To opt for approaches or models, which require so much data, input give insufficient results since in most cases the defaults inbuilt in these approaches are used instead of the actual data from field.

Field measurements are the basis of recharge investigations since they give a realistic idea on recharge processes. So models must work hand in hand with them for better estimations of groundwater recharge.

For further estimates of lake contribution towards the aquifer in the southern part of the lake, a more complex mixing model is recommended, which includes assigning different transmissivity values and piezometric heads for all the wells used.

It is of good idea for the future studies to apply and compare quite a number of approaches in groundwater recharge estimations. Other techniques like the application of chloride mass balance should be conducted in unsaturated zone. And since the unsaturated zone in the study is quite thick more advanced techniques other than hand augering should be applied in order to exploit the deeper layers.

Isotopic soil sampling should be carried out on quite a number of sites to have a wider view on isotopic variations.

The combination of available local data, remote sensing and Geo-information Science technology promise for a better understanding and quantification of recharge over large areas (Simmers et al., 2002). It is now clearly proved that the acacia trees do extract a reasonable amount of water from both the unsaturated and saturated zones, adding to what (Farah, 2001) researched on evapotranspiration using remote sense techniques, a research on the distribution of acacia trees in the study area should be investigated by remote sensing in order to determine how much they affect the recharge on a regional scale.

Since SWAP model uses Darcy's law, it is advisable to be applied in (semi-) arid regions where water tables are shallow(Scanlon et al., 2002).

The reliability of recharge estimates using different techniques is variable, the techniques based on surface-water and unsaturated zone data provide estimates of potential recharge whereas those based on groundwater data generally provide estimates of actual recharge (Scanlon et al., 2002). There is a need for application of multiple techniques to increase reliability of recharge estimates. There after, the estimated recharge should be assigned in the 3-D hydrogeological Model constructed by (Nabide, 2002), during its calibration.

REFERENCES

Allen, G.R., L.S. Pereira, D. Raes, and M. Smith. 1998. Crop Evapotranspiration: Guidelines for computing Crop Water requirements FAO, Rome.

Allison, G.B. 1987. A review of the Physical Chemical and Isotopic techniques available for Estimating Groundwater Recharge., p. 49-72, *In* I. Simmers, ed. Estimation of Natural Groundwater Recharge, Vol. 222. D. Reidel Publishing Company, Amsterdam.

Allison, G.B., G.W. Gee, and S.W. Tyler. 1994. Vadose-zone techniques for estimating groundwater recharge in arid and semiarid regions. Soil Science Society of America Journal 58:6-14.

Atkilt, G., G.R. Dr. David, D.W. Siderius, and I.R. Henneman. 2001. Soils of the Lake Naivasha Area, Kenya: Summary of investigations 1997-200, by the Soil Science Division. ITC, Enschede, pp 34.

Balek, J. 1987. Groundwater Recherge Concepts, p. 3-9, *In* I. Simmers, ed. Estimation of Natural Groundwater Recharge, Vol. 222. D. Reidel Publishing Company, Amsterdam.

Benders, E. 2000. Savanna Plant [Online] http://www.blueplanetbiomes.org/savanna_plant_page.htm.

Buttle, J.M. 1998. Fundamentals of Small Catchment Hydrology, p. 1-49, *In* J. J. McDonnell, ed. Isotope Tracers in Catchment Hydrology, Vol. Chapter 1. Elsevier Science B.V., Amsterdam.

Clarke, M.C.G., D.G. Woodhall, D. Allen, and G. Darling. 1990. Geological, Volcanological and Hydrogeological controls on the occurrence of Geothermal activity in the area surrounding Lake Naivasha, Kenya Ministry of Energy, Kenya Government, Nairobi.

De Vries, J.J., E.T. Selaolo, and H.E. Beekman. 2000. Groundwater Recharge in the Kalahari, with reference to paleo-hydrologic conditions. Journal of Hydrology 238:110-123.

Farah, H.O. 2001. Estimation of Regional Evaporation under different weather condition from Satellite and Meteorological data : A case study in the Naivasha basin, Kenya. PhD thesis, Wageningen University, Wageningen, pp 170.

Fetter, C.W. 1994. Applied Hydrogeology. 4th ed. Prentice Hall, upper Saddle river, New Jersey.

Kendall, C., and E.A. Caldwell. 1998. Fundamentals of isotope Geochemisitry, p. 51-86, *In* J. J. McDonnell, ed. sotope Traces in Catchment Hydrology. Elsevier Science B.V., Amsterdam.

Kroes, J.G., J.C. Van Dam, J. Huygen, and R.W. Vervoort. 1998. User's Guide of SWAP version 2.0; Simulation of Water flow, Solute transport and Plant growth in the Soil-Water-Atmosphere-Plant Environment. Technical Document 0927-4499. Departament of Water Resources Wageningen Agricultural University
DLO-Staring Centrum, Wageningen.

Landon, J.R. 1984. Booker Tropical Soil manual : A handbook for Soil Survey and Agricultural Land evaluation in the Tropics and Subtropics Longman: Booker Agriculture International, London.

Landon, J.R. 1991. Booker Tropical Soil Manual : A handbook for Soil survey and Agricultural Land Evaluation in the Tropics and Subtropics. 2nd Edition ed. John Wiley & Sons, Inc., New York, London.

Leduc, C., J. Bromley, and P. Schroeter. 1997. Watertable fluctuation and Recharge in Semi-arid climate: some results of the HAPEX-Sahel hydrodynamic survey (Niger). Journal of Hydrology 189:123-138.

Lerner, D.N., A.S. Issar, and I. Simmers. 1990. Groundwater Recharge : A guide to understanding and estimating Natural Recharge. International Contributions to Hydrogeologists : IAH International Association 10.

Nabide, I.K. 2002. Development of 3-D conceptual hydrogeological model for Lake naivasha area : based on the integration of geology, hydrochemistry, isotopic analysis and boundary conditions. MSc-thesis, ITC, Enschede.

Ogoso Odongo, M.E. 1986. Geology and the Olkaria Geothermal field (Kenya). Geothermics 15:741-748.

Ojiambo, B.S. 1996. Characterization of Subsurface outflow from a closed - basin freshwater tropical lake, Rift valley, Kenya. PhD thesis, University of Nevada, Nevada. 141 pp.

Ojiambo, B.S., R.J. Poreda, and W.B. Lyons. 2001. Ground water and Surface water interactions in Lake Naivasha, Kenya. Ground Water 39:526-533.

Oppong-Boateng, R. 2001. Assessment of the use of groundwater for irrigation in the southern part of lake Naivasha, Kenya. MSc-thesis, ITC, Enschede, pp 95.

Owor, M. 2000. The Long-term interaction of Groundwater with Lake Naivasha, Kenya : A numerical simulation of the relationship between groundwater and lake allowing for fluctuating lake levels. MSc-thesis, ITC, Enschede, pp 110.

Rawls, J.W., L.R. Ahuja, D.L. Brakenseik, and A. Shirmohammadi. 1993. Infiltration and Soil Water Movement, p. 5.1 - 5.51, *In* D. R. Maidment, ed. Handbook of Hydrology, Vol. Chapter 5. R. R. Donnelley & Sons Company, New York.

Rozanski, K., P. Wachniew, and T. Kuc. 1993. Isotope composition of Carbonates in the Lake Gosciaz sediment based on the core G1/87, G2/87 and G1/90 analyses. Polish Botanical Studies, Guidebook Series 8:157-162.

Scanlon, B.R., P.G. Cook, and R.W. Healy. 2002. Choosing appropriate Techniques for quantifying Groundwater Recharge. International Association of Hydrogeologists : IAH International Association 10:18-39.

Scott, D.F., and D.C. Le Maitre. 1998. The Interaction between Vegetation and Groundwater 730/1/98. CSIR Division of Water, Environment and Forestry Technology, Stellenbosch.

Selaolo, E.T. 1998. Tracer studies and Groundwater Recharge Assessment in the Eastern Fringe of Botswana Kalahari. Publishing Company Botswana Limited., Botswana.

Simmers, I. 1987. Estimation of Natural Groundwater Recharge. D. Reidel Publishing Company, Amsterdam.

Simmers, I., J.J. De Vries, and J. Jacobus. 2002. Groundwater recharge: An overview of processes and challenges. International Association of Hydrogeologists : IAH International Association 10:8-16.

APPENDICES

Appendix 1: Initial soil moisture conditions for the four locations in the study area.

Kedong		Ndabibi		Three point		Marula	
Depth (cm)	Soil moisture (%)	Depth (cm)	Soil moisture (%)	Depth (cm)	Soil moisture (%)	Depth (cm)	Soil moisture (%)
36.5	3.5	60	4.9	10	9.1	20	15.6
65.5	5.2	100	7.2	56	6.1	50	17.0
83	5.5	150	3.5	100	20.5	120	17.4
100	9.3	190	8.4	150	22.6	140	17.6
123	16.8	250	5.9	200	17	170	11.5
137	18.2	290	6.9	250	28.5	240	5.2
162	20.1	300	2.4	350	29.8	390	3.9
190	34.7	350	5.9	400	29.9	425	3.1
250	36.5	380	7.0	450	31.2	500	7.5
290	32.5			470	24.3	530	15.6
300	15.1			500	19.9		
360	15.6						
400	15.6						

Appendix 2: Data set of soil hydraulic functions, Carsel and Parish, 1988), USDA texture classes.

Texture	θ_{res} (cm^3cm^{-3})	θ_{sat} (cm^3cm^{-3})	α (cm^{-1})	n (-)	K_{sat} ($cm\ d^{-1}$)
Sand	0.045	0.43	0.145	2.68	712.8
Loamy sand	0.057	0.41	0.124	2.28	350.2
Sandy loam	0.065	0.41	0.075	1.89	106.1
Loam	0.078	0.43	0.036	1.56	25.0
Silt	0.034	0.46	0.016	1.37	6.0
Silt loam	0.067	0.45	0.020	1.41	10.8
Sandy clay loam	0.100	0.39	0.059	1.48	31.4
Clay loam	0.095	0.41	0.019	1.31	6.2
Silty clay loam	0.089	0.43	0.010	1.23	1.7
Sandy clay	0.100	0.38	0.027	1.23	2.9
Silty clay	0.07	0.36	0.005	1.09	0.5
Clay	0.068	0.38	0.008	1.09	4.8

Appendix 3: Infiltration measurements for Ndabibi and Three Point area.

Ndabibi			Three Point					
Day	**Soil moisture (%)**	**Depth (cm)**	**Day**	**Depth (cm)**	**Soil moisture (%)**	**Day**	**Depth (cm)**	**Soil moisture (%)**
2nd	27.18	0	**1st**	0	40.69	**5th**	0	30.84
	10.99	7		5	39.84		10	34.62
	6.98	9		19	39.18		18	35.25
4th	35.91	0		28	38.8		28	35.18
	32.12	5		34	36.53		40	35.7
	30.97	9		40	34.57		58	36.25
5th	31.08	0	**2nd**	0	34.65		62	35.54
	25.18	5		8	31.88		70	35.66
	25.38	10		12	35.5		78	32.28
	22.15	13		17	37.72	**7th**	5	34.5
	22.48	20		28	36.33		15	34.13
6th	29.5	0		35	35.95		30	36.28
	26.48	6		50	32.92		50	30.68
	23.98	15		60	24.4		60	20.6
	16.13	25	**3rd**	0	34.74	**8th**	15	32.8
7th	26.58	0		8	36		30	34.78
	22.14	12		12	33.8		50	35.5
	16.48	20		17	33.73		66	35.8
8th	20.26	20		24	34.76	**9th**	15	27.52
	16.78	25		30	34.1		30	32.64
9th	15.35	20		44	35.84		50	21.02
	9.62	25		50	36.68		70	17.07
	8.92	-32		60	36.5		80	18.2
10th	17.8	10		70	34.58	**10th**	15	24.7
	14.88	30	**4th**	0	39.79		30	27
	10.28	40		6	43.47		50	21.1
	3.52	50		16	43.43		65	18.6
Last	11.9	-10		24	43.06		76	17.2
	8	-30		33	42.06		100	17.1
	6.4	-50		42	31.78		120	17.6
	10	70		52	28.23		150	10.9
	9.5	100		64	26.34		200	11
	5.5	150		68	24.1			
				72	23.4			

Appendix 4: Infiltration measurements for Marula and Kedong area.

Marula			Kedong					
Day	**Depth (cm)**	**Soil moisture (%)**	**Day**	**Depth (cm)**	**Soil moisture (%)**	**Day**	**Depth (cm)**	**Soil moisture (%)**
1st	0	39.71	**1st**	0	36.96	**10th**	10	9
	10	37.4		2	28.7		20	5.97
	16	38.82	**2nd**	0	21.14		30	4.82
	28	39.02		13	15.7		40	4.57
	40	34.14		15	14.03		50	4.6
2nd	0	33.92	**3rd**	0	20.17		60	6.37
	8	35.38		10	16.58		70	9.95
	13	34.88		13	11.76		80	12.45
	28	35.6	**4th**	0	16.76		90	15.25
	38	33.68		5	16.32	**11th**	0	4.3
	0	33.07		13	12.35		10	4.5
3rd	10	35.24		18	8.6		20	4.7
	15	36.52	**6th**	0	14.78		40	4.8
	28	36.6		8	13.56		60	6.4
	40	32.72		14	12.14		80	12.9
	49	30.06		20	5.4		100	18.3
	15	35.42	**7th**	0	12.32		120	21.2
4th	30	36.5		8	12.64		150	30.9
	40	35.6		16	12.68		200	33.6
	60	31.9		20	7.4		250	38
	70	20.2	**8th**	0	11.45		270	33.2
	15	30.6		8	12.54			
5th	30	34.4		15	12.14			
	50	32.74		18	11.36			
	70	32.2		24	4.9			
	90	20.9		90	15.25			

	95	15.4						
	20	34						
6th	30	32.7						
	40	29.5						
	60	24.4						
	70	20.2						
	100	22.8						
	120	19						
	150	9.4						
	170	8.1						
	200	11.8						
	220	14.4						
	250	12.9						
	300	22.9						
	320	19.9						
	350	13.4						
	400	6.3						

Appendix 5: Laboratory analysis for SWAP modelling.

Sample name	Dry weight sand, N	Dry weight, silt, F	Dry weight, clay, H	Net weight clay, K	Net weight silt, P	Net weight sand, N	K+P+N	% Clay	% Silt	% Sand	% Organic Matter	Soil moisture (%)	K (sat) (cm/day)
KD_GL 84cm	14.4897	0.1057	0.0417	1.82	3.035	14.4897	19.3447	9.4083	15.6891	74.9027	1.1732	5.88	178.8
KD_GL 138cm	11.9409	0.1523	0.0517	2.32	4.865	11.9409	19.1259	12.1301	25.4367	62.4331	0.8212	18.36	44.7
KD_GL 190cm	10.1488	0.1553	0.06	2.735	4.6	10.1488	17.4838	15.6431	26.3101	58.0469	1.6424	18.36	44.7
KD_GL 250cm	5.6522	0.2022	0.0581	2.64	7.04	5.6522	15.3322	17.2187	45.9164	36.8649	1.0559	34.57	31.3
KD_GL 360cm	10.8282	0.1889	0.0447	1.925	7.15	10.8282	19.9032	9.6718	35.9239	54.4043	0.5866	34.57	40.2
KD_GL 400cm	10.8388	0.154	0.0322	1.345	5.925	10.8388	18.1088	7.4273	32.7189	59.8538	0.8212	15.43	40.2
3PT 30cm	14.4897	0.3185	0.1741	8.44	7.055	14.4897	29.9847	28.1477	23.5287	48.3236	14.8601		
3PT 56cm	5.6522	0.3055	0.1826	8.865	5.98	5.6522	20.4972	43.2498	29.1747	27.5755	2.9329	7.6	13.4
3PT 100cm	1.5045	0.3391	0.1455	7.01	9.515	1.5045	18.0295	39.2906	53.5735	7.1359	1.8696	20.5	13.4
3PT 150cm	2.6997	0.3138	0.0401	1.74	13.52	2.6997	17.9597	43.5258	44.3071	12.1671	1.3641	19.8	89.4
3PT 200cm	0.8231	0.3281	0.0951	4.49	11.485	0.8231	16.7981	26.0527	68.3883	5.559	1.0559	29.85	89.4
3PT 369cm	1.1806	0.3129	0.0608	2.775	12.44	1.1806	16.3956	47.7835	47.5495	4.6671	1.7286	22.1	13.4
3PT 500cm	12.358	0.1261	0.0532	2.395	3.48	12.358	18.233	14.499	18.9489	66.5521	0.5866		
ND 20cm	1.2406	0.3635	0.1163	5.55	12.195	1.2406	18.9856	29.2327	64.2329	6.5344	3.8715	4.9	89.4
ND 100cm	4.4016	0.3267	0.0796	3.715	12.19	4.4016	20.3066	18.2945	60.0297	21.6757	1.8771		
ND 150cm	3.9259	0.3566	0.0602	2.745	14.655	3.9259	21.3259	12.8717	68.7193	18.4091	1.0516	5.35	89.4
ND 200cm	4.8311	0.3092	0.1114	4.635	10.1	4.8311	19.5661	23.6889	51.6199	24.6912	1.3994	7.15	44.7
ND 300cm	15.8446	0.1289	0.038	0.965	4.755	15.8446	21.5646	4.4749	22.05	73.475	0.8212	4.65	44.7
ND 320cm	12.3894	0.1768	0.0387	1.625	6.845	12.3894	20.8594	7.7903	32.8149	59.3948	0.5866		
ND 350cm	16.5295	0.0932	0.0462	1.375	2.56	16.5295	20.4645	6.719	12.5095	80.7716	0.4693	5.9	35.6
ND 420cm	16.6135	0.0913	0.0393	1.03	2.81	16.6135	20.4535	5.0358	13.7385	81.2257	0.5717	7	35.6
MRU 120cm	1.9752	0.3401	0.215	9.815	6.465	1.9752	18.2552	53.7655	35.4146	10.8199	0.352	16.67	26.8
MRU 155cm	5.144	0.2784	0.1636	7.245	5.95	5.144	18.339	39.506	32.4445	28.0495	1.0251	17.6	26.8

MRU 255cm	10.4673	0.2544	0.1374	5.935	6.06	10.4673	22.4623	26.422	26.9785	46.5994	0.4601		
MRU 285cm	7.0394	0.2562	0.1393	6.03	6.055	7.0394	19.1244	31.5304	31.6611	36.8085	0.706	8.4	26.8
MRU 305cm	1.7814	0.3496	0.0734	2.735	14.02	1.7814	18.5364	14.7548	75.635	9.6103	0.3551		
MRU 500cm	10.2985	0.2072	0.0709	3.235	6.755	10.2985	20.2885	15.945	33.2947	50.7603	0.2335	4.83	22.4
MRU 550cm	7.0152	0.2451	0.0841	3.895	7.99	7.0152	18.9002	20.6082	42.2747	37.1171	0.7144	15.6	22.4

Appendix 6: Calculation of Eto using FAO – Penman Monteith

Day	Year	RH	e^o(Tmax) kPa	e^o(Tmin) kPa	e_s kPa	Δ (kPa/^{o}C)	e_a kPa	e_s-e_a (kPa)	u_2 (m/s)	Rnl	Rad (MJ/m2/day) Rn	Rad (KJ/m2/day) Rn	γ (kPa/^{o}C)	ETo (mm/d)
1	1990	66	4.4926	1.1481	2.8203	0.1447	1.8614	0.9589	1.5	3.0636	16.6544	16654.38	0.053223	2.028
2	1990	70	4.2431	1.2280	2.7355	0.1447	1.9149	0.8207	1.6	2.9683	16.7609	16760.92	0.053223	1.936
3	1990	65	4.0057	1.2280	2.6168	0.1409	1.7009	0.9159	1.5	3.1525	16.5887	16588.67	0.053223	1.970
4	1990	53	5.3193	0.9351	3.1272	0.1447	1.6574	1.4698	1.2	3.4167	16.3371	16337.09	0.053223	2.277
5	1990	56	4.0057	0.9351	2.4704	0.1262	1.3834	1.0870	1.6	3.5115	16.2556	16255.64	0.053223	2.213
6	1990	58	4.7548	0.9351	2.8449	0.1371	1.6501	1.1949	1.6	3.3370	16.4441	16444.11	0.053223	2.350
7	1990	57	5.3193	1.1481	3.2337	0.1569	1.8432	1.3905	1.5	3.2066	16.5892	16589.20	0.053223	2.492
8	1990	56	4.0057	1.2280	2.6168	0.1409	1.4654	1.1514	1.4	3.4154	16.3957	16395.70	0.053223	2.145
9	1990	56	4.7548	1.2280	2.9914	0.1528	1.6752	1.3162	1.7	3.3088	16.5181	16518.10	0.053223	2.569
10	1990	69	4.2431	1.3127	2.7779	0.1487	1.9167	0.8611	1.7	2.9668	16.8766	16876.64	0.053223	2.051
11	1990	38	5.3193	1.2280	3.2736	0.1611	1.2440	2.0296	1.6	3.9324	15.9280	15928.00	0.053223	3.214
12	1990	42	5.0301	1.1481	3.0891	0.1528	1.2974	1.7917	1.9	3.8114	16.0665	16066.52	0.053223	3.309
13	1990	56	5.0301	1.0728	3.0515	0.1487	1.7088	1.3426	1.8	3.3145	16.5816	16581.60	0.053223	2.688
14	1990	48	5.6227	1.1481	3.3854	0.1611	1.6250	1.7604	1.5	3.5005	16.4141	16414.12	0.053223	2.855
15	1990	56	4.7548	1.0728	2.9138	0.1447	1.6317	1.2821	1.3	3.3585	16.5751	16575.12	0.053223	2.209
16	1990	58	4.7548	1.1481	2.9514	0.1487	1.7118	1.2396	1.4	3.2682	16.6849	16684.90	0.053223	2.259
17	1990	54	5.0301	1.2280	3.1291	0.1569	1.6897	1.4394	1.8	3.3365	16.6366	16636.58	0.053223	2.801
18	1990	58	4.7548	1.3127	3.0337	0.1569	1.7596	1.2742	1.3	3.2155	16.7778	16777.79	0.053223	2.227
19	1990	63	4.0057	1.3127	2.6592	0.1447	1.6753	0.9839	1.9	3.1812	16.8327	16832.75	0.053223	2.309
20	1990	63	5.6227	1.0728	3.3477	0.1569	2.1091	1.2387	1.1	2.9624	17.0725	17072.54	0.053223	2.056
21	1990	59	3.7799	1.2280	2.5039	0.1371	1.4773	1.0266	1.8	3.3578	16.6984	16698.40	0.053223	2.294
22	1990	61	4.7548	1.2280	2.9914	0.1528	1.8247	1.1666	1.7	3.1449	16.9329	16932.88	0.053223	2.420
23	1990	32	4.7548	1.2280	2.9914	0.1528	0.9572	2.0341	2.1	4.2318	15.8678	15867.75	0.053223	3.842
24	1990	53	4.7548	1.3127	3.0337	0.1569	1.6106	1.4232	1.6	3.3836	16.7379	16737.91	0.053223	2.621
25	1990	51	5.6227	1.3127	3.4677	0.1699	1.7685	1.6992	2.3	3.3343	16.8094	16809.39	0.053223	3.554
26	1990	52	4.7548	1.0019	2.8783	0.1409	1.4967	1.3816	1.5	3.5171	16.6489	16648.90	0.053223	2.491
27	1990	41	5.3193	0.8133	3.0663	0.1371	1.2572	1.8091	1.2	3.9164	16.2720	16272.02	0.053223	2.590
28	1990	43	5.3193	0.8723	3.0958	0.1409	1.3312	1.7646	1.4	3.8191	16.3919	16391.87	0.053223	2.786

29	1990	49	5.3193	1.0019	3.1606	0.1487	1.5487	1.6119	1.6	3.5475	16.6860	16685.99	0.053223	2.835
30	1990	51	5.0301	1.0728	3.0515	0.1487	1.5562	1.4952	1.5	3.4927	16.7634	16763.40	0.053223	2.615
31	1990	49	5.6227	1.0728	3.3477	0.1569	1.6404	1.7073	1.4	3.4840	16.7947	16794.68	0.053223	2.726

Appendix 7: Calculation of Short wave (Solar) Radiation using Angstrom Formula

Day	Year	X	Tan delta	tan phi		sin WS	Ra	N	n	Rs
1	1990	0.999968	-0.42398	0.013387	1.576472	0.999984	36.06208	12.04336	11.75	26.29065
2	1990	0.999968	-0.42228	0.013387	1.57645	0.999984	36.08233	12.04319	11.75	26.30564
3	1990	0.999968	-0.42044	0.013387	1.576425	0.999984	36.10385	12.043	11.75	26.32158
4	1990	0.999969	-0.41846	0.013387	1.576399	0.999984	36.12662	12.0428	11.75	26.33844
5	1990	0.999969	-0.41635	0.013387	1.57637	0.999984	36.15061	12.04258	11.75	26.35622
6	1990	0.999969	-0.41411	0.013387	1.57634	0.999985	36.17579	12.04235	11.75	26.37488
7	1990	0.99997	-0.41173	0.013387	1.576308	0.999985	36.20212	12.04211	11.75	26.3944
8	1990	0.99997	-0.40922	0.013387	1.576275	0.999985	36.22957	12.04185	11.75	26.41475
9	1990	0.99997	-0.40658	0.013387	1.576239	0.999985	36.25811	12.04158	11.75	26.43591
10	1990	0.999971	-0.40381	0.013387	1.576202	0.999985	36.28769	12.0413	11.75	26.45786
11	1990	0.999971	-0.40092	0.013387	1.576164	0.999986	36.31828	12.041	11.75	26.48055
12	1990	0.999972	-0.3979	0.013387	1.576123	0.999986	36.34983	12.04069	11.75	26.50397
13	1990	0.999972	-0.39476	0.013387	1.576081	0.999986	36.38231	12.04037	11.75	26.52807
14	1990	0.999973	-0.3915	0.013387	1.576037	0.999986	36.41566	12.04004	11.75	26.55283
15	1990	0.999973	-0.38811	0.013387	1.575992	0.999987	36.44985	12.03969	11.75	26.57822
16	1990	0.999973	-0.38461	0.013387	1.575945	0.999987	36.48481	12.03934	11.75	26.60419
17	1990	0.999974	-0.38099	0.013387	1.575897	0.999987	36.52052	12.03897	11.75	26.63072
18	1990	0.999974	-0.37726	0.013387	1.575847	0.999987	36.55691	12.03858	11.75	26.65777
19	1990	0.999975	-0.37341	0.013387	1.575795	0.999988	36.59393	12.03819	11.75	26.68529
20	1990	0.999976	-0.36946	0.013387	1.575742	0.999988	36.63153	12.03779	11.75	26.71325
21	1990	0.999976	-0.36539	0.013387	1.575688	0.999988	36.66967	12.03737	11.75	26.74161
22	1990	0.999977	-0.36122	0.013387	1.575632	0.999988	36.70827	12.03694	11.75	26.77034
23	1990	0.999977	-0.35694	0.013387	1.575575	0.999989	36.7473	12.03651	11.75	26.79939
24	1990	0.999978	-0.35256	0.013387	1.575516	0.999989	36.78668	12.03606	11.75	26.82871
25	1990	0.999978	-0.34808	0.013387	1.575456	0.999989	36.82637	12.0356	11.75	26.85827
26	1990	0.999979	-0.3435	0.013387	1.575395	0.999989	36.8663	12.03513	11.75	26.88802
27	1990	0.999979	-0.33883	0.013387	1.575332	0.99999	36.90642	12.03465	11.75	26.91793

28	1990	0.99998	-0.33406	0.013387	1.575269	0.99999	36.94667	12.03417	11.75	26.94794
29	1990	0.999981	-0.3292	0.013387	1.575203	0.99999	36.98699	12.03367	11.75	26.97802
30	1990	0.999981	-0.32425	0.013387	1.575137	0.999991	37.02731	12.03316	11.75	27.00812
31	1990	0.999982	-0.31921	0.013387	1.57507	0.999991	37.06758	12.03265	11.75	27.03818

Regression constants (a and b) are fractions of extraterrestrial radiation reaching the earth on clear days.

a = 0.29

b = 0.45

$$Rs = Ra\ (a + b * \frac{n}{N})$$

Appendix 8: Simple 1-D Mixing model; variation in isotopic composition of $\delta^{18}O$ from the Lake.

Simple 1-D mixing model												
		Width model is unit (1 meter)										
Constant head left	1888	m										
Transimissivity	3500	m2/day										
Recharge	4E-05	m/day		14.6		3.65	mm/yr					
Cell size	1000	m				25.55	mm/yr					
Constanthead right	1884	m				14.6	mm/yr	average				
Concentration lake	6.6	o/oo										
Concentration recharge	-3	o/oo										
Heads of the area	1888	1887.65	1887.29	1886.92	1886.5	1886	1885.7	1885.32	1884.9	1884	1884	m
Distance right side	0	1000	2000	3000	4000	5000	6000	7000	8000	9000	10000	m
flow right side	1.22	1.26	1.3	1.34	1.38	1.42	1.46	1.5	1.54	1.58	1.58	m3/day
matter flux rightside	8.052	7.932	7.812	7.692	7.572	7.452	7.332	7.212	7.092	6.972	6.852	g/day
concentration	6.6	6.29524	6.00923	5.7403	5.487	5.248	5.0219	4.808	4.6052	4.413	4.33671	g/m3
% percentage lakewater	100	96.8254	93.8462	91.0448	88.406	85.92	83.562	81.3333	79.221	77.22	77.2152	
Sampled Borehole	Lake	Osluswa	C4366	Heather	C562	C2071	C210	C579	C562	C210	Kongoni M13	
measured $d^{18}O$	6.6	3.25	3.4	4.19	4.3	3.4	3.1	3.9	4.3	3.1	3.25	
measured $d^{2}H$	36	23.9	21	29.2	25	18	20.1	22	25	20.1	23	

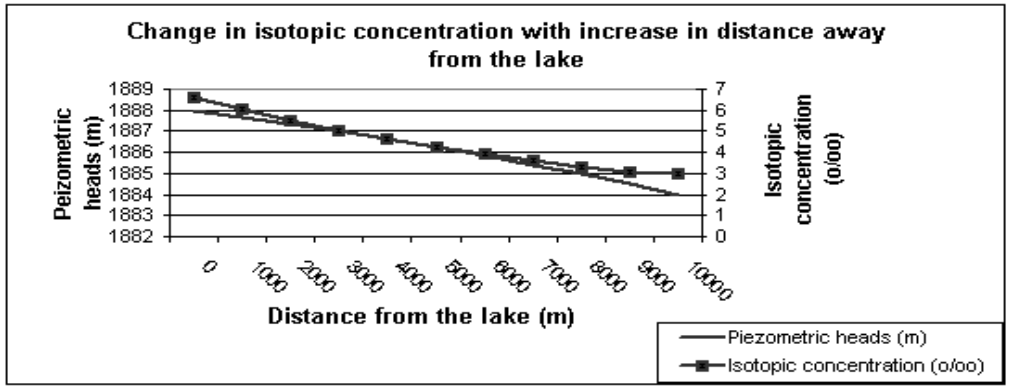

Appendix 9: Simple 1-D Mixing model; variation in isotopic composition of δD from the Lake.

Simple 1-D mixing model												
		Width model is unit (1 meter)										
Constant head left		1888	m									
Transmissivity		3500	m2/day									
recharge		0.00009	m/day		32.85		10.95	mm/year				
cell size		1000	m				32.85	mm/year				
constanthead right		1884	m									
Concentration lake		36	o/oo									
Concentration recharge		-3	o/oo									
Heads of the area	1888.0	1887.7	1887.4	1887.1	1886.7	1886.3	1885.9	1885.5	1885.0	1884.5	1884.0	m
Distance right side	0	1000	2000	3000	4000	5000	6000	7000	8000	9000	10000	m
flow right side	0.995	1.085	1.175	1.265	1.355	1.445	1.535	1.625	1.715	1.805	1.805	m3/day
matter flux rightside	35.82	35.55	35.28	35.01	34.74	34.47	34.2	33.93	33.66	33.39	33.12	g/day
concentration	36	32.765	30.0255	27.6759	25.64	23.85	22.28	20.88	19.63	18.499	18.349	g/m3
% percentage lakewater	100	91.7051	84.6809	78.6561	73.43	68.86	64.82	61.231	58.02	55.125	55.125	
Sampled Borehole	Lake	Osluswa	C4366	Heather	C562	89	C210	C579	C562	C210	C2071	Kongoni M13
measured $d^{18}O$	6.6	3.25	3.4	4.19	4.3	3.25	3.1	3.9	4.3	3.1	3.4	
measured $d^{2}H$	36	23.9	21	29.2	25	23	20.1	22	25	20.1	18	

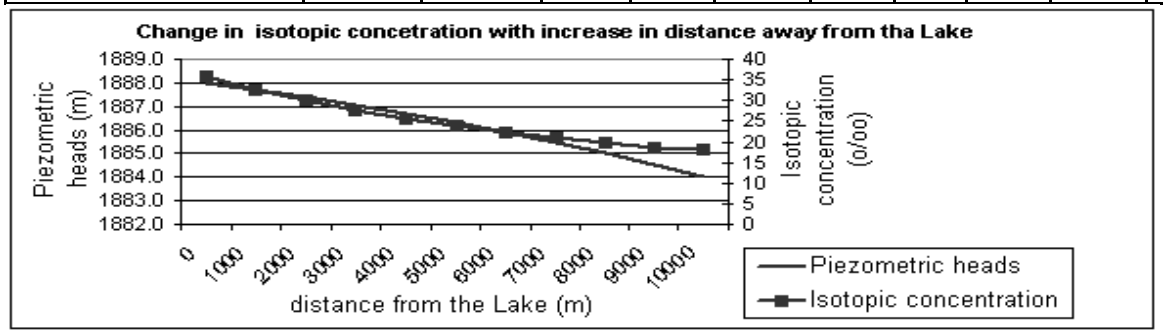

Appendix 10: Stable isotopes of Water Samples collected during fieldwork, 2000.

Dataset 1: Analysis carried out at Royal University of Groningen, The Netherlands.

Sample	X	Y	$\delta^{18}O$(‰)	δD(‰)
River Malewa	209119	9926378	-2.74	-6.2
Crater Lake	194929	9913682	12.43	59.3
L.Naivasha Mid.	205000	9915000	6.56	36
Gorge Spring	205000	9903000	4.47	25.5
Oloidian bay	195312	9909880	10.24	56.7
Heather BH	214281	9909564	4.19	29.2
Sulmac farms	207857	9908376	2.9	19.1
3 Point farms BHM	213065	9924682	-4.33	-17.6
Golf course down BH	201390	9925438	0.05	5.3
Olsuswa water supply	204888	9908150	3.53	23.9
Kongoni M13	194823	9909906	3.25	23
Kedong C210	208867	9909074	3.1	20.1
Golf course BH	201563	9926482	-0.37	2.8
Moi Ndabi BH2	189657	9911938	-4.86	-20.7
Ngodi BH	187796	9909094	-5.29	-31.9
Marula BH2	203819	9938994	-3.59	-15

Appendix 11: Isotope data set 2 : darling et.al.,1996.

Site	Sample type	$\delta^{18}O$(‰o)	δD(‰o)
Naivasha	L	6.6	36
C4178	B	-4.1	-24
C5002	B	-4.4	-22
OW-2	G	2.1	3
OW-5	G	3.7	18
OW-16	G	3.1	10
OW-21	G	2.8	8
OW-22	G	2.7	13
OW-23	G	3.6	13
OW-26	G	2.6	11
OW-703	G	4.5	34
OW-705	G	3.7	25
OW-706	G	2.2	21
OW-715	G	1	4
EW-1	G	-2.1	-9
B: Borehole	**G: Geothermal well**	**L: Lake**	

Appendix 12: Isotope Data set 3: University of Nevada, 1992.

Site	Sample type	$\delta^{18}O$(‰)	δD(‰)
Naivasha	Rain (regional)	-5.1	-32.8
Naivasha	Rain (local)	-6.4	-39
River	R	-2.7	-13
L. Naivasha	L	4.8	23
Ololdian bay	L	6.6	36
Crater lake	L	11	39
C729	B	0.7	-8
C1404	B	-4.6	-28
C563	B	5.6	32
C210	B	3.7	18
133/4/138	B	4.1	7
OW-2	G	3	10.5
OW-4	G	5.4	32.6
OW-5	G	4.3	21.5
OW-6	G	4	17.4
OW-10	G	5	27.8
OW-11	G	3.8	18.2
OW-13	G	4.5	25.3
OW-14	G	4.8	25
OW-15	G	5.5	23.6
OW-16	G	3.7	14
OW-17	G	6.4	32
OW-18	G	5.5	25.5
OW-19	G	5.9	29
OW-20	G	4.4	20.2
OW-21	G	4.8	22.7
OW-22	G	3.8	18.6
OW-23	G	4.7	18
OW-24	G	4.2	20.3
OW-25	G	3.8	17.8
OW-26	G	3.4	18.1
OW-701	G	3.5	24
OW-703	G	4.3	32.9
X-2	G	2.5	5
B: Borehole	**G: Geothermal well**	**L: Lake**	

Appendix 13: Isotope Dataset 4: University of Nevada, 1996.

Sample	Type	$\delta^{18}O$(‰o)	δD(‰o)
R.Murindati,r-4	R	-2.6	-8
Little Gilgil, r-5	R	-3.3	-15
R.Malewa (m),r-6	R	-3	-9
R.Kianjogu, r-7	R	-3.6	-14
Gathiriga str., r-8	R	-2.4	-6
Nandarashi str., r-9	R	-3.3	-12
R.Turasha,r-10	R	-3.8	-19
R.Karati (up), r-11	R	-1.9	-5
R.Karati (mi), r-12	R	-1.6	-5
L.Naivasha, Ik-001	L	6.4	39
Oloidian Bay Ik-002	L	10.6	60
Mini-piez.mpzl-1	B	5.6	34
Mini-piez.mpzl-2	B	5.8	33
C3366	B	-3.9	-21
C3677	B	-4.2	-22
C3675	B	-2.7	-16
C210	B	3.5	19
C562	B	4.3	25
C567	B	4.2	23
C7829	B	3.9	26
C4397	B	4.2	21
C4420	B	3.7	22
C2071	B	3.4	18
C579	B	3.9	22
C4366	B	3.4	21
UW-1	B	3.6	21
C630-D	B	3.6	23
C3767	B	2.1	17
C2660	B	4.1	22
OW101	G	3.1	4
OW-2	G	3.4	17.6
OW-26	G	3.7	23
OW-725	G	3.4	24
OW-728	G	3.7	29
G: Geothermal well	**B: Borehole**	**L: Lake**	

Appendix 14: Isotope Dataset 5: Arc Seibersdorf research, Vien, Austria, 2002

Natural areas	Year	X	Y	$\delta^{18}O$(‰)	δD(‰)	Sample type
Kedong	2002	211875	9904706	-3.03	-17.7	Un
Ndabibi	2002	194432	9914858	-1.42	-21.1	Un
Three point	2002	213398	9924946	-3.78	-26.7	Un
Marula	2002	208448	9930834	-2.8	-23.6	Un
Kihoto, K 1	2002	214125	9919894	3.21	23	B
Kihoto, K 2	2002	213219	9919782	3.78	25.5	B

Where, Un: Unsaturated zone below rooting depth B: Borehole

PLATES

Plates 1: The behaviour of different types of vegetation during dry seasons, Kedong area.

Plates 2: Fractured volcanic rock from a quarry at Kedong area.

Plates 3: Acacia, the yellow Fever species.

Plates 4: Acacia, the Whistling Thorn species.

Plates 5: The Pumice sand, volcano origin, Three Point area.

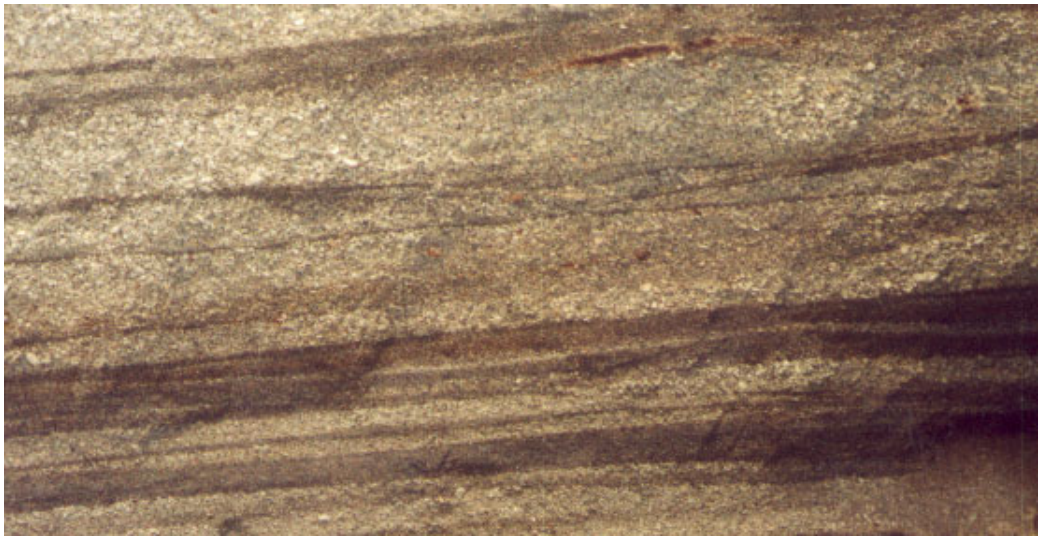

Plates 6: Well-bedded trachytic pumice, lower plains of Mt.Longonot.

PLATES 1

Conditions of vegetation during fieldwork, Kedong area.

The effect of dry seasons on grassland in the study area.

Fractured volcanic rock from a quarry at Kedong area.

Acacia, the yellow Fever species

Acacia, the Whistling Thorn species